

MACROMOLECULAR CHARACTERIZATION OF ADIPOSE TISSUES IN
INBRED OBESE MOUSE MODELS

A THESIS SUBMITTED TO
THE GRADUATE SCHOOL OF NATURAL AND APPLIED SCIENCES
OF
MIDDLE EAST TECHNICAL UNIVERSITY

BY

İLKE ŞEN

IN PARTIAL FULFILLMENT OF THE REQUIREMENTS
FOR
THE DEGREE OF MASTER OF SCIENCE
IN
BIOLOGY

AUGUST 2012

Approval of the thesis:

**MACROMOLECULAR CHARACTERIZATION OF ADIPOSE TISSUES
IN INBRED OBESE MOUSE MODELS**

submitted by **İLKE ŞEN** in partial fulfillment of the requirements for the degree
of **Master of Science in Biology Department, Middle East Technical
University** by,

Prof.Dr.Canan Özgen
Dean, Graduate School of **Natural and Applied Sciences**

Prof. Dr. Musa Doğan
Head of Department, **Biology Dept., METU**

Prof. Dr. Feride Severcan
Supervisor, **Biology Dept., METU**

Examining Committee Members:

Prof.Dr.Feride Severcan
Biology Dept., METU

Prof. Dr. Sevgi Haman Bayarı
Physics Education Dept., Hacettepe University

Assist.Prof.Dr.Sreeparna Banerjee
Biology Dept., METU

Assist.Prof.Dr. Tülin Yanık
Biology Dept., METU

Dr. Ayça Doğan

Date: 03.08.2012

I hereby declare that all information in this document has been obtained and presented in accordance with academic rules and ethical conduct. I also declare that, as required by these rules and conduct, I have fully cited and referenced all material and results that are not original to this work.

Name, Last name : İLKE ŞEN

Signature :

ABSTRACT

MACROMOLECULAR CHARACTERIZATION OF ADIPOSE TISSUES IN INBRED OBESE MOUSE MODELS

ŞEN, İlke

M.Sc., Department of Biology

Supervisor: Prof.Dr. Feride SEVERCAN

Co-Supervisor: Assist. Prof. Dr. Sreeparna BANERJEE

August 2012, 110 pages

Obesity is a metabolic disorder that results in elevated levels of free fatty acids and triglycerides in the blood circulation, which further leads to accumulation of lipids within various tissues. Like in other similar metabolic disorders, obesity is thought to be originated from structural and regulatory changes in macromolecular assemblies. This current study aims to investigate the effects of obesity on macromolecular alterations in order to characterize Berlin fat mouse inbred (BFMI) lines which are new models for the obesity research that may contribute to understanding of spontaneous obesity without induction of a high fat diet. Attenuated Total Reflectance - Fourier Transform Infrared (ATR-FTIR) spectroscopy was used to characterize content and structure of macromolecules in male and female control (DBA/2J) and BFMI lines; namely BFMI856, BFMI860 and BFMI861, in two different adipose tissues; inguinal fat (IF) which is subcutaneous adipose tissue (SAT), gonadal fat (GF) which is visceral adipose

tissue (VAT). Structural and compositional alterations in proteins, lipids, saturated and unsaturated lipid contents, nucleic acid, collagen and glycogen contents and variations in the lipid chain length were determined. BFMI860 and BFMI861 lines were found to be the most affected lines since they showed the indications of lipid peroxidation and insulin resistance more severely as they had lower glycogen content in all tissues and lower unsaturated lipid content especially in IF adipose tissues. Moreover, structural changes in lipids were observed especially in male GF adipose tissues of BFMI856 and BFMI861 lines. Protein content decreased significantly specifically in female IF adipose tissues but no change was observed in the structure. Furthermore, BFMI852 line was found to be affected different than other lines and had an effect on especially female IF. To conclude, obesity induced changes differ in BFMI lines according to the gender, adipose tissue type and distinctness in the strains.

Keywords: Obesity, BFMI, adipose tissue, IF, GF, FTIR spectroscopy, macromolecule

ÖZ

İNBRED OBEZ FARE MODELLERİ ADİPOZ DOKULARININ MAKROMOLEKÜLER KARAKTERİZASYONU

ŞEN, İlke

Yüksek Lisans, Biyoloji Bölümü

Tez Yürütücüsü: Prof.Dr. Feride SEVERCAN

Ortak Tez Yürütücüsü: Assist. Prof. Dr. Sreeparna BANERJEE

Ağustos 2012, 110 sayfa

Obezite, serbest yağ asitlerinin ve trigliseritlerin kan dolaşımındaki miktarlarının artması ile birçok dokuda lipit birikimine sebep olan metabolik bir rahatsızlıktır. Diğer hastalıklara benzer olarak obezitenin de, dokulardaki moleküllerin ve membran gibi makromoleküler toplulukların yapısal ve regülatör değişimleri sonucu oluşan bazı işleyiş bozukluklarından kaynaklandığı düşünülmektedir. Bu çalışma, obezitenin makromoleküler değişimleri incelemeyi ve Berlin fat mouse inbred (BFMI) ırklarını karakterize etmeyi amaçlamıştır. Obezite çalışmalarında kullanılmak üzere oluşturulan bu yeni fare modelleri, yüksek yağ içerikli diyet ile tetiklenmemiş kendiliğinden oluşan obezitenin anlaşılmasına katkıda bulunacaktır. Bu amaç doğrultusunda, Attenuated Total Reflectance-Fourier Transform Infrared (ATR-FTIR) spektroskopi tekniği kullanılarak BFMI852, BFMI856, BFMI860, BFMI861 (BFMI) ve kontrol DBAJ farelerinin subkütan adipoz doku olan (SAT) inguinal (IF) ve viseral adipoz doku (VAT)

olan gonadal (GF) adipoz dokularındaki makromoleküllerin yapı ve içeriği karakterize edilmiştir. Protein, doymuş ve doymamış lipit, nükleik asit, kolajen ve glikojen miktar ve yapısındaki değişimler ve lipit zincir uzunluğundaki farklılıklar belirlenmiştir. Özellikle dişi ve erkek fare IF adipoz dokusunda doymamış yağ ve glikojen içeriği en az belirlenen ve dolayısı ile lipit peroksidasyonu ve insulin direnci belirtilerini en belirgin gösteren BFMI860 ve BFMI861 ırkları en çok etkilenen ırklar olarak belirlenmiştir. Buna ek olarak, lipitlerde oluşan yapısal değişikliklerin en çok BFMI856 ve BFMI861 ırklarının erkek fare GF adipoz dokularında olduğu tespit edilmiştir. Protein içeriğinin spesifik olarak dişi fare IF adipoz dokularında azaldığı belirlenmiş fakat proteinlerin yapısında anlamlı bir değişim bulunamamıştır. Ayrıca, BFMI852 ırkının diğer BFMI ırklarından daha farklı etkilendiği ve bu ırkta özellikle dişi fare IF adipoz dokusunun etkilendiği tespit edilmiştir. Sonuç olarak, BFMI ırklarının adipoz dokularında obeziteden kaynaklanan etkinin cinsiyete, adipoz doku tipine ve ırklarda görülen farklılıklara bağlı olarak değiştiği saptanmıştır.

Anahtar sözcükler: Obezite, BFMI, adipoz doku, IF, GF, FTIR spektroskopisi, makromolekül

To my parents Nilgün and Bekir Ersin Şen,

ACKNOWLEDGEMENTS

I would first like to express my gratitude to my supervisor Prof. Dr. Feride Severcan for her guidance, encouragement and supervision during my thesis study.

I am also grateful to Assoc. Prof. Dr. Sreeparna Banerjee for her valuable suggestions and guidance.

I would compassionately express my thanks to Özlem Bozkurt, Nihal Şimşek Özek, Ceren Aksoy, Şebnem Garip and Sherif Abbas owing to their precious help and lovely attitude both in the course of experimental period and in the course of writing this thesis.

I would like to extend my thanks to my close friends, Damla Güldağ, Seza Ergün, and Ebru Aras, and to all my other lab mates for their friendship, care and support. All these years have passed very pleasant, worthy and notable on account of you.

I would also thank to Özlem Mavi and Okan Tezcan for their endless support and sincere friendship.

I would like to thank to Aslı Sade Memişoğlu, Deniz Sezlev and Canan Kurşungöz for their endless help and friendship.

I would like to send my ultimate appreciation to my mother Nilgün Şen, my father Bekir Ersin Şen, my brothers Mehmet Ege Şen and Erdem Tüzen, my intimate friends Başak Karatoprak, Hande Yapıcı and İrem Durmaz also to Bora Başkaner for their absolute patience, understanding, encouragement, support and also for their endless love.

TABLE OF CONTENTS

ABSTRACT	iv
ÖZ	vi
ACKNOWLEDGEMENTS	ix
LIST OF FIGURES.....	xii
LIST OF TABLES	xv
LIST OF ABBREVIATIONS	xvii

CHAPTERS

1. INTRODUCTION	1
1.1 Obesity	1
1.1.1 Diagnosis of Obesity	2
1.1.2 Causes of Obesity.....	3
1.2 Adipose Tissue	4
1.2.1 Distribution and Localization of Adipose Tissue.....	4
1.2.2 Adipose Tissue Cytotypes.....	6
1.2.2.1 White Adipose Tissue	7
1.2.2.2 Brown Adipose Tissue	8
1.2.3 Adipocytes	8
1.2.3.1 Adipocyte Differentiation and Function	8
1.2.4 Adipose Tissue as an Endocrine Organ	9
1.2.5 Visceral and Subcutaneous Adipose Tissue.....	11
1.2.5.1 Subcutaneous Adipose Tissue (SCAT).....	11
1.2.5.2 Visceral Adipose Tissue.....	12
1.2.5.3 Physiological and Functional Differences Between VAT and SCAT.....	12
1.3 Adipose and Non-adipose tissues Affected During Obesity and Their Relation with Metabolic Complications.....	14

1.4 Adipocyte Stress in Obesity	16
1.4.1 Oxidative Stress	16
1.4.2 Endoplasmic Reticulum (ER) Stress	17
1.4.3 Mitochondrial Stress	18
1.5 Gender Effect in Obesity	19
1.6 BFMI Lines As New Mouse Models For Obesity	20
1.7 Electromagnetic Radiation and Basics of Spectroscopy	22
1.7.1. Infrared (IR) Spectroscopy	25
1.7.1.1 Fourier Transform Infrared (FTIR) Spectroscopy	27
1.7.1.1.1 Attenuated Total Reflectance (ATR) – FTIR Spectroscopy	28
1.7.1.1.2 The Advantages of FTIR Spectroscopy	30
1.8 Aim of the Study	31
2. MATERIALS AND METHODS	33
2.1 Animal Models	33
2.2 Feeding and Husbandry Conditions	34
2.3 Sample Collection	34
2.4 Experimental Groups	34
2.5 FTIR spectroscopic sample preparation, data acquisition and analysis	35
2.6 Statistics	36
3. RESULTS	37
3.1 General FTIR Spectrum and Band Assingment of the Adipose Tissues ..	37
3.2 Comparisons of the Band Wavenumber and Band Area Values of Control and Obese Mice.....	46
3.2.1 Comparisons of the Band Wavenumber and Band Area Values of Control and Obese Mice in the C-H Region (3025-2800 cm ⁻¹).....	46
3.2.2 Comparisons of the Band Wavenumber and Band Area Values of Control and Obese Mice in Fingerprint Region (1800-950 cm ⁻¹).....	48
3.3 Comparisons of the Band Area Ratio Values of Control and Obese Mice:	60
3.4 Comparison of the Bandwidth Values of Control and Obese Mice.....	71
4. DISCUSSION	77
5. CONCLUSION	90
REFERENCES.....	93

LIST OF FIGURES

FIGURES

Figure 1. Co-morbidities associated with obesity (Gupta et al, 2011).....	2
Figure 2. BMI values and classification of obesity.....	3
Figure 3 Multifactorial causes of obesity (Balaban & Silva, 2004).....	4
Figure 4. Localization of VAT and SAT in the body.....	5
Figure 5. Different cell types in adipose tissue (Fruhbeck, 2008)	6
Figure 6. Cytotypes of Adipose Tissue, BAT and WAT phenotype (Cinti, 2006)	7
Figure 7. Adipokines released from adipose tissue during obesity (Fruhbeck, 2008)	10
Figure 8. Comparison of visceral and subcutaneous adipose tissue functions (Freedland, 2004)	14
Figure 9. Lipid accumulation in non-adipose tissues and its relation with the metabolic diseases (van Herpen & Schrauwen-Hinderling, 2008)	15
Figure 10. Illustration of the contribution of accumulated fat in metabolic syndrome to increased ROS production (Furukawa et al, 2004).	17
Figure 11. Mechanism of the formation of ER and mitochondrial stress due to the dysfunctional adipocytes (Mittra et al, 2008).....	19
Figure 12. Hematoxylin and eosin stained section of reproductive (RPF), retroperitoneal (RF), and inguinal (IF) adipose tissue and oil-red staining of liver sections of B6 and BFMI mice on standard maintenance diet (SMD) and of BFMI mice on high-fat diet (HFD) at 10 weeks (Wagener et al, 2010).	22
Figure 13. An electromagnetic wave.....	23
Figure 14. Typical energy-level diagram showing the ground, excited states and vibrational levels. Long arrow represents a possible electron transition between the ground state and the fourth vibrational level of the first excited state. Short arrow represents a vibrational transition within the ground state (Freifelder, 1982).	23

Figure 15. The IR regions of the electromagnetic spectrum (Marcelli et al, 2012).	25
Figure 16. Types of linear vibrations modes of triatomic molecules.....	26
Figure 17. Types of non-linear vibrations modes of triatomic molecules (Marcelli et al, 2012).....	26
Figure 18. Components of FTIR Spectroscopy (Stuart, 1997)	27
Figure 19. A multiple reflection ATR system (Wang et al, 2007).....	29
Figure 20. The representative infrared spectra of control groups of IF and GF adipose tissues in the 4000-950 cm^{-1} region. The spectra were normalized with respect to the amide A band located at 3307 cm^{-1}	38
Figure 21. Representative spectra of GF adipose tissue of male control DBA/J2 and obese BFMI860 line in 4000-950 cm^{-1} region. The spectra were normalized with respect to the amide A band located at 3307 cm^{-1}	40
Figure 22. Representative spectra of GF adipose tissue of male control DBA/J2 Sand obese BFMI860 line in 3025-2800 cm^{-1} region The spectra were normalized with respect to the amide A band located at 3307 cm^{-1}	41
Figure 23. Representative spectra of GF adipose tissue of male control DBA/J2 and obese BFMI860 line in 1800-950 cm^{-1} region. The spectra were normalized with respect to the amide A band located at 3307 cm^{-1}	42
Figure 24. Representative spectra of IF adipose tissue of male control DBA/J2 and obese BFMI860 line in 4000-950 cm^{-1} region. The spectra were normalized with respect to the amide A band located at 3307 cm^{-1}	43
Figure 25. Representative spectra of IF adipose tissue of male control DBA/J2 and obese BFMI860 line in 3025-2800 cm^{-1} region. The spectra were normalized with respect to the amide A band located at 3307 cm^{-1}	44
Figure 26. Representative spectra of IF adipose tissue of male control DBA/J2 and obese BFMI860 line in 1800-950 cm^{-1} region. The spectra were normalized with respect to the amide A band located at 3307 cm^{-1}	45
Figure 27. The triglyceride/total lipid band area ratio.	61
Figure 28. The CH_3 anti-symmetric stretching/total lipid ratio band area ratio..	62
Figure 29. The olefinic stretching/total lipid band area ratio.....	63
Figure 30. The unsaturated/saturated lipid band area ratio.....	64

Figure 31. The lipid/protein band area ratio.....	65
Figure 32. The CH ₂ anti-sym. str./CH ₃ anti-sym. str. band area ratio.....	66
Figure 33. The CH ₂ anti-sym. str./total lipid band area ratio.....	67
Figure 34. The amide I / amide II band area ratio.....	68
Figure 35. The amide II/ 1345 cm ⁻¹ band area ratio..	69

LIST OF TABLES

TABLES

Table 1. Physical properties of commonly used ATR crystal materials	30
Table 2. General band assignment of FTIR spectrum of adipose tissues.....	39
Table 3. Detailed numerical summary of the differences in the wavenumber value of the bands observed in female control (DBA/2J) and obese (BFMI lines) mice GF adipose tissues.....	52
Table 4. Detailed numerical summary of the differences in the wavenumber value of the bands observed in male control (DBA/2J) and obese (BFMI lines) mice GF adipose tissues.....	53
Table 5. Detailed numerical summary of the differences in the wavenumber value of the bands observed in female control (DBA/2J) and obese (BFMI lines) mice IF adipose tissues.....	54
Table 6. Detailed numerical summary of the differences in the wavenumber value of the bands observed in male control (DBA/2J) and obese (BFMI lines) mice IF adipose tissues.....	55
Table 7. Detailed numerical summary of the differences in the band area value of the bands observed in female control (DBA/2J) and obese (BFMI lines) mice GF adipose tissues.....	56
Table 8. Detailed numerical summary of the differences in the band area value of the bands observed in male control (DBA/2J) and obese (BFMI lines) mice GF adipose tissues.....	57
Table 9. Detailed numerical summary of the differences in the band area value of the bands observed in female control (DBA/2J) and obese (BFMI lines) mice IF adipose tissues.....	58
Table 10. Detailed numerical summary of the differences in the band area value of the bands observed in male control (DBA/2J) and obese (BFMI lines) mice IF adipose tissues.....	59

Table 11. Detailed numerical summary of the differences in the bandwidth value of the bands observed in female control (DBA/2J) and obese (BFMI lines) mice GF adipose tissues.	73
Table 12. Detailed numerical summary of the differences in the bandwidth value of the bands observed in male control (DBA/2J) and obese (BFMI lines) mice GF adipose tissues.	74
Table 13. Detailed numerical summary of the differences in the bandwidth value of the bands observed in female control (DBA/2J) and obese (BFMI lines) mice IF adipose tissues.	75
Table 14. Detailed numerical summary of the differences in the bandwidth value of the bands observed in male control (DBA/2J) and obese (BFMI lines) mice IF adipose tissues.	76

LIST OF ABBREVIATIONS

ATR	Attenuated total reflectance
BAT	Brown adipose tissue
BFMI	Berlin fat mouse inbred
FFA	Free fatty acid
FTIR	Fourier transform infrared
GF	Gonadal fat
IF	Inguinal fat
SAT	Subcutaneous adipose tissue
TG	Triglyceride
VAT	Visceral adipose tissue
WAT	White adipose tissue

CHAPTER 1

INTRODUCTION

This current study aims to investigate the effects of obesity on macromolecular alterations in order to characterize 10 week old BFMI mice, new models for obesity research, which will contribute to understanding of spontaneous obesity without induction of a high fat diet. For this purpose, Attenuated Total Reflectance - Fourier Transform Infrared (ATR-FTIR) spectroscopy was used to characterize content and structure of macromolecules in female and male control (DBA/2J) and BFMI lines; namely BFMI852, BFMI856, BFMI860 and BFMI861, in two different adipose tissues; inguinal fat (IF) which is a subcutaneous adipose tissue (SAT) and gonadal fat (GF) which is a visceral adipose tissue (VAT).

1.1 Obesity

Obesity arises from the imbalance between energy intake and energy consumed with the effect of genetic susceptibility and environmental factors, which further leads to secondary metabolic disorders such as insulin resistance, hypertension, hyperlipidemia, cardiovascular diseases and many other diseases (Figure 1). Since, there is an increment in consumption of high fat included food intake and decrease in the physical activity in modern lifestyle, obesity is becoming one of the major health problems in the world (Reaven, 1997; Weisberg et al, 2003). There is a variety in body fat distribution and metabolic profile in obese patients according to the heterogeneous property of obesity (Ibrahim, 2010). According to World Health Organisation (WHO) approximately 1.6 billion people in all around the world were found to be overweight and 400 million of them were in obese state in 2005. Also, it is expected that approximately 2.3 billion people will

BMI	Classification
18.5–24.9	Normal weight
25.0–29.9	Overweight
30.0–34.9	Obese
34.9- 39.9	Morbid Obese
40.0 and above	Super Obese

Figure 2. BMI values and classification of obesity

1.1.2 Causes of Obesity

Environmental factors such as excessive dietary calories and lack of physical activity are the major factors that may lead obesity. Moreover, endocrine disorders, some medications, psychiatric illness can also make contribution to the formation of obesity (Gupta et al, 2011).

In addition to these factors, genetic susceptibility is an important factor for obesity, which may arise from a single gene mutation. Leptin and leptin receptor, pro-opiomelanocortin (POMC) and melanocortin-4 receptor (MC4R) are important genes and if there is a mutation in these genes monogenic obesity occurs (Andreasen & Andersen, 2009). Furthermore, growing evidences show that single-nucleotide polymorphisms (SNP) may also have a role in obesity. As an example, obesity-associated gene (FTO) was the first gene found with a genome-wide association (GWA) study for identifying a SNP located in the fat mass and its association with increase risk of obesity (Frayling et al, 2007). Moreover, recent association studies have been giving promising results for the new findings of gene mutations and these studies elucidate to the understanding of the genetic background of the obesity (Speliotes et al, 2010).

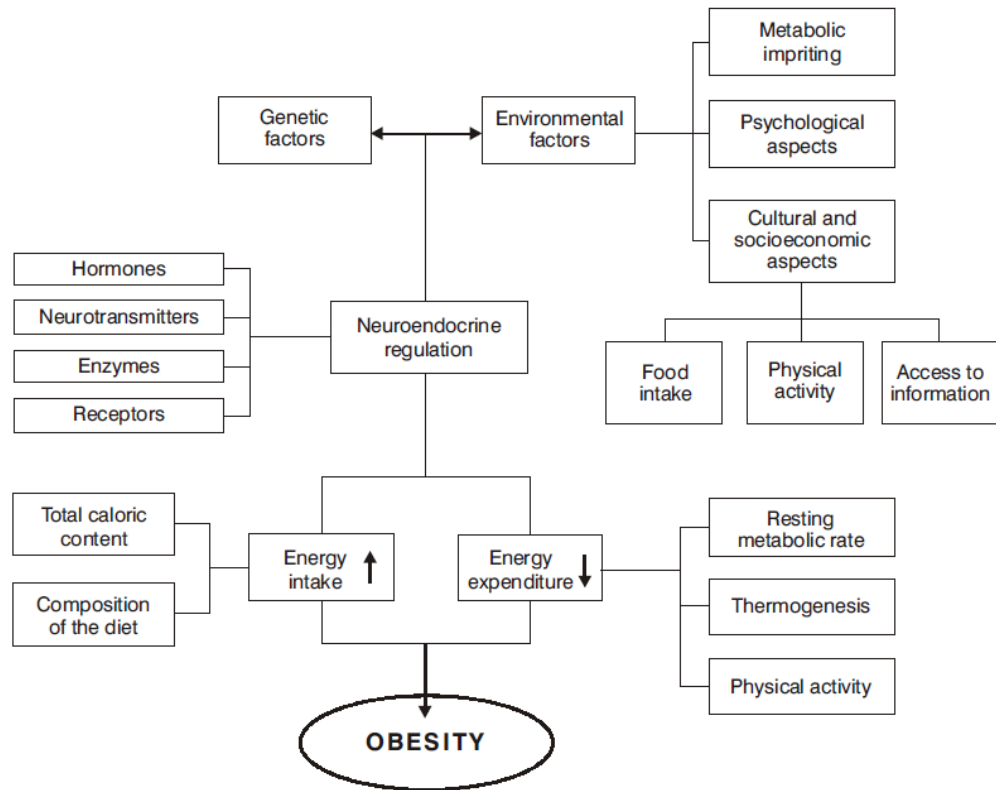


Figure 3 Multifactorial causes of obesity (Balaban & Silva, 2004)

1.2 Adipose Tissue

1.2.1 Distribution and Localization of Adipose Tissue

Adipose tissue is an essential, complex and metabolically active endocrine organ which is distributed in a variety of locations in the body different than the other organs (Figure 4) (Cinti, 2005; Kershaw & Flier, 2004).

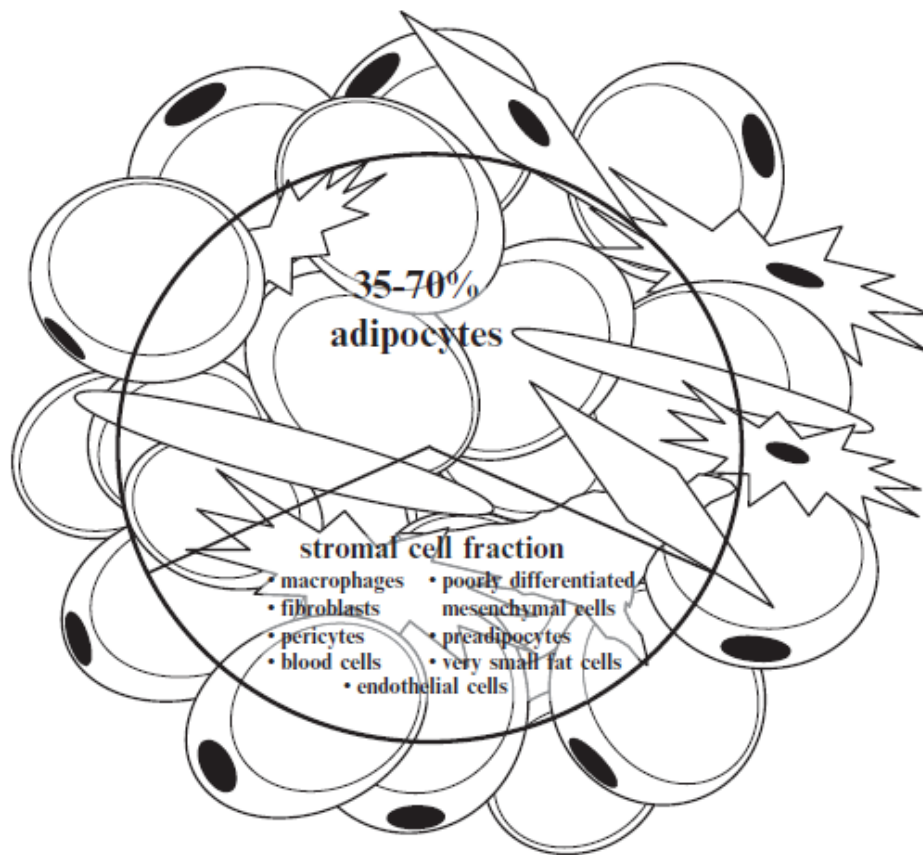


Figure 5. Different cell types in adipose tissue (Fruhbeck, 2008)

1.2.2 Adipose Tissue Cytotypes

Adipose tissue depots are composed of two cytotypes. These cytotypes are white adipose tissue (WAT) and brown adipose tissue (BAT). Their amounts in body represent variety according to the strain, gender, age, nutritional environmental factors. These adipose tissues are separated due to their colours since there is a difference on the histological composition of WAT and BAT. WAT is composed of white adipocytes whereas BAT is constituted from brown adipocytes (Figure 6) (Cinti, 2006).

1.2.2.2 Brown Adipose Tissue

Brown adipocytes have a completely different role than white adipocytes in the adipose organ since they are responsible for thermogenesis. They transfer the energy achieved from nutrition to thermal energy (Cannon & Nedergaard, 2004; Klaus et al, 1991). Uncoupling protein 1 (UCP1) which is only expressed in BAT is responsible for this transformation of the energy that is not used in oxidative metabolism (Cannon et al, 1982). Noradrenaline is responsible for the activation of beta-3-adrenoceptors which induce BAT to produce heat. When BAT is not stimulated adrenergically, it loses most of its brown characteristics and transdifferentiate into WAT like adipocytes due to the transformation of brown mitochondria into white mitochondria (Cinti, 2006; Cinti, 2008). This morphological transformation occurs with the activation of leptin gene activation and UCP-1 gene inhibition but it is reversible (Cancello et al, 1998). In rodents, BAT phenotype in adipose tissues is very important for the prevention of many metabolic diseases such as obesity and diabetes (Cinti, 2006).

.

1.2.3 Adipocytes

Adipocytes which are the major cellular component of adipose tissue have an important role in energy homeostasis as they are the main storage depots of the free fatty acids (FFAs) as triglycerides (TG) droplets and after food intake release FFAs into circulation in order for the regulation of energy status during the fasting state (Ahima, 2006; Hajer et al, 2008; Ibrahim, 2010). They also secrete adipokines for the regulation of immunity, thermogenesis, feeding and neuroendocrine function (Ahima, 2006).

1.2.3.1 Adipocyte Differentiation and Function

Adipocytes are formed by the differentiation of pre-adipocytes which are originated from a multipotent stem cell and have the potential for the generation of new adipocytes during the entire life of the organism (Otto & Lane, 2005).

Newly formed smaller adipocytes act as buffers during satiety since they absorb FFAs and TGs which are energy-rich molecules having important metabolic functions. In addition, fatty acids are one of the major membrane components in the cells. They can influence membrane fluidity and moreover they can affect functions of receptor and channels. Their excess accumulation and storage as TGs are seen in obesity. Moreover hormone-like effects of fatty acids and derivatives of fatty acids have been correlated with the regulation of gene expression profiles in preadipocytes and so, they affect adipocyte proliferation and differentiation directly (Duplus et al, 2000; Garaulet et al, 2006). Adipocytes cannot function properly as they grow larger (hypertrophy). Insulin has an important role in the regulation of adipocyte fat content, since it is a powerful inhibitor of hormone sensitive lipase (HSL) which is responsible for the hydrolysis of TGs to FFAs and an important activator of lipoprotein lipase (LPL) for enhancing FFA uptake by providing hydrolysis of TGs in triglyceride-rich lipoproteins such as very low-density lipoprotein-cholesterol (VLDL-c) and chylomicrons during postprandial phase (Hajer et al, 2008). Although, smaller adipose cells are more insulin sensitive, large adipocytes become insulin resistant and since they also gain hyperlipolytic property, they cannot respond to the anti-lipolytic effect of insulin. These complications lead to metabolic disorder obesity (Freedland, 2004; Garaulet et al, 2006; Ibrahim, 2010; Rajala & Scherer, 2003).

1.2.4 Adipose Tissue as an Endocrine Organ

Adipose tissue has been considered as an endocrine organ in recent years since it is involved in the secretion of wide range of protein factors and number of pathways as a connection of adipose tissue metabolism with the immune system in addition to its role in energy storage. During obesity, due to the expand in adipose tissue mass and adipocyte size, adipocytes are induced to secrete chemokines which attract monocytes as a starting point of low-grade inflammation (Weisberg et al, 2003). Then, the macrophages within the adipose tissue secrete cytokines. However, these cytokines make a paracrine effect on this tissue that causes low-grade inflammation with a decreased sensitivity to insulin among the adipocytes nearby (Schenk et al, 2008). WAT plays a critical role in

the formation of low-grade systemic inflammation (Federico et al, 2010). WAT includes many secretory cells and all the releasing molecules from these cells represent the secretome (Trayhurn & Wood, 2004). The adipocyte secretome comprises a variety of lipids and proteins. At first, these proteins were termed as “adipocytokines” but later on “adipokines” were assigned (Trayhurn et al, 2011). However, their role in regulation of obesity-related inflammation and metabolism is not well understood (Gesta et al., 2007 ; Wozniak et al., 2009 ; Juge-Aubry et al., 2005). As well as, adipokines have autocrine and paracrine effects on adipose tissue, they participate in the endocrine cross-talk of adipose tissue with other tissues such as skeletal muscle and liver (Hevener & Febbraio, 2010; Hotamisligil, 2006; Trayhurn et al, 2011). During obesity adipokine amounts change as adipocytes become dysfunctional (Figure 7) (Fruhbeck, 2008; Haugen & Drevon, 2007; Kershaw & Flier, 2004; MacDougald & Burant, 2007; Ouchi et al, 2000; Trayhurn & Wood, 2004).

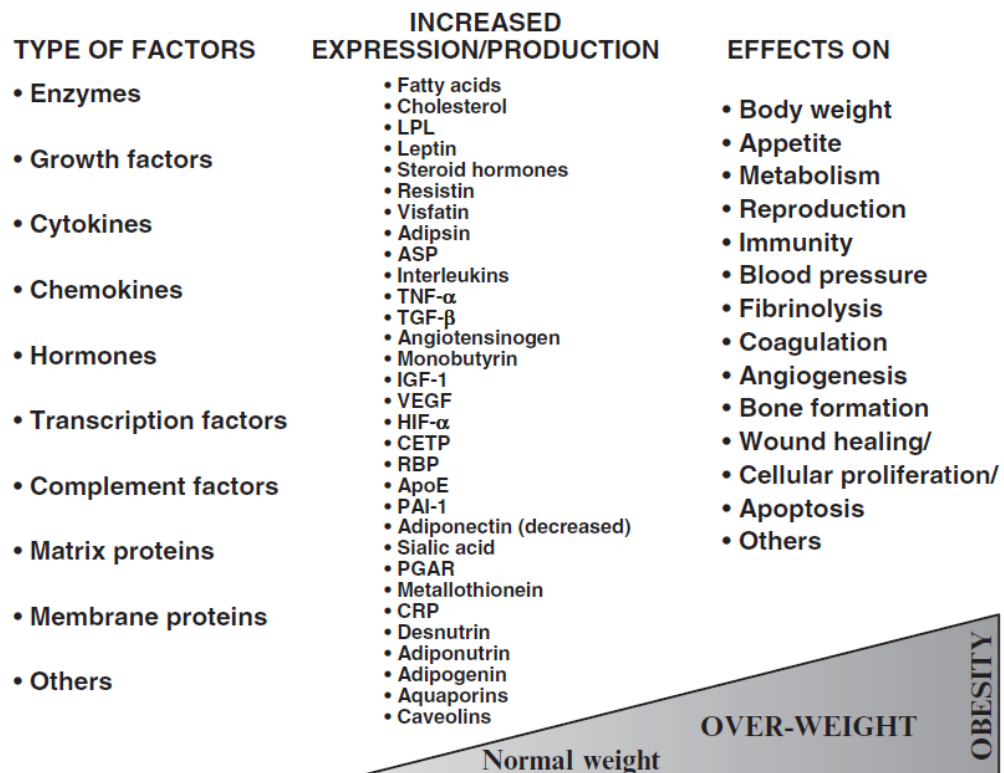


Figure 7. Adipokines released from adipose tissue during obesity (Fruhbeck, 2008)

1.2.5 Visceral and Subcutaneous Adipose Tissue

It has been shown that the regional fat distribution is more important than overall fat content related to obesity linked metabolic disorders (Oka et al, 2010). In adults, approximately more than 80% of total body fat consists of subcutaneous adipose tissue (SCAT) in the body and nearly 10–20% constituted from visceral adipose tissue (VAT) in adults (Abate et al, 1995). The type of adipocytes, lipolytic activity of the adipocytes, endocrine functions and their response to insulin and to the other hormones vary between SCAT and VAT (Ibrahim, 2010). Although, abdominal obesity is detected by the accumulation of both SCAT and VAT in the body, excessive accumulation of VAT seems to play more important role in the pathogeny of obesity (Freedland, 2004).

1.2.5.1 Subcutaneous Adipose Tissue (SCAT)

The abdominal SCAT is located under the skin and top of the abdominal musculature and SCAT which is stored in the femerogluteal regions, predominantly forms the lower body fat and they are drained into the caval vein (Lafontan & Berlan, 2003; Montague & O'Rahilly, 2000; Rytka et al, 2011; Wajchenberg, 2000). Differentiation capacity of SCAT preadipocytes is greater than VAT preadipocytes since preadipocyte differentiation into lipid storing mature adipocytes is regulated by peroxisome proliferators activated receptor (PPAR) which is a nuclear hormone receptor. The differentiation pathway is stimulated by this receptor when it is activated by natural ligands (such as prostaglandin metabolites) or synthetic ligands (such as thiazolidinediones (TZDs)) (Adams et al, 1997; Hauner et al, 1988) and the number of newly formed small adipocytes within SCAT increases. These new adipocytes become more willing to uptake TGs and FFAs. Therefore newly formed adipose tissues including these new and smaller adipocytes which are more sensitive to insulin behave like great buffers that stores circulating fatty acids and TGs during posprantial period (Frayn, 2002; Miyazaki et al, 2002). This regulation supplies protection to the body by preventing the accumulation of TGs and FFAs within non-adipose tissues and so that protect organism from type 2 diabetes and so

metabolic syndrome (Danforth, 2000; Frayn, 2002). However, if they reach their full capacity, they can never act as a protective SCAT adipocyte anymore. Excess accumulation of lipids within these tissues make these protective adipocytes dysfunctional (Freedland, 2004; Hajer et al, 2008).

1.2.5.2 Visceral Adipose Tissue

Visceral adipose tissues (VAT) depots are densely located at abdominal viscera beneath the abdominal muscles distributed in mesentery and omentum body cavity. Also, small amount of VAT is located retroperitoneally. VAT constitutes approximately 20 percent of total body fat in men and 5 to 8 percent in women (Freedland, 2004). VAT is different from the adipose tissue SAT presented in subcutaneous areas in the body since visceral adipocytes are metabolically more active and have more lipolytic activity than subcutaneous adipocytes (Arner, 1995; Lemieux & Despres, 1994). In addition to, VAT is thought to have a role in lipolysis of central SCAT results in acceleration in the release of peripheral FFAs (Freedland, 2004). VAT is also thought to play an important role in the expression of inflammatory cytokines and secretion of wide range of hormones responsible for the metabolic complications of obesity since it has unique position near portal circulation (Bjorntorp, 1990; Freedland, 2004; Ibrahim, 2010; Oka et al, 2010; Rytko et al, 2011).

1.2.5.3 Physiological and Functional Differences Between VAT and SCAT

Adipocytes in VAT includes large, more dysfunctional adipocytes with a greater amount when it is compared to SCAT which has insulin-sensitive, smaller adipocytes that are more willing to store FFAs and TG preventing their accumulation in non-adipose tissues (Marin et al, 1992; Misra & Vikram, 2003) BMI and waist circumference anthropometric indices which are used for the diagnosis of obesity, have higher correlation with SCAT than VAT. Moreover, both VAT and SAT are responsible for the regulation of the blood pressure in both sexes (men and women) independently (Ibrahim, 2010).

In addition to, VAT is more sensitive to the catecholamine (hormone has a role in lipolytic activity) induced lipolysis and less susceptible to the anti-lipolytic action of insulin so that VAT has higher rate of glucose uptake due to insulin stimulation and becomes more insulin-resistant than adipocytes in SCAT (Abate et al, 1995; Arner, 1999; Frayn, 2000). According to this, visceral abdominal obesity expressive subjects have lower glucose oxidation and disposal, also they have greater lipid oxidation in comparison to the subjects having peripheral obesity (Ibrahim, 2010). VAT and SCAT have different capacity to produce and secrete adipokines. One of the major adipokine leptin is expressed in particular levels according to the size of adipose tissue. Leptin levels increase as the storage of TG in adipose tissue increases (Tritos & Mantzoros, 1997). Since SCAT adipocytes can store more TGs, they are the major source of leptin hormone (Wajchenberg, 2000). Another important adipokine adiponectin is more abundantly expressed in VAT in comparison to SCAT (Freedland, 2004; Motoshima et al, 2002). It has been also thought that although, VAT has more effect on adiponectin plasma levels, SCAT adipocytes are the major adiponectin sources in subjects having obesity and insulin resistance. In addition, plasma adiponectin levels are negatively correlated with body weight significantly (Hajer et al, 2008). There are more infiltrated inflammatory cells within VAT than SCAT. Therefore, more pro-inflammatory cytokines such as TNF- α , IL-6 and CRP are observed in VAT in comparison to SCAT (Weisberg et al, 2003). Redundant levels of inflammatory markers are observed in abdominal obesity. C-reactive protein (CRP) which is one of the most important inflammatory markers, is correlated with WC and abundantly found in VAT during obesity (Pepys & Hirschfield, 2003). Also, VAT contains higher levels of MCP-1 compared to SCAT (Pou et al, 2007). After liver, adipose tissue is a significant source of angiotensinogen that has a role in the regulation of blood pressure and this peptide hormone is highly expressed in VAT in comparison to SCAT (Dusserre et al, 2000). Furthermore, PAI-1 levels increases during obesity and PAI-1 expression is higher in VAT compared to SCAT (Figure 8) (Alessi et al, 1997).

VAT	vs	SCAT
<ul style="list-style-type: none"> ■ Major predictor of IR /Metabolic Syndrome ■ Less responsive to insulin's adipogenic effects ■ More lipolytic ■ Portal Drainage ■ May enhance truncal SCAT lipolysis ■ Produces more IL-6, PAI-1 ■ More glucocorticoid receptors ■ High density of androgen receptors 		<ul style="list-style-type: none"> ■ Preadipocytes have greater differentiation capacity ■ May replenish VAT ■ Estrogen promotes ■ Produces Leptin ■ ? Role in IR ■ May be protective

Figure 8. Comparison of visceral and subcutaneous adipose tissue functions (Freedland, 2004)

1.3 Adipose and Non-adipose tissues Affected During Obesity and Their Relation with Metabolic Complications

“Obesity is due to a chronic positive energy balance, which increases the amount of TGs in adipose tissue” (van Herpen & Schrauwen-Hinderling, 2008). Increase in the amount of the adipose tissue may also lead the formation of other diseases rather than metabolic complications of obesity such as exophthalmus, and Crohn’s disease (Klein et al, 2007; Westcott et al, 2005). However, TGs may also be stored in non-adipose tissues such as liver, muscle, pancreas and heart. Excessive deposition of TGs in these tissues during obesity is termed as ectopic fat deposition or steatosis. And excessive accumulation of these lipids within the non-adipose tissues may lead to cell dysfunction or cell death, which is called lipotoxicity (Schaffer, 2003; Unger & Orci, 2001).

Lipid accumulation and the storage of these lipids in adipocytes during obesity induce hyperplasia (increased cell number) and hypertrophy (increased cell size),

which lead the formation of dysfunctional adipocytes (Couillard et al, 2000; Sjostrom & William-Olsson, 1981). Since the subcutaneous adipose tissue storage capacity is limited due to the increase in hypertrophy progresses, excess lipids also accumulate in the visceral adipose tissue stores. This process results in free fatty acid and pro-inflammatory adipokine secretion into the portal vein. These factors contribute to the ectopic lipid accumulation in different tissues (Figure 9) (van Herpen & Schrauwen-Hinderling, 2008). Accumulation of lipids in skeletal muscles results in muscle insulin resistance, and in hepatocytes (hepatic steatosis) hepatic insulin resistance and non-alcoholic steatohepatitis (Ferris & Crowther, 2011; Mendez-Sanchez et al, 2007). Moreover, excess accumulation of lipids results in pancreatic β cells failure and cardiomyopathy in heart muscle cells (Figure 5) (van Herpen & Schrauwen-Hinderling, 2008).

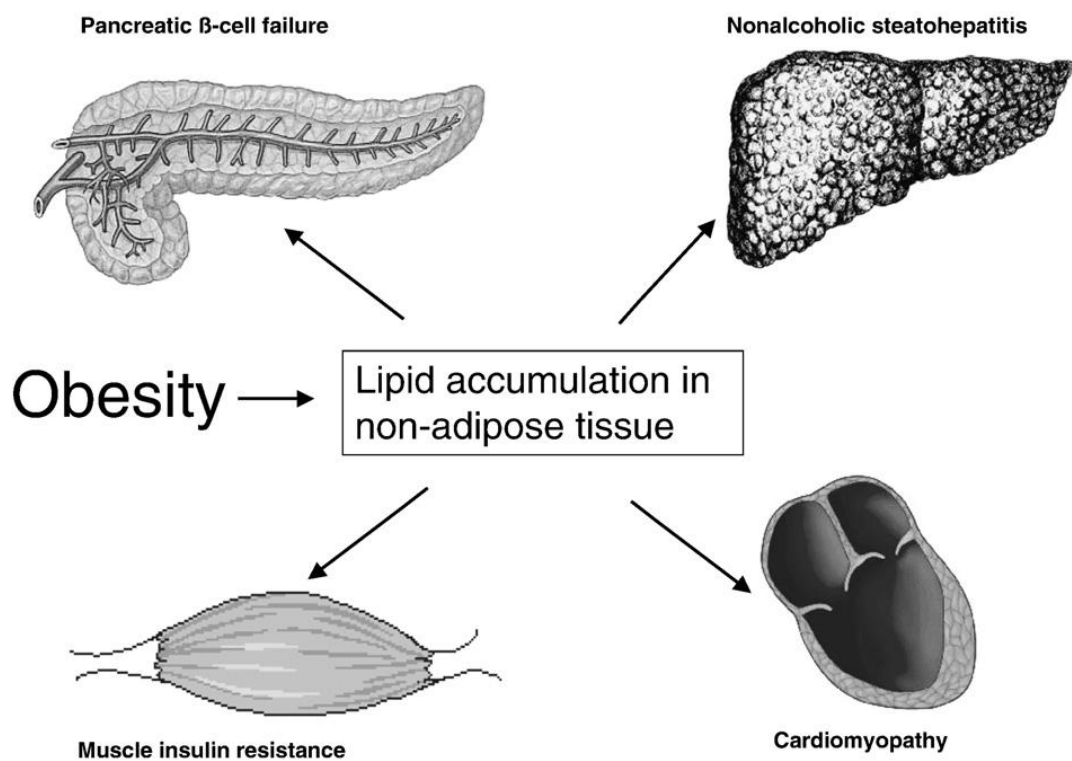


Figure 9. Lipid accumulation in non-adipose tissues and its relation with the metabolic diseases (van Herpen & Schrauwen-Hinderling, 2008)

1.4 Adipocyte Stress in Obesity

Adipose tissue may induce many stress factors in obesity such as oxidative, endoplasmic reticulum (ER) and mitochondrial stresses (Mittra et al, 2008).

1.4.1 Oxidative Stress

Oxidative stress is defined as an accumulation of oxidative products caused by the impaired balance between antioxidant capacity and free radical production. Reactive oxygen species (ROS) includes oxygen molecules with or without unpaired electrons and they are highly reactive within tissues. There should be low concentrations of ROS, free radicals and other nitrogen species for normal cell redox status, intracellular signaling and cell function (Vincent & Taylor, 2006). It has been shown that excess free radicals and high concentrations of ROS damage DNA, proteins, carbohydrate, lipids and constitute alterations in cell function in many pathological conditions (Sies, 1997; Yu, 1994) and that is why oxidative stress has an important role in relation with many diseases (Brownlee, 2001; Vendemiale et al, 1999). In diabetes, oxidative stress causes impairment in glucose uptake in fat and muscle cells (Maddux et al, 2001; Rudich et al, 1998) and also affects pancreatic β cells by decreasing insulin secretion from these cells (Matsuoka et al, 1997). Moreover, oxidative stress was found to be increased in other metabolic diseases such as hypertension and atherosclerosis (Nakazono et al, 1991; Ohara et al, 1993) In obesity, oxidative stress in accumulated fat is an indicator of obesity related metabolic syndrome. It was found in a study that obese mice produce increased level of ROS in lipid accumulated fat tissue but not in muscle and liver (Furukawa et al, 2004). Increase in ROS production in lipid accumulated adipocyte causes elevated oxidative stress and increased oxidative stress in dysfunctional lipid accumulated adipocytes causes dysregulated adipokine production. Furthermore, ROS secretion into peripheral blood from these dysfunctional adipocytes leads to impaired insulin secretion by β cells and induction of insulin resistance in skeletal muscle and adipose tissue. Therefore, oxidative stress in adipose tissue involves in the pathogenesis of several diseases such as atherosclerosis and hypertension and acts as a causative effect of the

transcription, which leads the activation of IRE1 α leads to the activation of c-Jun N-terminal kinase (JNK). JNK activity results in several downstream effects, such as obesity induced inflammation (release of adipokines), insulin resistance and apoptosis leading cell death (Figure 11) (Mittra et al, 2008). Conversely, it may also be possible that obesity induced inflammation can activate UPR and another possible reason may be the oxidative stress as a causative factor of obesity-related ER stress previously shown in the studies that ROS can activate the UPR (Furukawa et al, 2004; Gregor & Hotamisligil, 2007; Holtz et al, 2006)

1.4.3 Mitochondrial Stress

Mitochondria is responsible for the energy transformation but it also has many important metabolic functions such as cellular proliferation and apoptosis, hormone synthesis and regulation of redox state of the cells. Although, mitochondria have an efficient phosphorylation process, some electrons may prematurely reduce oxygen and eventually leads formation of the toxic free radicals. Moreover, in some conditions, uncoupling proteins (UCPs) enable protons to re-enter the mitochondrial matrix, which leads high level production of free radicals by mitochondria (Fernandez-Sanchez et al, 2011). Formation of the free radicals from these processes lead to mitochondrial dysfunction. In obesity, over-production of ROS due to the impairments in electron transport chain in mitochondria and release of inflammatory cytokines, and antioxidant defenses have been reported. Together with these factors, increased FFA and glucose levels causes increment in substrate oxidation and secondary increase in the formation of ROS and eventually mitochondrial stress (Figure 11) (Martinez, 2006; Mittra et al, 2008).

have shown that, females have a greater energy expenditure of than males because they have higher thermogenic activity and a greater oxidative capacity with a more effective antioxidant mechanism (Catala-Niell et al, 2008; Valle et al, 2005).

1.6 BFMI Lines As New Mouse Models For Obesity

Animal models enable scientists to investigate diseases and treatments with eliminations of the variety of factors such as genetics, individual disease characteristics and life style (Nissen-Meyer et al, 2008). Up till now, for the studies on characterication of the metabolic diseases such as obesity and insulin resistance, different kinds of animal models were generated and used. Some of them are; Zucker rats having (fa/fa) mutation that causes abnormalities in leptin receptors leading spontaneous obesity (Phillips et al, 1996) , leptin deficient (Lepob/Lepob) mice (Zhang et al, 1994), C/EBP- α transcription factor knock-out Cebp α mouse models and PPAR γ 2 transcription factor knock-out Pparg mice having abnormalities in adipocyte (Lefterova & Lazar, 2009), Agpat2 knock-out mice (Cortes et al, 2009) and Cav1 knock-out mice (Razani et al, 2001).

The Berlin fat mouse inbred line (BFMI) is a new animal model which is affected by obesity due to hyperphagia and altered lipid metabolism (Meyer et al, 2009; Neuschl et al, 2010; Wagener et al, 2006). BFMI mice do not develop type II diabetes even they were fed with high-fat diet, although they are affected by severe obesity (Hantschel et al, 2011). These lines are genetically complex mice which are not generated by knock-out mutations as a causative effect for the generation of spontaneous obesity phenotype. That is why, according to their polygenic nature underlying obesity phenotypes, the BFMI lines (BFMI852, BFMI856, BFMI860, BFMI861) are excellent models for the study of obesity induced changes in humans (Brockmann et al, 2009; Wagener et al, 2006).

When these lines were compared with each other, BFMI860 line was found to have the highest fat percentage and different than the other lines, it was found to have the highest amount of total WAT. Moreover, BFMI860 line in female mice

represented much more obese phenotype than the other lines. However, according to the differences due to the gender, male mice was found to have higher body weight than female mice. Since BFMI861 line was found to have the smallest reproductive fat depots, these mice line had the least amount of WAT and male mice in this line had lower body weight than female mice. Furthermore, BFMI861 line was found to have the highest blood glucose concentration among the BFMI lines and BFMI856 line had the lowest blood glucose concentration (Wagener et al, 2006). Additionally, in a study BFMI three types of adipose tissues and liver tissue were investigated by hematoxylin and eosin staining method and hypertrophy (enlargement of adipose tissues) and increase in fat accumulation in liver were determined even in mice fed with standart breeding diet compared to control B6 mice line (Figure 12) (Wagener et al, 2010).

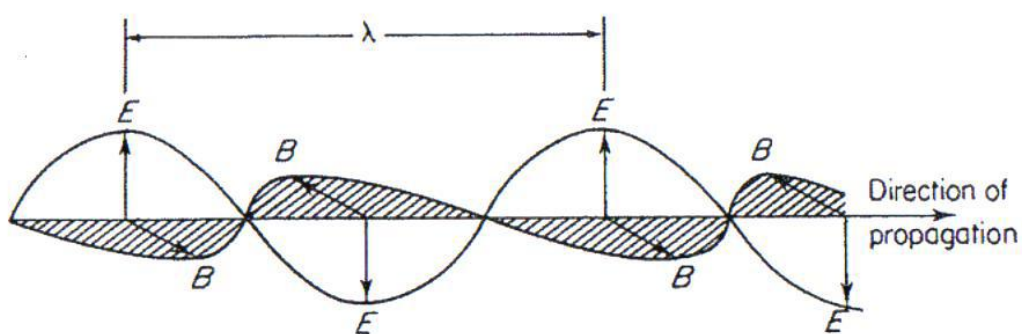


Figure 13. An electromagnetic wave

When an electromagnetic radiation interacts with a matter, the waves can be absorbed, emitted or scattered. And, if the waves are absorbed, molecules within the matter are excited to a higher energy level. The excited molecule may gain a quantum of energy which is equal to the difference between the energy levels of the molecule described by the laws of quantum mechanics. Electronic energy levels achieved from the spacial distributions of the electrons are represented by an energy-level diagram in Figure 14. Electrons in the ground state have the lowest energy level and all other electrons except the ones in the ground state are in excited states (Campbell & Dwek, 1984).

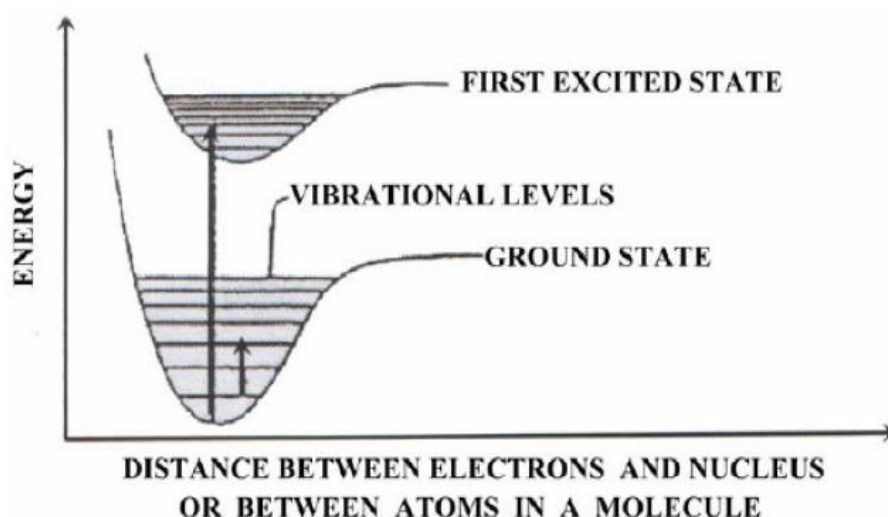


Figure 14. Typical energy-level diagram showing the ground, excited states and vibrational levels. Long arrow represents a possible electron transition between

the ground state and the fourth vibrational level of the first excited state. Short arrow represents a vibrational transition within the ground state (Freifelder, 1982).

“For most purposes, it is convenient to treat a molecule as if it possesses several distinct reservoirs of energy.” The total energy is given by:

$$E_{\text{total}} = E_{\text{transition}} + E_{\text{vibration}} + E_{\text{rotation}} + E_{\text{electronic}} + E_{\text{electron spin orientation}} + E_{\text{nuclear spin orientation}}$$

The energy (E) of the electromagnetic wave is formulized by the following equation as:

$$E = h \cdot \nu$$

where h the is Planck's constant and its value is equal to $6.63 \cdot 10^{-34}$ J s and ν is the frequency of the electromagnetic radiation applied.

$$\lambda = c / \nu$$

where λ is the wavelength of the radiation, c is the speed of wave in vacuum and its value is equal to 3.0×10^8 ms⁻¹. These two equations mentioned above are used for the identification of the wavenumber as a spectral unit which is denoted by ν with a unit cm⁻¹.

$$\nu = \text{wavenumber} = (1 / \lambda)$$

$$E = h \cdot \nu = h \cdot c / \lambda = h \cdot c \cdot \nu$$

According to these formulas given above, wavenumber and frequency values are proportional to energy directly. The plot representing the energy which is absorbed, scattered or emitted as a function of λ , ν or ν is termed “spectrum”.

All of the spectroscopic techniques are based on the interaction of electromagnetic radiation and matter. Monitoring of the absorption and emission of the

1.7.1.1 Fourier Transform Infrared (FTIR) Spectroscopy

Fourier transform infrared (FTIR) spectroscopy has found increasing favor in laboratories recently. This method is based on the ideas of the interference of radiation between two beams to yield an interferogram. An interferogram is a signal produced as a function of the change of pathlength between the two beams. The two domains of distance and frequency are interconvertible by the mathematical method Fourier transformation. The basic optical component of FTIR instrument is the Michelson interferometer. The basic components of an FTIR spectrometer are shown schematically in Figure 18.

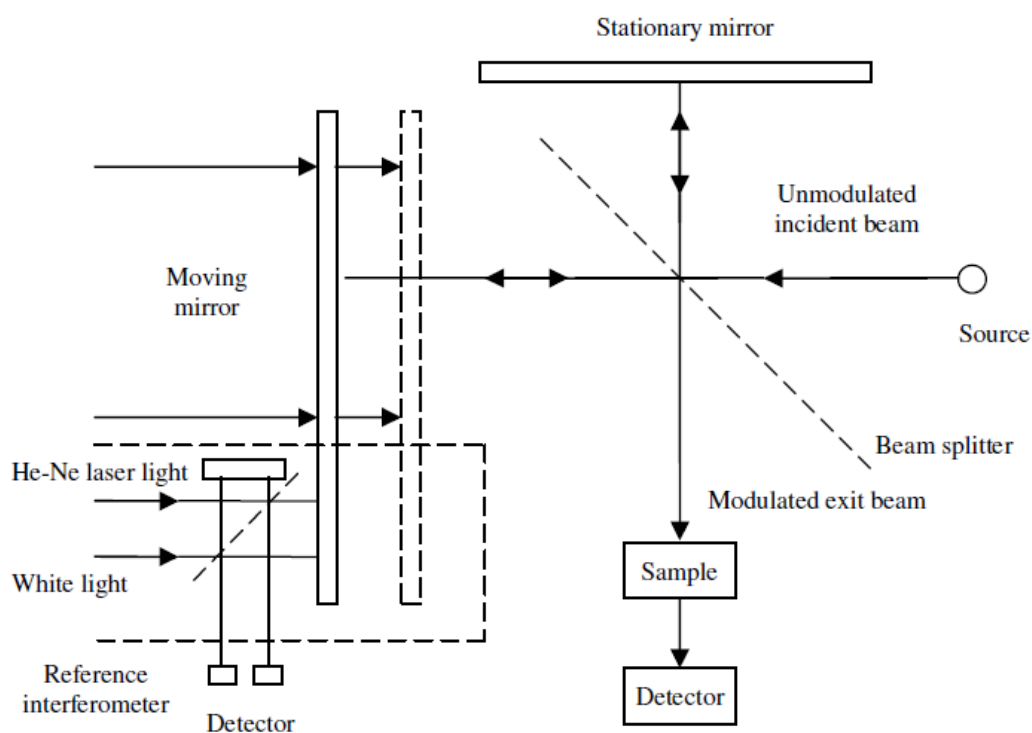


Figure 18. Components of FTIR Spectroscopy (Stuart, 1997)

The radiation emerging from the source is passed through an interferometer to the sample before reaching a detector. Upon amplification of the signal, in which high-frequency contributions have been eliminated by a filter, the data are converted to a digital form by an analog-to-digital converter and then transferred to the computer for Fourier transformation to be carried out. Michelson

interferometer consists of two perpendicularly plane mirrors, one of which can travel in a direction perpendicular to the plane. A semi-reflecting film, the beamsplitter, bisects the planes of these two mirrors. The beamsplitter material has to be chosen according to the region to be examined. Materials such as germanium or iron oxide are coated on to an infrared-transparent substrate such as potassium bromide or caesium iodide to produce beamsplitters for the mid-or near-infrared regions. Thin organic films, such as poly(ethylene terephthalate), are used in the far-infrared region. If a collimated beam of monochromatic radiation of wavelength λ is passed into an ideal beamsplitter, fifty percent of the incident radiation will be transmitted to the other mirror. The two beams are reflected from these mirrors, then returning to the beamsplitter where they recombine and interfere. Fifty percent of the beam reflected from the fixed mirror is transmitted through the beamsplitter and fifty percent is reflected back in the direction of the source. The beam which emerges from the interferometer at 90° to the input beam is called transmitted beam and this is the beam detected in FTIR spectrometry.

The mathematics of the conversion of an interference pattern into a spectrum is done by using the Fourier transformation method.

The essential equations which relate the intensity falling on the detector, $I(\delta)$, to the spectral power density at a particular wavenumber, are the cosine Fourier transform pairs. These pairs are interconvertible by Fourier transformation method. The essential experiment for obtaining an FTIR spectrum is to produce an interferogram with and without a sample in the beam and then transform these interferograms into spectra of the source with sample absorptions and the source without sample absorptions. The ratio of the former and the latter corresponds to a double-beam dispersive spectrum. Finally a plot of absorbance against wavenumber (cm^{-1}) is achieved by the deconvolution of the computer (Stuart, 1997).

1.7.1.1.1 Attenuated Total Reflectance (ATR) – FTIR Spectroscopy

Attenuated Total Reflectance (ATR) spectroscopy utilises the phenomenon of total internal reflection. A beam of radiation entering a crystal will undergo total internal reflection when the angle of incidence at the interface between the sample

and the crystal is greater than the critical angle. The critical angle is a function of the refractive indices of the two surfaces. The beam penetrates a fraction of a wavelength beyond the reflecting surface and when a material which selectively absorbs radiation is in close contact with the reflecting surface and when a material which selectively absorbs radiation is in close contact with the reflecting surface, the beam loses energy at the wavelength where the material absorbs. The resultant attenuated radiation is measured and plotted as a function of the wavelength by the spectrometer and gives rise to the absorption spectral characteristics of the sample (Figure 19) (Stuart, 1997).

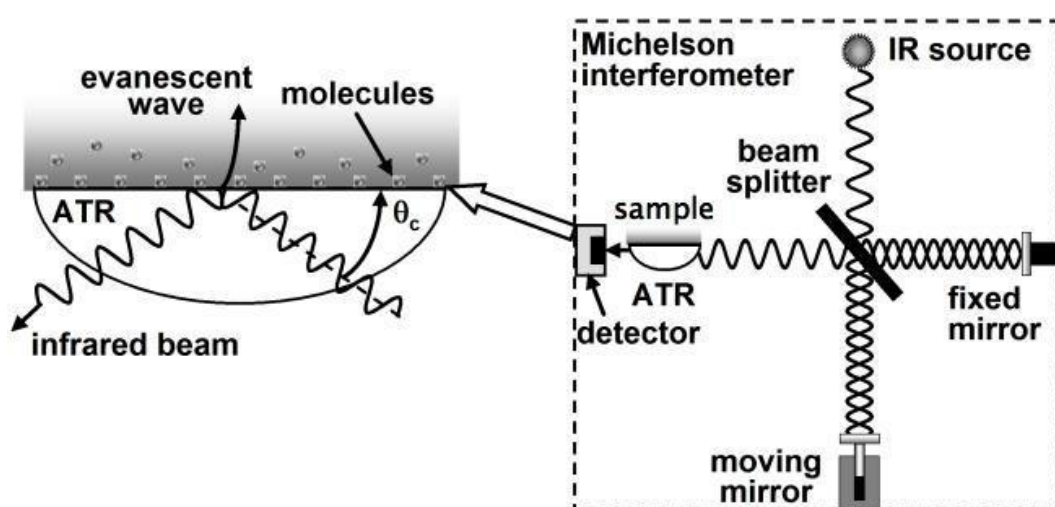


Figure 19. A multiple reflection ATR system (Wang et al, 2007).

The crystals used in ATR cells are made from materials which have low solubility in water and are very high refractive index. The physical properties of ATR crystals are given in Table 1. Among these ATR crystals, diamond and zinc selenide are the most convenient ones for the usage in the mid-IR region since these crystals are relatively cheaper than the other materials and resistant to many chemicals such as acids and alkalis. According to the water resistant property of these crystals which can be cleaned easily, enables to study and analyze wet or aqueous samples.

Table 1. Physical properties of commonly used ATR crystal materials

Material	Wavelength (cm ⁻¹)	Refractive Index	Observations
CaF ₂	1150 – 50.000	1.4	Very hard, for high pressure application
ZnSe	500 – 20.000	2.4	Hard, brittle, insoluble in water
ZnS	830 – 17.000	2.2	Insensitive to thermal and mechanical shocks
NaCl	625 – 40.000	1.5	Soft, cheap, not water resistant
KRS-5	250 – 17.000	2.4	Soft, slightly water soluble
Ge	550 – 5.000	4.0	Hard, brittle, chem. stable

1.7.1.1.2 The Advantages of FTIR Spectroscopy

The advantages of FTIR spectroscopy are;

- FTIR spectroscopy is a rapid, sensitive and non-destructive technique which can be used in order to obtain structural, functional and compositional information about the system (Aksoy et al, 2012; Cakmak et al, 2003; Haris & Severcan, 1999; Melin et al, 2000),
- FTIR spectroscopy increases signal to noise ratio by signal averaging the numbers of scans per sample (Stuart, 1997),
- Samples can be prepared very easily in a short time either in gaseous, liquid, or solid states,
- Very small amounts of the samples is sufficient for the analysis (Mendelsohn & Mantsch, 1986),
- Any kind of material such as solutions, suspensions, inhomogeneous solids viscous liquids or powders can be used in FTIR spectroscopy and also analysis can be applied to these variety of systems (Colthup et al, 1975) and also kinetic and time-resolved studies can be done with this technique (Haris & Severcan, 1999; Mantsch, 1984; Mendelsohn & Mantsch, 1986),
- FTIR spectroscopy can be used for biological samples obtained from several environments,
- Spectral data can be obtained rapidly and qualitative interpretation can be done,

- FTIR spectroscopy is a cheaper technique in comparison to other spectroscopic techniques especially NMR spectroscopy, X-ray crystallography, ESR and CD spectroscopy (Diem, 1993),
- Measurements can be done without any need of external calibration (Ci et al, 1999; Rigas et al, 1990),
- Any changes in the functional groups of the macromolecules in the system can be detected simultaneously within the same spectrum (Garip et al, 2007; Kneipp et al, 2000),
- And, the software used for FTIR spectroscopy allows the storage of the achieved data permanently, which enables user to make manipulations on the data together with quantitative calculations (Ci et al, 1999; Manoharan et al, 1996; Rigas et al, 1990; Yano et al, 1996).

1.8 Aim of the Study

Obesity arises from the imbalance between energy intake and energy consumed with the effect of genetic susceptibility and environmental factors, which further leads to secondary metabolic disorders such as insulin resistance, hypertension, hyperlipidemia, cardiovascular diseases and many other diseases. It is characterized by adipocyte hypertrophy, the expansion of visceral adipose tissues (VAT) and subcutaneous adipose tissue (SAT) mass in the body, and alterations in cellular biology, such as disturbed glucose and lipid metabolism. Despite the fact that information on this subject is still lacking, these alterations are expected to be based on variations in macromolecular content, structure and function.

The Berlin fat mouse inbred line (BFMI) is an important new model for obesity which has a complex genetic background and generates spontaneous obesity, even on standard breeding diet

In the literature, there are many studies based on the complications of obesity on various tissues. However, contradictory results were found in these studies, which remained insufficient to elicit the effect of obesity on different adipose tissues and gender effect in obesity. Therefore, this current study aims to investigate the effects of obesity on macromolecular alterations in order to characterize BFMI

mice models for obesity research, which will contribute to understanding of; spontaneous obesity without induction of a high fat diet, macromolecular alterations in different adipose tissues and gender effect in obesity. For this purpose, Attenuated Total Reflectance-Fourier Transform Infrared (ATR-FTIR) spectroscopy was used to characterize content and structure of macromolecules in male and female control (DBA/2J) and BFMI lines; namely BFMI856, BFMI860 and BFMI861, in two different adipose tissues; IF which is SAT, GF which is VAT.

CHAPTER 2

MATERIALS AND METHODS

2.1 Animal Models

All experimental protocols regarding treatment of animals were approved by the German Animal Welfare Authorities (approval no. G0171/10). Founder animals of the Berlin Fat Mouse lines were originally purchased from several pet shops in Berlin, Germany.

The selection process composed of several phases. Firstly, animals were selected according to their low protein content over 23 generations when they were 60 days-old . In the second phase, animal selection was done according to their low body weight and high fat content at the age of 42 days. At the final phase, 9 week-old mice which had high fatness phenotype were selected. Thus, the Berlin Fat Mouse line was created. By using this new line, 20 families were produced per generation with the mating ratio of one male to three females. This period continued for 10 generations. After that, 40 families per generation were achieved with the mating ratio of one male to two females. In each generation, 40 breeding pairs of BFMI line were kept between 24th to 50th generation. After 50th generation, 30 breeding pairs were selected and maintained for each generation. By selection during 58 generations, BFMI line's inbred derivatives were generated and these lines were created by brother and sister mated randomly chosen sib-pairs of the selected lines (Wagener et al, 2006). For characterization, male and female BFMI852, BFMI856, BFMI860 and BFMI861 inbred lines have been used after six generations of inbreeding.

As controls female and male DBA/J2 mouse line was used, which is an unselected commercially available inbred line that is often used as standard mice showing a wildtype-like phenotype. Moreover, DBA/2J showed the highest weight gain in response to a high fat diet among 43 inbred strains (Hageman et al, 2010; Svenson et al, 2007). Therefore, DBA/2J is one of the most suitable inbred lines for the usage as control in studies with BFMI mice lines (Svenson et al., 2007; Hageman et al., 2010).

2.2 Feeding and Husbandry Conditions

Mice were maintained under conventional conditions and controlled lighting with a 12:12h light/dark cycle at a temperature of $22\pm 2^{\circ}\text{C}$ and a relative humidity of 65%. They were reared in groups of two to three mice in macrolon cages with a 350 cm^2 floor space (E. Becker & Co (Ebeco) GmbH, Castrop-Rauxel, Germany) and with bedding type S 80/150, dust-free (Rettenmeier Holding AG, Wilburgstetten, Germany). All mice had *ad libitum* access to food and water. After weaning at the age of 3 weeks, animals were fed with a rodent standard breeding diet (SBD). The SBD (V1534-000, ssniff R/M-H, Ssniff Spezialdiäten GmbH, Soest/Germany) contains 12.8 MJ/kg of metabolisable energy and biggest amount from carbohydrates with 58% (33% from proteins and 9% from fat). The SBD derived its fat from soy oil (Hantschel et al., 2011).

2.3 Sample Collection

Inguinal fat and gonadal fat adipose tissues of the 10 week-old mice were dissected and directly transferred to a plastic tube, snap-frozen in liquid nitrogen and then stored at -80 degrees until further examination.

2.4 Experimental Groups

Female and male mice were separated into 5 groups which consisted of control group, DBA/J2 mice (n=6) and four obese groups, BFMI852 (n=6), BFMI856 (n=6), BFMI860 (n=6), and BFMI861 (n=6) mice. For each tissue, female and

male mice groups were both investigated. 30 female and 30 male mice per each adipose tissue (60 samples for IF and 60 samples for GF), totally 120 samples were analyzed.

2.5 FTIR spectroscopic sample preparation, data acquisition and analysis

ATR-FTIR spectroscopy technique was used in this study in order to achieve information about the relative amounts of macromolecules (lipid, protein, carbohydrates, and nucleic acids and collagen) and dynamics and structural properties of these macromolecules within the IF and GF adipose tissues were detected. Using ATR-FTIR spectroscopy technique, before taking the samples from atmospheric CO₂ and H₂O absorption bands in the spectrum to eliminate the ambient air sample was taken and the spectrum obtained through a computer program mathematically subtracted. This process was repeated for all spectra. Thus, the effect of atmospheric water vapor samples were eliminated on the spectrum bands.

ATR-FTIR spectra of adipose tissues were obtained using a Universal ATR accessory (Perkin-Elmer Inc., Norwalk, CT, USA) that is attached to a Perkin-Elmer Spectrum 100 FTIR spectrometer (Perkin-Elmer Inc., Boston, MA, USA) equipped with a MIR TGS detector. Collection of spectra and all data manipulations were carried out using Spectrum One software (Perkin-Elmer). The interfering spectrum of air was recorded together as background and subtracted automatically. A small amount of tissue samples were cut and placed directly on the Diamond/ZnSe (Di/ZnSe) crystal plate of the Universal ATR unit of the FTIR spectrometer and scanned in 4000-650 cm⁻¹ region for 50 scans with a resolution of 4 cm⁻¹ at room temperature. Three different aliquots of each sample were scanned, all of which gave identical spectra. While carrying out the detailed data analysis, the non-normalized average spectra of these replicates were considered. In order to remove the noise, the spectra were first smoothed with the thirteen point smooth factor by using Savitzky-Golay smooth function. Then the determination of the mean values for the peak positions and band area values were performed using Spectrum One software. The band positions were measured

using the wavenumber corresponding to the center of weight of each band. The bandwidth values of specific bands were calculated as the width at 0.75x height of the signal in terms of cm^{-1} . After detailed analysis, the spectra were baseline corrected and normalized with respect to specific bands for visual demonstration.

2.6 Statistics

The results were expressed as 'mean \pm standard error of mean (SE)'. The differences in variance were analyzed statistically using one-way ANOVA test. Tukey's test was used as a post-hoc test and the results of each group were compared with each other. The p values less than or equal to 0.05 were considered as statistically significant (such as $*p \leq 0.05$; $**p \leq 0.01$; $***p \leq 0.001$). The degree of significance was denoted by * for the comparison of control DBA/J2 line with BFMI lines, by # for the comparison of BFMI852 with other BFMI lines, by ‡ for the comparison of BFMI856 with other BFMI lines and by † for the comparison of BFMI860 with other BFMI lines.

CHAPTER 3

RESULTS

This study was carried out to investigate obesity induced changes on different adipose tissues inguinal fat (IF) and gonadal fat (GF) of the BFMI lines, BFMI852, BFMI856, BFMI860, BFMI861 and characterize these lines according to the macromolecular alterations within these tissues by using ATR-FTIR spectroscopy technique.

3.1 General FTIR Spectrum and Band Assignment of the Adipose Tissues

In this current study, 5 (five) experimental groups; Control DBA/J2 (n=6), BFMI852 (n=6), BFMI856 (n=6), BFMI860 (n=6), BFMI861 (n=6) were used. Totally 120 samples including 30 samples for female GF, 30 samples for female IF, 30 samples for male GF and 30 samples for male IF, were examined by ATR-FTIR spectroscopy. Figure 20 shows the representative infrared spectra of control groups of IF and GF adipose tissues in the 4000-950 cm^{-1} region. The main bands are labelled in the figures and detailed band assignments are given in Table 2 (Bozkurt et al, 2010; Cakmak et al, 2006; Cakmak et al, 2011; Jackson et al, 1998; Lyman & Murray-Wijelath, 1999; Melin et al, 2000; Movasaghi et al, 2008; Ozek et al, 2010; Rigas et al, 1990; Takahashi et al, 1991; Toyran et al, 2006; Wong et al, 1991). Figures 20-25 show the average spectrum of GF and IF adipose tissue of control DBA/J2 and obese BFMI860 line in the 4000-950 cm^{-1} , 3050-2800 cm^{-1} and 1800-950 cm^{-1} regions, respectively. All average spectra were baseline corrected and normalized to amid A band and spectra were presented in the figures only for visual demonstration for the the band assignment in control groups and discrimination of the obese and control spectra.

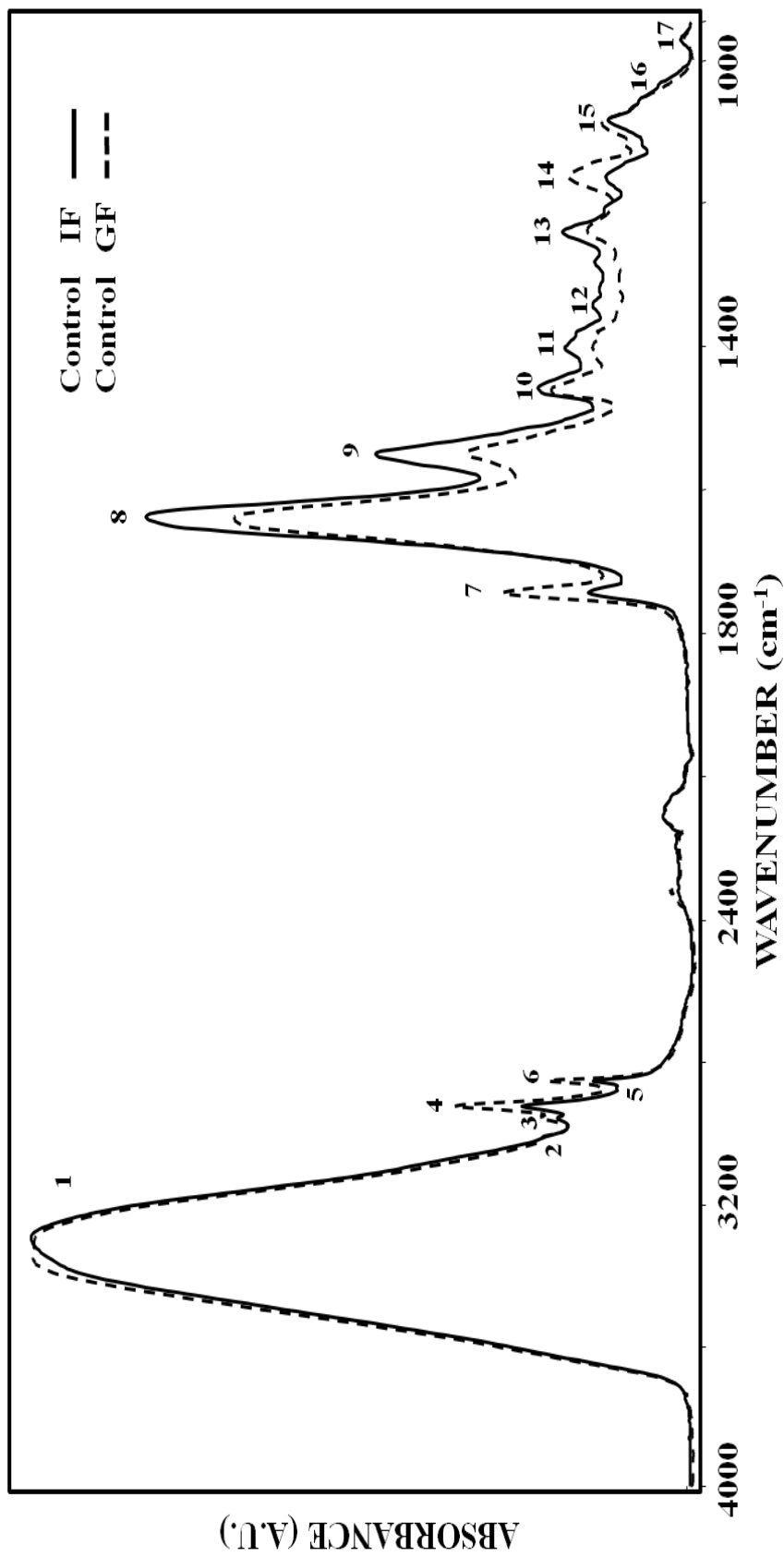


Figure 20. The representative infrared spectra of control groups of IF and GF adipose tissues in the 4000-950 cm^{-1} region. The spectra were normalized with respect to the amide A band located at 3307 cm^{-1}

Table 2. General band assignment of FTIR spectrum of adipose tissues

Band No	Wavenumber (cm⁻¹)	Definition of the spectral assignment
1	3307	Mainly N–H stretching (amide A) of amide groups of proteins, with the little contribution from O–H stretching of polysaccharides and intermolecular H bonding
2	3009	Olefinic=CH stretching vibration: unsaturated lipids, cholesterol esters
3	2957	CH ₃ anti-symmetric stretching: lipids, protein side chains, with some contribution from carbohydrates and nucleic acids
4	2924	CH ₂ anti-symmetric stretching: mainly lipids, with some contribution from proteins, carbohydrates, nucleic acids
5	2873	CH ₃ symmetric stretching: protein side chains, lipids, with some contribution from carbohydrates and nucleic acids
6	2854	CH ₂ symmetric stretching: mainly lipids, with some contribution from proteins, carbohydrates, nucleic acids
7	1743	Ester C=O stretch: triglycerides
8	1642	Amide I (protein C=O stretching)
9	1551	Amide II (protein N–H bend, C–N stretch)
10	1456	CH ₂ bending: lipids
11	1400	COO ⁻ symmetric stretching: fatty acids
12	1343	CH ₂ side chain vibrations of collagen Sulfate stretch from proteoglycans, collagen
13	1237	amide III vibration with significant mixing with CH ₂ wagging vibration from the glycine backbone and proline sidechain
14	1160	CO–O–C asymmetric stretching: phospholipids, triglycerides and cholesterol esters
15	1083	PO ₂ ⁻ symmetric stretching: nucleic acids and phospholipids. C–O stretch: glycogen, polysaccharides, glycolipids
16	1052	C–O stretching: polysaccharides (glycogen)
17	971	C–N+–C stretch: nucleic acids, ribose-phosphate main chain vibrations of RNA

3.2 Comparisons of the Band Wavenumber and Band Area Values of Control and Obese Mice

Numerical comparisons of the wavenumber and band area values of these selected bands for adipose tissues were given in Table 3-10.

3.2.1 C-H Region (3025-2800 cm⁻¹)

Bands located at the 3025-2800 cm⁻¹ region arise from the C-H stretching vibrations of the olefinic HC=CH groups, the CH₃ anti-symmetric stretching vibrations, the CH₂ anti-symmetric stretching vibrations, the CH₃ symmetric stretching vibrations and the CH₂ symmetric stretching vibrations (Bozkurt et al, 2010; Cakmak et al, 2006; Ozek et al, 2010; Severcan et al, 2005; Severcan et al, 2000a). Alterations in the CH₂ anti-symmetric, the CH₂ symmetric and CH₃ anti-symmetric stretching vibration band wavenumber and band area values in this region represent changes in lipid structure and content. Alterations in the CH₃ symmetric stretching vibration band intensity and band area values give information about the changes in protein structure and protein content (Bozkurt et al, 2010; Cakmak et al, 2011; Mantsch, 1984).

Band located around 3010 cm⁻¹ arises from the C-H bond stretching vibrations of HC=CH groups in unsaturated lipids. Band area and wavenumber of the olefinic band gives information about unsaturation of hydrocarbon chains (Bozkurt et al, 2010; Cakmak et al, 2003; Cakmak et al, 2011; Melin et al, 2000; Ozek et al, 2010; Severcan et al, 2005; Takahashi et al, 1991). According to the area values of this band, there was an increase in unsaturated lipid content in GF of BFMI860, BFMI861 female mice. In female IF, BFMI852, BFMI856, BFMI860 and BFMI861 had significantly lower concentration of unsaturated lipid with respect to the control DBA/2J mice. In male IF, there was a significant decrease in unsaturated fat content in BFMI852, BFMI860 and BFMI861 in comparison to the control group. Especially, in male IF tissues, BFMI860 line represented the lowest band area value (Table 7-10). The decrease in the olefinic band area was thought to be originated from the increase in lipid peroxidation due to the

decrease in the unsaturated fatty acid content within the tissues (Bozkurt et al, 2010; Bruch & Thayer, 1983; Cakmak et al, 2011; Curtis et al, 1984).

Band wavenumber shift to the lower values in the olefinic band is an indicator of an increase in the order of unsaturated fatty acid structures located in the membrane (Bizeau et al, 2000; Severcan & Haris, 2003). As it is also seen in Table 3-6, there was no significant change in the wavenumber values of olefinic band in BFMI lines in both sexes and tissues in comparison to control. However, significant alterations were observed in the CH₃ ve CH₂ anti-symmetric stretching band wavenumber values. The CH₃ anti-symmetric stretching band gives structural and functional information about methyl groups in lipid acyl chains and moreover, from the CH₂ anti-symmetric and symmetric stretching bands, structural and functional information about lipid acyl chains can be achieved (Takahashi et al, 1991). In the CH₃ anti-symmetric stretching band wavenumber value, there was a significant decrease in BFMI856 line in both male and female GF. In female IF of BFMI852 and BFMI856 lines, significant decrease was observed in comparison to the control group as an indicator of an increase in lipid order. According to the area values of the CH₃ anti-symmetric stretching band, there was an increase in BFMI856 line in female and male GF and also in male IF adipose tissues compared to the control, which is an indicator of higher amount of methyl groups in the lipids in BFMI856 line. In addition, BFMI861 line represented the lowest band area value in the same adipose tissues among all lines including the control as an indicator of lower amount of methyl groups in the lipids belonging to these adipose tissues.

Furthermore, in the CH₂ antisymmetric stretching band, value of wavenumber decreased significantly in BFMI852, BFMI856 and BFMI861 lines in male GF adipose tissue. The CH₂ anti-symmetric and symmetric band positions give information about lipid acyl chain flexibility and so, information about conformational disorders of the lipids can be obtained from these bands (Bozkurt et al, 2010; Casal & Mantsch, 1984; Umemura et al, 1980).

Moreover, the CH₃ symmetric stretching band is comprised of mainly proteins with a contribution of lipids (Bozkurt et al, 2010; Cakmak et al, 2011). There was no significant change in wavenumber value of this band in both tissues and sexes. However, BFMI856 line had the highest band area value among all BFMI lines and control line in GF tissue of male mice.

3.2.2 Fingerprint Region (1800-950 cm⁻¹)

Band located around 1743 cm⁻¹ in fingerprint region of the spectra of BFMI lines and control group GF and IF adipose tissues arise from ester C=O stretching of triglycerides (Nara et al, 2002). There were not any significant changes in band area and wavenumber values in all BFMI lines in female IF and GF adipose tissues. However, BFMI860 in male IF and BFMI856, BFMI860 lines in male GF represented significant increase in band area value as an indicator of increment in triglyceride content compared to control DBA/J2 group. In addition, BFMI856 and BFMI861 lines in GF adipose tissues of male mice showed significantly lower band wavenumber values in comparison to the control, which indicated that structural changes might occur in triglycerides due to obesity.

The amide I band which is located at 1642 cm⁻¹ wavenumber in fingerprint region, originates from proteins consist of C=O stretching vibrations at the rate of 80%, C-N stretching vibrations at the rate of 10% and N-H bending vibrations at the rate of 10%, the amide II band which is located at 1551 cm⁻¹ wavenumber, also derives from proteins with the rate of 60% N-H bending and 40% C-N stretching vibrations (Bozkurt et al, 2010; Cakmak et al, 2006; Dogan et al, 2007; Haris & Severcan, 1999; Ozek et al, 2010; Stuart, 1997; Takahashi et al, 1991; Wong et al, 1991). In Tables 3-10, area and wavenumber values of the amide I and amide II bands are given. Changes in wavenumber values of the amide I and amide II bands give information about alterations in protein secondary structures (Garip et al, 2010; Haris & Severcan, 1999; Jackson et al, 1998; Lyman & Murray-Wijelath, 1999). There was no change observed in the amide I wavenumber value in both sexes and adipose tissues compared to the control. However, in female GF adipose tissue, BFMI856 line had a higher wavenumber

value at the amide II band in comparison to the control. This increase indicated that there might be alterations in the protein secondary structure in GF adipose tissue of BFMI856 line. Moreover, according to the area values of the amide I and amide II bands, there was a significant decrease in all BFMI lines in female IF with respect to the control group. This decrease indicated that in female IF, all BFMI lines had lower protein content significantly compared to the control (Bozkurt et al, 2010; Ozek et al, 2010).

The CH₂ bending band located around 1456 cm⁻¹, mostly consists of lipids with a little contribution of proteins and gives information about lipid structure and lipid content (Simsek Ozek et al, 2010). Wavenumber value of the CH₂ bending band did not change in BFMI lines with respect to the control group. However, when band area values were taken into consideration, there was a decrease in all BFMI lines, significantly in BFMI852 in female GF. BFMI852 line showed the lowest band area value in both female and male GF tissues. In males, BFMI860 line represented the highest band area value in both tissues.

The COO⁻ symmetric stretching band located at 1400 cm⁻¹, arises from fatty acids and aminoacids (Cakmak et al, 2006; Movasaghi et al, 2008). According to the wavenumber value of this band, BFMI856 line represented a significant decrease in male GF adipose tissue in comparison to the control. This alteration was the indicator of structural changes in fatty acids and aminoacids in BFMI856 line. There were alterations also in the band area values. In female IF, significant decrease was observed in BFMI852, BFMI860, BFMI861 lines with respect to control. Especially, BFMI861 line showed the lowest band area value among all BFMI lines and compared to the control mice in both sexes and adipose tissues, which indicated a significant decrease in aminoacid and fatty acid content of the adipose tissues of BFMI861 obese line.

The CH₂ side chain vibration band which is located around 1343-1345 cm⁻¹ arises from collagens (Camacho et al, 2001; Gough et al, 2003; West et al, 2004). Wavenumber value of this band can be used for observing the order of triple helix structure of collagens (Bozkurt et al, 2010; West et al, 2004). However, there was

no significant change in the wavenumber value of this band in all BFMI lines in both IF and GF compared to control. Also, area value of this band gives information about the concentration of collagens within the tissues. In male GF, BFMI860 line and in female IF, BFMI852 and BFMI861 lines represented a decrease in area value of this band with respect to control. This decrease in the band area value indicated lower content of collagen within the tissues and mice lines mentioned above.

Bands located at 1300-1000 cm^{-1} in the spectra of IF and GF adipose tissues mostly consist of absorbance of P=O bonds of phosphate (PO_2^-) groups within nucleic acids and phospholipids (Bozkurt et al, 2010; Cakmak et al, 2006; Cakmak et al, 2011; Diem et al, 1999; Dovbeshko et al, 2000). These bands give important information about head groups of membrane phospholipids (Bozkurt et al, 2010; Cakmak et al, 2011; Mendelsohn & Mantsch, 1986). In PO_2^- symmetric stretching band which was located around 1237 cm^{-1} , there was no significant difference in wavelength values in all lines in both adipose tissues compared to the control group. However, in the area value of this band, there were significant alterations as seen in Tables 7-10. In female IF, there was a significant decrease in all BFMI lines except BFMI860 line and in male GF and IF, BFMI861 line showed the lowest band area value among all lines including the control line. Therefore, it was interpreted as reduction of nucleic acids and/or membrane phospholipids in male BFMI861 line in both GF and IF adipose tissues. Although, there was not a significant alteration in female GF adipose tissues, all BFMI lines were seem to have lower nucleic acid and/or membrane phospholipid content compared to control (Severcan et al, 2003).

Band located at 1080 cm^{-1} gives information about the strength of hydrogen bonding in the nucleic acid backbone and phospholipids in membrane structures (Rigas et al, 1990). Any changes in the wavenumber of this band relate to the phosphate groups in the lipid bilayer polar region and in DNA and RNA conformation (Dovbeshko et al, 2000). However, no significant changes were observed in both band wavenumber and area values in both female and male adipose tissues.

Band located at 1050 cm^{-1} arises from the C–O stretching vibrations of polysaccharides especially glycogen within the tissues (Ozek et al, 2010). There was no significant decrease in the wavenumber value of this band in both female and male, IF and GF adipose tissues compared to the control group. However, in band area values, all lines represented a decrease in female GF and IF adipose tissues. In addition to this, BFMI860 and BFMI861 lines had significantly lower band area values in both IF and GF adipose tissue of male mice. Importantly, BFMI861 line seemed to have the lowest value of band area. The decrease in the area value of this band indicated the decrease in glycogen content of the tissues (Ozek et al, 2010; Toyran et al, 2006).

The C-N+-C stretching vibration band located at $970\text{-}971\text{ cm}^{-1}$ arises from nucleic acids especially ribose-phosphate main chain vibrations (Banyay et al, 2003; Chiriboga et al, 2000). There was not any significant change in the wavenumber value of this band in both sexes and tissues. In band area values, there was a decrease in all lines in female IF and in BFMI860 and BFMI861 lines in male IF compared to the control. BFMI861 had the lowest band area value in IF adipose tissues of the female and male mice. The decrease in band area values represented the lower RNA content in the lines and tissues indicated above.

Table 3. Detailed numerical summary of the differences in the wavenumber value of the bands observed in female control (DBA/2J) and obese (BFMI lines) mice GF adipose tissues.

Band No	Control	BFMI852	BFMI856	BFMI860	BFMI861
2	3009.11 ± 0.14	3008.73 ± 0.22	3008.96 ± 0.14	3009.22 ± 0.17	3009.10 ± 0.09
3	2957.75 ± 0.04	2957.59 ± 0.04	2957.36 ± 0.06 **↓	2957.76 ± 0.10 ‡‡↑	2957.67 ± 0.09 ‡↑
4	2923.66 ± 0.23	2923.62 ± 0.22	2923.18 ± 0.22	2923.82 ± 0.16	2923.78 ± 0.21
5	2873.16 ± 0.03	2873.22 ± 0.03	2873.13 ± 0.03	2873.23 ± 0.03	2873.20 ± 0.03
6	2853.72 ± 0.07	2853.71 ± 0.07	2853.53 ± 0.07	2853.77 ± 0.05	2853.68 ± 0.08
7	1743.08 ± 0.08	1742.93 ± 0.10	1742.84 ± 0.10	1742.87 ± 0.22	1742.95 ± 0.13
8	1642.10 ± 0.31	1641.72 ± 0.24	1642.07 ± 0.66	1641.93 ± 0.43	1641.71 ± 0.47
9	1549.30 ± 0.61	1550.78 ± 0.22	1551.95 ± 0.60*↑	1550.59 ± 0.35	1551.21 ± 0.90
10	1457.42 ± 0.82	1456.37 ± 0.07	1456.37 ± 0.08	1456.30 ± 0.19	1457.01 ± 0.60
11	1400.24 ± 0.04	1400.84 ± 0.29	1401.49 ± 0.43	1400.46 ± 0.44	1400.54 ± 0.14
12	1345.46 ± 0.20	1345.78 ± 0.16	1345.13 ± 0.33	1344.97 ± 0.41	1345.96 ± 0.08
13	1235.72 ± 0.14	1236.23 ± 0.33	1236.49 ± 0.34	1236.29 ± 0.68	1236.24 ± 0.33
14	1159.65 ± 0.37	1158.55 ± 0.27	1158.58 ± 0.17	1159.38 ± 0.80	1159.63 ± 0.35
15	1091.56 ± 0.72	1092.84 ± 0.72	1092.94 ± 0.83	1091.86 ± 0.63	1092.31 ± 0.49
16	1052.40 ± 0.97	1053.57 ± 0.88	1054.26 ± 0.23	1053.54 ± 0.23	1053.06 ± 0.79
17	970.16 ± 0.78	970.64 ± 0.45	969.52 ± 1.06	970.37 ± 0.88	970.64 ± 0.70

The values are the mean ± standard error of the mean for each group. Comparison was performed by one-way ANOVA and Tukey's test was used as a post test. The degree of significance was denoted with * for the comparison of control DBA/12 strain with other BFM lines, with ‡ for the comparison of BFM852 with other BFM lines, with ‡ for the comparison for BFM856 and with † for the comparison of BFM860 with other BFM lines. *P* values less than or equal to 0.05 were considered as statistically significant; * $p \leq 0.05$; ** $p \leq 0.01$; *** $p \leq 0.001$.

Table 4. Detailed numerical summary of the differences in the wavenumber value of the bands observed in male control (DBA/2J) and obese (BFMI lines) mice GF adipose tissues.

Band No	Control	BFMI852	BFMI856	BFMI860	BFMI861
2	3008.90 ± 0.16	3009.22 ± 0.08	3009.01 ± 0.09	3009.13 ± 0.13	3009.01 ± 0.16
3	2957.77 ± 0.08	2957.57 ± 0.06	2957.27 ± 0.04 ***;##↓	2957.66 ± 0.04 †††↑	2957.63 ± 0.04 †††↑
4	2923.98 ± 0.36	2923.18 ± 0.14 *↓	2922.95 ± 0.19 **↓	2923.33 ± 0.12	2923.14 ± 0.06*↓
5	2873.18 ± 0.05	2873.23 ± 0.03	2873.11 ± 0.05 #↓	2873.22 ± 0.04	2873.19 ± 0.03
6	2853.92 ± 0.16	2853.63 ± 0.06	2853.58 ± 0.11*↓	2853.68 ± 0.04	2853.53 ± 0.01 *↓
7	1743.04 ± 0.06	1743.13 ± 0.07	1743.05 ± 0.08	1743.21 ± 0.07	1743.15 ± 0.06
8	1642.22 ± 0.52	1642.94 ± 0.44	1642.67 ± 0.58	1643.45 ± 0.66	1643.04 ± 0.27
9	1550.58 ± 0.71	1550.90 ± 0.50	1552.78 ± 1.25	1550.91 ± 0.60	1551.97 ± 0.47
10	1457.87 ± 0.87	1456.47 ± 0.04	1456.42 ± 0.12	1457.52 ± 1.12	1457.74 ± 0.71
11	1400.41 ± 0.52	1399.75 ± 0.19	1398.49 ± 0.77 *↓	1399.74 ± 0.14	1399.74 ± 0.12
12	1345.68 ± 0.17	1345.78 ± 0.17	1345.23 ± 0.50	1345.48 ± 0.36	1345.77 ± 0.21
13	1235.42 ± 0.37	1235.22 ± 0.21	1235.48 ± 0.46	1235.04 ± 0.22	1235.00 ± 0.13
14	1159.04 ± 0.57	1158.51 ± 0.29	1158.24 ± 0.30	1158.03 ± 0.13	1158.40 ± 0.21
15	1092.10 ± 1.87	1094.61 ± 0.69	1093.40 ± 1.99	1095.25 ± 0.64	1095.55 ± 0.42
16	1052.27 ± 1.48	1052.65 ± 1.37	1053.29 ± 1.32	1053.64 ± 1.47	1054.84 ± 0.27
17	969,0 ± 0.85	968.49 ± 1.07	968.83 ± 1.09	967.73 ± 0.67	968.68 ± 0.55

The values are the mean ± standard error of the mean for each group. Comparison was performed by one-way ANOVA and Tukey's test was used as a post test. The degree of significance was denoted with * for the comparison of control DBA/12 strain with other BFM lines, with # for the comparison of BFM852 with other BFM lines, with † for the comparison for BFM856 and with ‡ for the comparison of BFM860 with other BFM lines. *P* values less than or equal to 0.05 were considered as statistically significant; * $p \leq 0.05$; ** $p \leq 0.01$; *** $p \leq 0.001$.

Table 5. Detailed numerical summary of the differences in the wavenumber value of the bands observed in female control (DBA/2J) and obese (BFMI lines) mice IF adipose tissues.

Band No	Control	BFMI852	BFMI856	BFMI860	BFMI861
2	3009.47 ± 0.38	3009.40 ± 0.25	3008.72 ± 0.23	3008.93 ± 0.32	3009.15 ± 0.21
3	2958.31 ± 0.10	2957.84 ± 0.09 *↓	2957.70 ± 0.15 **↓	2958.06 ± 0.09	2957.91 ± 0.07
4	2926.33 ± 0.64	2925.16 ± 0.29	2925.82 ± 0.77	2926.59 ± 1.21	2925.33 ± 0.39
5	2873.36 ± 0.06	2873.36 ± 0.05	2873.26 ± 0.06	2873.36 ± 0.11	2873.21 ± 0.08
6	2854.69 ± 0.30	2854.28 ± 0.12	2854.55 ± 0.30	2854.60 ± 0.20	2854.19 ± 0.20
7	1735.55 ± 4.06	1742.44 ± 0.15	1740.84 ± 1.63	1739.48 ± 3.53	1742.51 ± 0.16
8	1639.57 ± 0.30	1640.58 ± 0.18	1640.57 ± 0.19	1640.56 ± 0.47	1640.53 ± 0.22
9	1550.15 ± 0.44	1551.32 ± 0.66	1552.48 ± 0.47	1552.00 ± 0.90	1551.70 ± 0.48
10	1453.89 ± 0.24	1455.01 ± 0.28	1454.95 ± 0.39	1455.07 ± 0.38	1455.10 ± 0.43
11	1403.23 ± 0.21	1402.78 ± 0.17	1403.04 ± 0.29	1402.74 ± 0.62	1402.08 ± 0.49
12	1340.99 ± 0.00	1343.18 ± 1.00	1343.53 ± 0.83	1341.53 ± 0.54	1343.27 ± 1.02
13	1239.41 ± 0.15	1238.94 ± 0.26	1239.07 ± 0.33	1238.87 ± 0.67	1238.56 ± 0.49
14	1189.73 ± 8.19	1168.99 ± 6.69	1168.45 ± 6.92	1175.20 ± 8.83	1175.28 ± 8.74
15	1082.21 ± 0.29	1083.79 ± 0.66	1084.33 ± 1.10	1084.53 ± 1.88	1085.27 ± 1.26
16	1051.33 ± 0.48	1052.05 ± 0.72	1053.02 ± 0.45	1053.43 ± 0.27	1051.50 ± 0.52
17	971.81 ± 0.09	971.82 ± 0.19	972.00 ± 0.23	971.42 ± 0.65	971.73 ± 0.25

The values are the mean ± standard error of the mean for each group. Comparison was performed by one-way ANOVA and Tukey's test was used as a post test. The degree of significance was denoted with * for the comparison of control DBA/12 strain with other BFM lines, with † for the comparison of BFM852 with other BFM lines, with ‡ for the comparison of BFM856 and with † for the comparison of BFM860 with other BFM lines. *P* values less than or equal to 0.05 were considered as statistically significant; **p* ≤ 0.05; ***p* ≤ 0.01; ****p* ≤ 0.001.

Table 6. Detailed numerical summary of the differences in the wavenumber value of the bands observed in male control (DBA/2J) and obese (BFMI lines) mice IF adipose tissues.

Band No	Control	BFMI852	BFMI856	BFMI860	BFMI861
2	3008.70 ± 0.23	3008.86 ± 0.18	3008.65 ± 0.20	3008.96 ± 0.21	3009.42 ± 0.47
3	2957.82 ± 0.08	2957.89 ± 0.14	2957.44 ± 0.13 #↓	2957.99 ± 0.12 ††↑	2957.85 ± 0.06
4	2925.36 ± 0.55	2925.91 ± 0.66	2925.56 ± 0.71	2925.43 ± 0.27	2925.22 ± 0.40
5	2873.32 ± 0.05	2873.46 ± 0.09	2873.13 ± 0.12 #↓	2873.39 ± 0.05	2873.24 ± 0.05
6	2854.32 ± 0.24	2854.59 ± 0.19	2854.82 ± 0.46	2854.47 ± 0.11	2854.29 ± 0.16
7	1742.72 ± 0.31	1742.32 ± 0.70	1742.14 ± 0.41	1743.23 ± 0.10	1742.91 ± 0.17
8	1640.89 ± 0.25	1640.58 ± 0.25	1640.87 ± 0.29	1640.90 ± 0.23	1641.14 ± 0.20
9	1551.64 ± 0.46	1552.51 ± 0.46	1552.36 ± 0.34	1552.48 ± 0.58	1553.14 ± 0.45
10	1455.88 ± 0.86	1454.89 ± 0.19	1454.75 ± 0.42	1457.52 ± 1.12	1455.63 ± 0.23
11	1402.81 ± 0.41	1403.53 ± 0.27	1403.74 ± 0.47	1402.47 ± 0.35	1401.92 ± 0.41 #, †↓
12	1341.66 ± 0.67	1341.00 ± 0.01	1342.48 ± 0.95	1342.44 ± 0.86	1343.21 ± 0.99
13	1239.07 ± 0.43	1239.85 ± 0.35	1239.69 ± 0.53	1239.18 ± 0.31	1238.97 ± 0.41
14	1169.27 ± 6.69	1162.67 ± 0.31	1175.23 ± 8.73	1161.53 ± 0.54	1161.22 ± 0.57
15	1084.73 ± 1.24	1082.87 ± 0.64	1083.69 ± 1.32	1085.07 ± 1.30	1087.11 ± 1.43
16	1050.93 ± 1.02	1051.28 ± 1.11	1053.19 ± 0.70	1053.10 ± 0.47	1052.59 ± 0.79
17	971.75 ± 0.30	972.23 ± 0.16	972.27 ± 0.24	972.20 ± 0.32	971.37 ± 0.17

The values are the mean ± standard error of the mean for each group. Comparison was performed by one-way ANOVA and Tukey's test was used as a post test. The degree of significance was denoted with * for the comparison of control DBA/12 strain with other BFMI lines, with # for the comparison of BFMI852 with other BFMI lines, with † for the comparison for BFMI856 and with † for the comparison of BFMI860 with other BFMI lines. *P* values less than or equal to 0.05 were considered as statistically significant; * $p \leq 0.05$; ** $p \leq 0.01$; *** $p \leq 0.001$.

Table 7. Detailed numerical summary of the differences in the band area value of the bands observed in female control (DBA/2J) and obese (BFMI lines) mice GF adipose tissues.

Band No	Control	BFMI852	BFMI856	BFMI860	BFMI861
2	1.54 ± 0.05	1.78 ± 0.04	1.74 ± 0.07	1.80 ± 0.06 *↑	1.83 ± 0.07 *↑
3	1.53 ± 0.02	1.57 ± 0.01	1.60 ± 0.01 *↑	1.44 ± 0.01 *,###,†††↓	1.34 ± 0.02 ***,###,†††,†↓
4	3.77 ± 0.19	3.75 ± 0.16	3.92 ± 0.28	3.59 ± 0.18	3.42 ± 0.25
5	0.34 ± 0.01	0.34 ± 0.01	0.32 ± 0.02	0.29 ± 0.01	0.31 ± 0.02
6	1.19 ± 0.08	1.17 ± 0.07	1.26 ± 0.11	1.18 ± 0.08	1.09 ± 0.10
7	2.48 ± 0.19	2.03 ± 0.14	2.29 ± 0.24	2.07 ± 0.20	2.03 ± 0.22
8	11.53 ± 0.64	11.02 ± 0.50	10.87 ± 0.68	11.18 ± 0.62	10.78 ± 0.64
9	4.32 ± 0.32	3.50 ± 0.24	3.44 ± 0.28	3.79 ± 0.32	3.57 ± 0.33
10	0.63 ± 0.01	0.50 ± 0.01 ***↓	0.54 ± 0.01 ***↓	0.58 ± 0.01 *↓###↑	0.57 ± 0.02 **↓###↑
11	0.62 ± 0.03	0.50 ± 0.03	0.50 ± 0.03	0.53 ± 0.03	0.48 ± 0.04 *↓
12	0.64 ± 0.02	0.60 ± 0.03	0.60 ± 0.02	0.58 ± 0.02	0.58 ± 0.03
13	1.62 ± 0.03	1.61 ± 0.03	1.71 ± 0.06	1.60 ± 0.03	1.61 ± 0.06
14	3.19 ± 0.26	2.86 ± 0.18	3.16 ± 0.36	2.86 ± 0.28	2.77 ± 0.29
15	1.06 ± 0.06	0.93 ± 0.04	1.01 ± 0.09	0.90 ± 0.06	0.90 ± 0.07
16	0.45 ± 0.03	0.32 ± 0.01 ***↓	0.42 ± 0.02	0.37 ± 0.02 *↓	0.27 ± 0.02 ***,†††,†↓
17	0.03 ± 0.00	0.03 ± 0.00	0.03 ± 0.00	0.03 ± 0.00	0.03 ± 0.00

The values are the mean ± standard error of the mean for each group. Comparison was performed by one-way ANOVA and Tukey's test was used as a post test. The degree of significance was denoted with * for the comparison of control DBA/12 strain with other BFM lines, with # for the comparison of BFM852 with other BFM lines, with † for the comparison for BFM856 and with ‡ for the comparison of BFM860 with other BFM lines. *P* values less than or equal to 0.05 were considered as statistically significant; **p* ≤ 0.05; ***p* ≤ 0.01; ****p* ≤ 0.001.

Table 8. Detailed numerical summary of the differences in the band area value of the bands observed in male control (DBA/2J) and obese (BFMI lines) mice GF adipose tissues.

Band No	Control	BFMI852	BFMI856	BFMI860	BFMI861
2	1.66 ± 0.07	1.60 ± 0.06	1.69 ± 0.11	1.55 ± 0.08	1.45 ± 0.04
3	1.41 ± 0.02	1.56 ± 0.01 ***↑	1.67 ± 0.04 ***↑ #↓	1.56 ± 0.01 ***↑ ‡↓	1.47 ± 0.01 ‡‡‡↓
4	3.52 ± 0.19	4.42 ± 0.21	4.65 ± 0.30 *↑	4.40 ± 0.32	4.04 ± 0.17
5	0.30 ± 0.01	0.36 ± 0.01	0.37 ± 0.02 *↑	0.33 ± 0.02	0.32 ± 0.01
6	1.10 ± 0.08	1.52 ± 0.09	1.53 ± 0.13	1.51 ± 0.14	1.29 ± 0.07
7	2.03 ± 0.21	2.68 ± 0.17	3.01 ± 0.24 *↑	3.29 ± 0.22 **↑	2.62 ± 0.07
8	10.74 ± 0.78	8.92 ± 0.69	9.12 ± 0.91	8.80 ± 0.67	8.48 ± 0.48
9	3.49 ± 0.42	2.66 ± 0.32	2.83 ± 0.42	2.63 ± 0.29	2.34 ± 0.21
10	0.57 ± 0.01	0.52 ± 0.00 **↓	0.59 ± 0.01 ###	0.66 ± 0.01 ***↑ ###, ‡‡‡↓	0.64 ± 0.00 ***↑ ###, ‡‡‡↓
11	0.47 ± 0.05	0.38 ± 0.03	0.41 ± 0.05	0.38 ± 0.03	0.32 ± 0.02
12	0.55 ± 0.03	0.49 ± 0.02	0.56 ± 0.03	0.40 ± 0.02 **, ‡‡↓	0.48 ± 0.01
13	1.59 ± 0.03	1.78 ± 0.02 *↑	1.79 ± 0.04 ***↑	1.52 ± 0.06 ###, ‡‡‡↓	1.37 ± 0.02 ***↑ ###, ‡‡‡, †↓
14	3.02 ± 0.30	3.74 ± 0.25	3.75 ± 0.38	3.87 ± 0.36	3.75 ± 0.18
15	0.97 ± 0.06	1.14 ± 0.05	1.15 ± 0.06	1.14 ± 0.08	1.05 ± 0.03
16	0.47 ± 0.02	0.43 ± 0.01	0.54 ± 0.05	0.37 ± 0.02 ‡‡↓	0.32 ± 0.01 **↓ #, ‡‡‡↓
17	0.04 ± 0.00	0.03 ± 0.00	0.03 ± 0.01	0.03 ± 0.00	0.04 ± 0.00

The values are the mean ± standard error of the mean for each group. Comparison was performed by one-way ANOVA and Tukey's test was used as a post test. The degree of significance was denoted with * for the comparison of control DBA/2J strain with other BFM lines, with # for the comparison of BFM852 with other BFM lines, with ‡ for the comparison for BFM856 and with † for the comparison of BFM860 with other BFM lines. *P* values less than or equal to 0.05 were considered as statistically significant; **p* ≤ 0.05; ***p* ≤ 0.01; ****p* ≤ 0.001.

Table 9. Detailed numerical summary of the differences in the band area value of the bands observed in female control (DBA/2J) and obese (BFMI lines) mice IF adipose tissues.

Band No	Control	BFMI852	BFMI856	BFMI860	BFMI861
2	1.87 ± 0.04	1.42 ± 0.02 ***↓	1.52 ± 0.03 ***↓	1.43 ± 0.06 ***↓	1.50 ± 0.03 ***↓
3	1.59 ± 0.05	1.66 ± 0.04	1.39 ± 0.02 *,##↓	1.44 ± 0.07 #↓	1.42 ± 0.03 ##↓
4	2.91 ± 0.17	3.27 ± 0.13	2.95 ± 0.07	3.23 ± 0.22	2.89 ± 0.05 ##,††↓
5	0.30 ± 0.02	0.33 ± 0.01	0.27 ± 0.00	0.33 ± 0.02	0.26 ± 0.01
6	0.76 ± 0.05	0.96 ± 0.05 *↑	0.85 ± 0.03	0.94 ± 0.08	0.84 ± 0.02
7	0.98 ± 0.08	1.22 ± 0.08	1.29 ± 0.11	1.36 ± 0.24	1.23 ± 0.13
8	17.32 ± 0.57	14.43 ± 0.52	14.39 ± 0.61	14.50 ± 1.08	13.97 ± 0.67 *↓
9	9.35 ± 0.55	6.30 ± 0.47 *↓	5.68 ± 0.47 **↓	6.72 ± 0.93	5.72 ± 0.64 **↓
10	0.96 ± 0.05	0.48 ± 0.10 ***↓	0.56 ± 0.03 **↓	0.72 ± 0.07	0.67 ± 0.05 *↓
11	1.47 ± 0.08	0.92 ± 0.06 **↓	1.17 ± 0.08	0.87 ± 0.11 ***↓	0.87 ± 0.09 ***↓
12	1.24 ± 0.05	0.84 ± 0.04 **↓	1.17 ± 0.08 #↑	0.98 ± 0.08	0.80 ± 0.06 ***,††↓
13	2.61 ± 0.15	1.87 ± 0.13 **↓	1.64 ± 0.09 ***↓	2.08 ± 0.19	1.73 ± 0.12 **↓
14	2.10 ± 0.10	1.94 ± 0.14	1.95 ± 0.09	2.23 ± 0.28	2.01 ± 0.12
15	0.98 ± 0.07	0.88 ± 0.07	0.80 ± 0.02	0.88 ± 0.09	0.91 ± 0.05
16	0.84 ± 0.08	0.39 ± 0.04 ***↓	0.40 ± 0.03 ***↓	0.53 ± 0.08 **↓	0.28 ± 0.03 ***,†↓
17	0.08 ± 0.01	0.04 ± 0.00 ***↓	0.03 ± 0.00 ***↓	0.05 ± 0.01 **↓	0.04 ± 0.00 ***↓

The values are the mean ± standard error of the mean for each group. Comparison was performed by one-way ANOVA and Tukey's test was used as a post test. The degree of significance was denoted with * for the comparison of control DBA/2J strain with other BFMI lines, with # for the comparison of BFMI852 with other BFMI lines, with † for the comparison for BFMI856 and with ‡ for the comparison of BFMI860 with other BFMI lines. *P* values less than or equal to 0.05 were considered as statistically significant; **p* ≤ 0.05; ***p* ≤ 0.01; ****p* ≤ 0.001.

Table 10. Detailed numerical summary of the differences in the band area value of the bands observed in male control (DBA/2J) and obese (BFMI lines) mice IF adipose tissues.

Band No	Control	BFMI852	BFMI856	BFMI860	BFMI861
2	1.81 ± 0.05	1.43 ± 0.04 ***↓	1.74 ± 0.06 ###↑	1.43 ± 0.03 *** ,†††↓	1.31 ± 0.03 *** ,†††↓
3	1.44 ± 0.05	1.66 ± 0.02 ***↑	1.92 ± 0.04 *** ,###↑	1.43 ± 0.03 ###↓	1.29 ± 0.01 * ,### ,†↓
4	3.07 ± 0.24	3.22 ± 0.18	3.73 ± 0.14 *↑	3.25 ± 0.11	2.84 ± 0.09 ††↓
5	0.28 ± 0.02	0.30 ± 0.01	0.42 ± 0.01 *** ,###↑	0.26 ± 0.01 †††↓	0.27 ± 0.01 †††↓
6	0.87 ± 0.09	1.00 ± 0.07	1.10 ± 0.06	1.01 ± 0.05	0.85 ± 0.04
7	0.97 ± 0.08	1.28 ± 0.11	1.29 ± 0.11	1.56 ± 0.12 *↑	1.49 ± 0.10
8	13.89 ± 0.67	14.69 ± 0.61	14.26 ± 0.85	14.00 ± 0.50	13.14 ± 0.63
9	5.93 ± 0.49	6.50 ± 0.35	6.25 ± 0.62	6.17 ± 0.51	4.75 ± 0.37
10	0.68 ± 0.05	0.61 ± 0.02	0.63 ± 0.05	0.79 ± 0.05 #↑	0.61 ± 0.02 †↓
11	0.81 ± 0.06	0.99 ± 0.04	0.99 ± 0.10	0.95 ± 0.07	0.66 ± 0.04 # ,† ,†↓
12	0.86 ± 0.05	0.96 ± 0.04	0.90 ± 0.09	0.91 ± 0.05	0.74 ± 0.04
13	1.87 ± 0.13	1.87 ± 0.07	1.91 ± 0.14	1.82 ± 0.13	1.51 ± 0.05
14	2.26 ± 0.25	1.59 ± 0.13	2.14 ± 0.19	2.29 ± 0.15	2.21 ± 0.14
15	0.79 ± 0.08	0.87 ± 0.05	0.86 ± 0.03	0.77 ± 0.03	0.70 ± 0.02
16	0.53 ± 0.05	0.46 ± 0.03	0.61 ± 0.04	0.45 ± 0.03 †↓	0.39 ± 0.02 ††↓
17	0.04 ± 0.00	0.03 ± 0.00	0.04 ± 0.00	0.02 ± 0.01 *** ,††↓	0.02 ± 0.00 * ,†↓

The values are the mean ± standard error of the mean for each group. Comparison was performed by one-way ANOVA and Tukey's test was used as a post test. The degree of significance was denoted with * for the comparison of control DBA/12 strain with other BFM lines, with # for the comparison of BFM852 with other BFM lines, with † for the comparison for BFM856 and with † for the comparison of BFM860 with other BFM lines. *P* values less than or equal to 0.05 were considered as statistically significant; * $p \leq 0.05$; ** $p \leq 0.01$; *** $p \leq 0.001$.

3.3 Comparisons of the Band Area Ratio Values of Control and Obese Mice:

Band area ratio values were given in Figures 26-34. Total lipid content was calculated by taking the sum of the areas of the olefinic, the CH₃ anti-symmetric stretching, the CH₂ anti-symmetric and symmetric stretching, the CH₂ bending and the C=O carbonyl stretching bands. The unsaturated/saturated lipid ratio was calculated by dividing the olefinic band area to the sum of the CH₂ anti-symmetric and symmetric stretching band area values and unsaturation amount was deduced from the ratio of the olefinic band area to total lipid content. In order to observe the methyl group amount in lipids, the ratio of area of the CH₃ anti-symmetric stretching band to total lipid content was calculated. In order to observe the triglyceride amount in total lipids, ratio of the C=O carbonyl stretching band area to total lipid area was calculated. The CH₂ anti-sym. str./CH₃ antisym. str. and the CH₂ anti-sym. str./total lipid band area ratios were calculated to achieve information about the hydrocarbon chain length of the lipids. The CH₂ sym. str./CH₃ sym. str. band area ratio was calculated in order for obtaining information about lipid to protein ratio. The amide I/ amide II ratio was calculated to obtain information about structural changes in proteins. The amide II/ 1345 cm⁻¹ band area ratio was calculated to achieve information about collagen integrity.

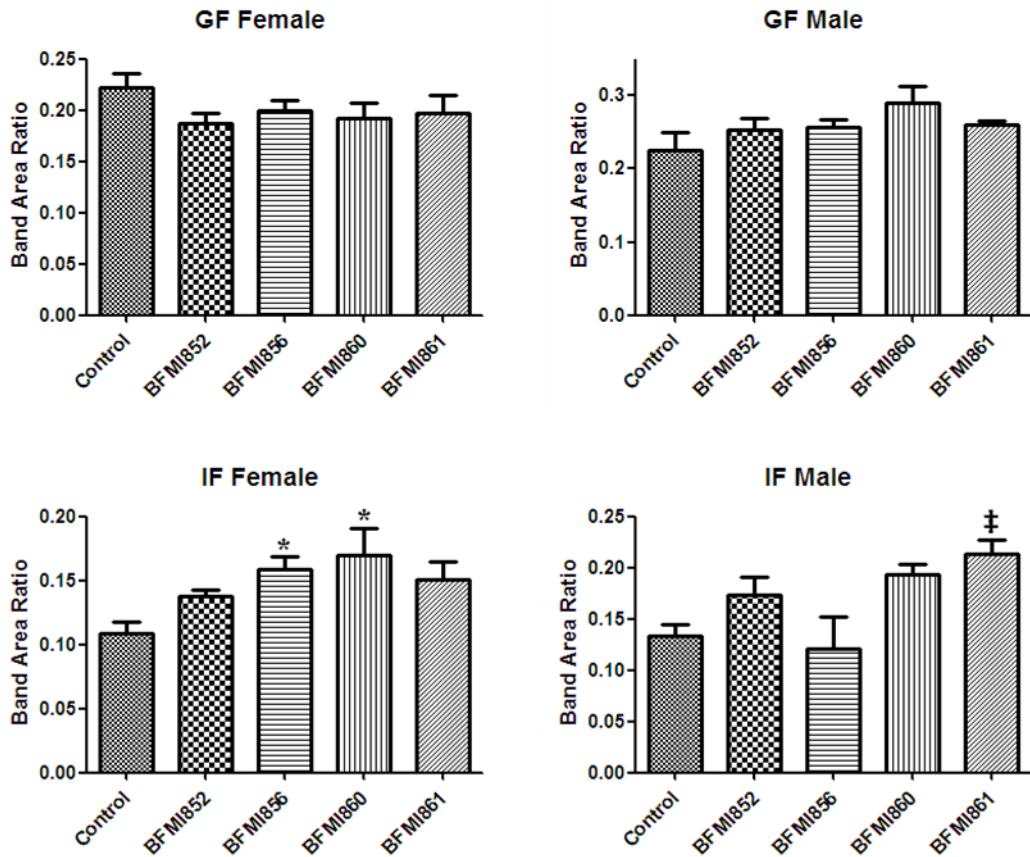


Figure 27. The triglyceride/total lipid band area ratio. The degree of significance was denoted with * for the comparison of control DBA/J2 strain with other BFM lines, with # for the comparison of BFM852 with other BFM lines, with ‡ for the comparison for BFM856 and with † for the comparison of BFM860 with other BFM lines. P values less than or equal to 0.05 were considered as statistically significant; * $p \leq 0.05$; ** $p \leq 0.01$; *** $p \leq 0.001$.

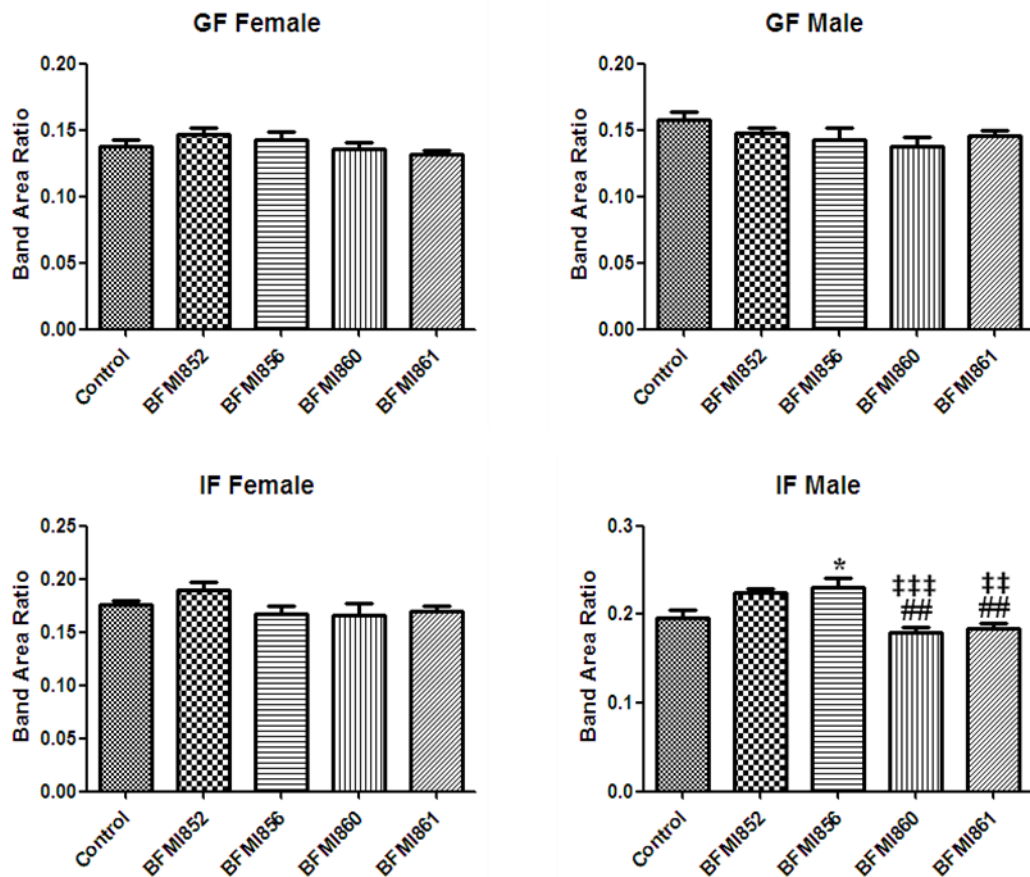


Figure 28. The CH₃ anti-symmetric stretching/total lipid ratio band area ratio. The degree of significance was denoted with * for the comparison of control DBA/J2 strain with other BFM lines, with # for the comparison of BFM852 with other BFM lines, with ‡ for the comparison for BFMI856 and with † for the comparison of BFM860 with other BFM lines. *P* values less than or equal to 0.05 were considered as statistically significant; **p* ≤ 0.05; ***p* ≤ 0.01; ****p* ≤ 0.001.

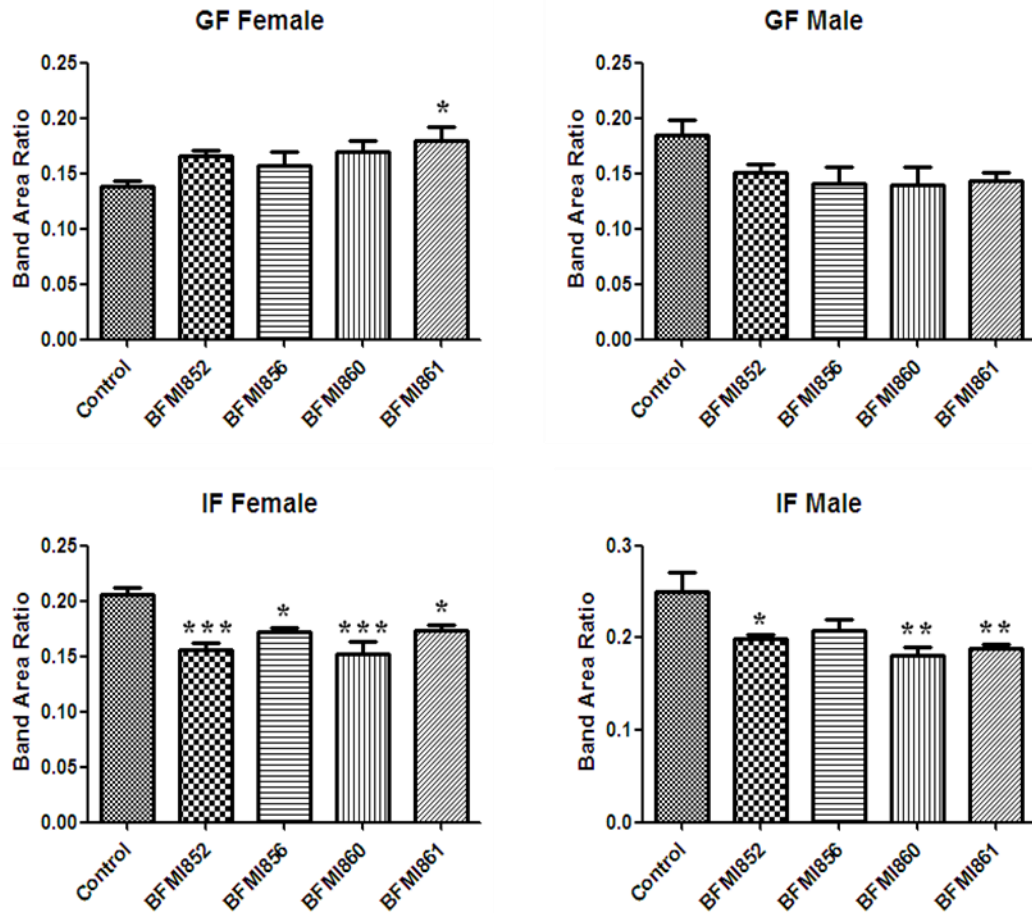


Figure 29. The olefinic stretching/total lipid band area ratio. The degree of significance was denoted with * for the comparison of control DBA/J2 strain with other BFM lines, with # for the comparison of BFM852 with other BFM lines, with ‡ for the comparison for BFM856 and with † for the comparison of BFM860 with other BFM lines. *P* values less than or equal to 0.05 were considered as statistically significant; **p* ≤ 0.05; ***p* ≤ 0.01; ****p* ≤ 0.001.

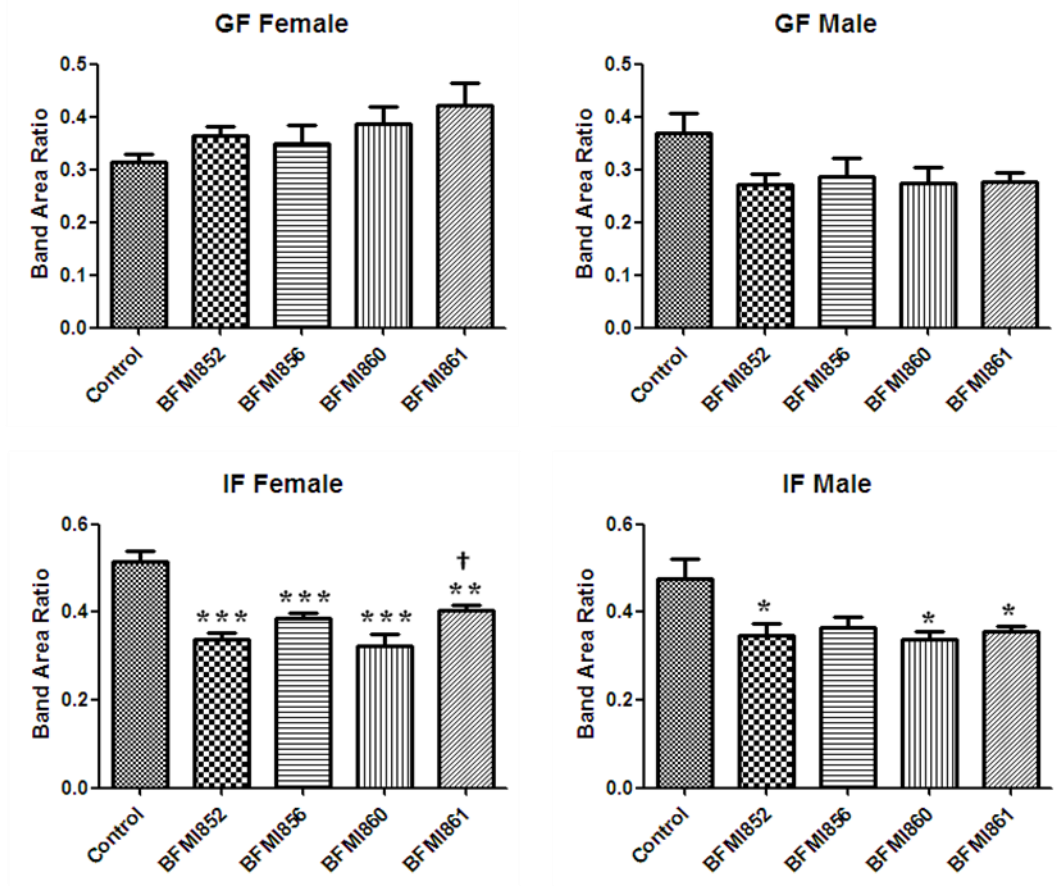


Figure 30. The unsaturated/saturated lipid band area ratio. The degree of significance was denoted with * for the comparison of control DBA/J2 strain with other BFM lines, with # for the comparison of BFM852 with other BFM lines, with ‡ for the comparison for BFMI856 and with † for the comparison of BFMI860 with other BFM lines. *P* values less than or equal to 0.05 were considered as statistically significant; **p* ≤ 0.05; ***p* ≤ 0.01; ****p* ≤ 0.001.

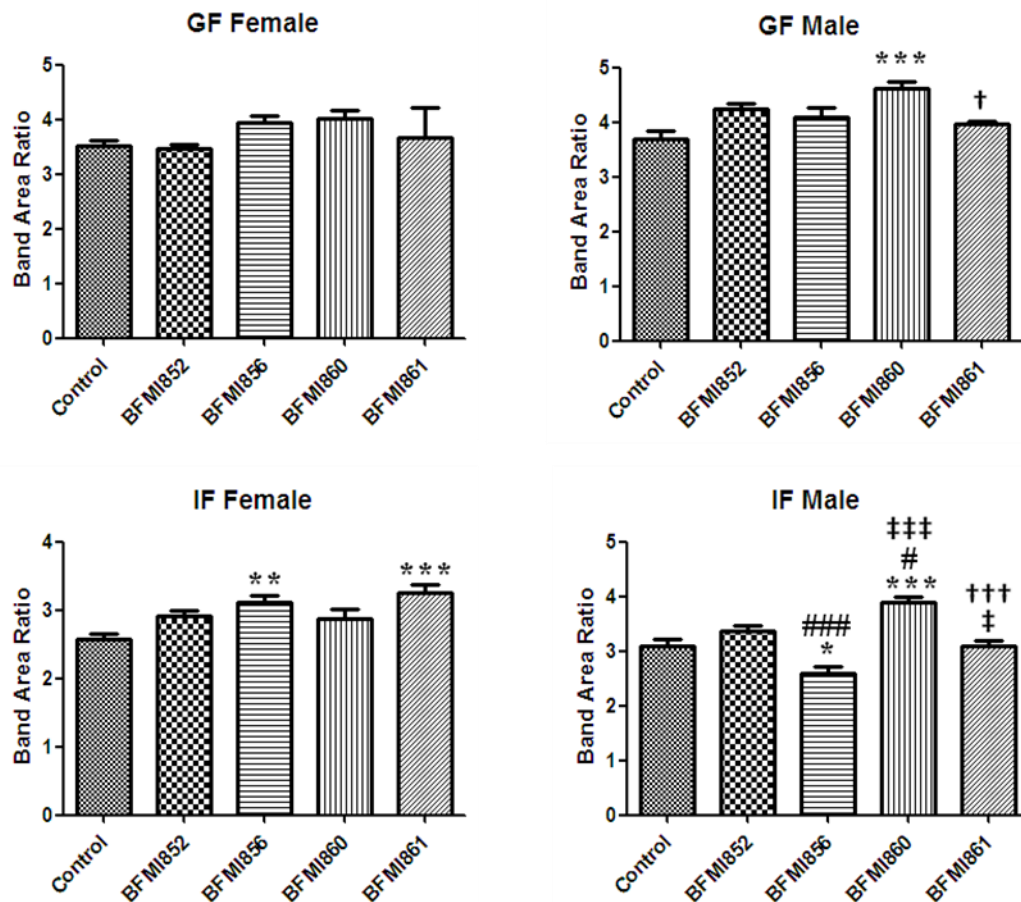


Figure 31. The lipid/protein band area ratio. The degree of significance was denoted with * for the comparison of control DBA/J2 strain with other BFM lines, with # for the comparison of BFM852 with other BFM lines, with ‡ for the comparison for BFMI856 and with † for the comparison of BFMI860 with other BFM lines. *P* values less than or equal to 0.05 were considered as statistically significant; **p* ≤ 0.05; ***p* ≤ 0.01; ****p* ≤ 0.001.

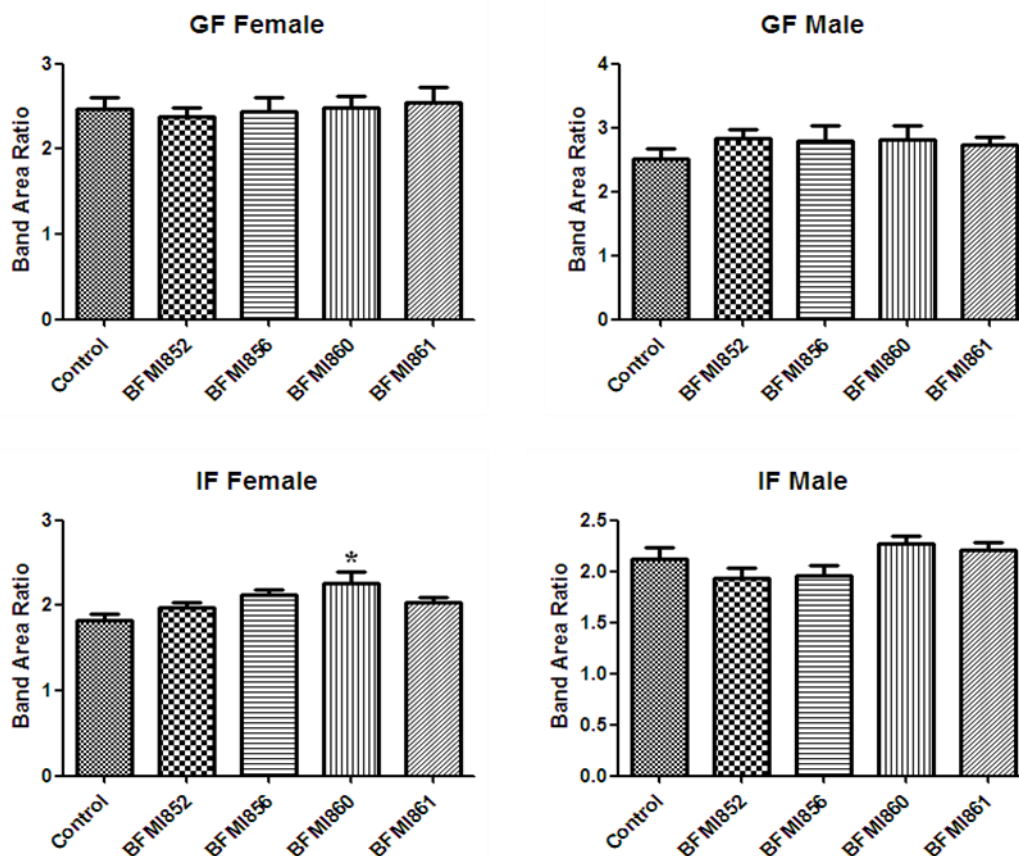


Figure 32. The CH₂ anti-sym. str./CH₃ anti-sym. str. band area ratio. The degree of significance was denoted with * for the comparison of control DBA/J2 strain with other BFM lines, with # for the comparison of BFM852 with other BFM lines, with ‡ for the comparison for BFM856 and with † for the comparison of BFM860 with other BFM lines. *P* values less than or equal to 0.05 were considered as statistically significant; **p* ≤ 0.05; ***p* ≤ 0.01; ****p* ≤ 0.001.

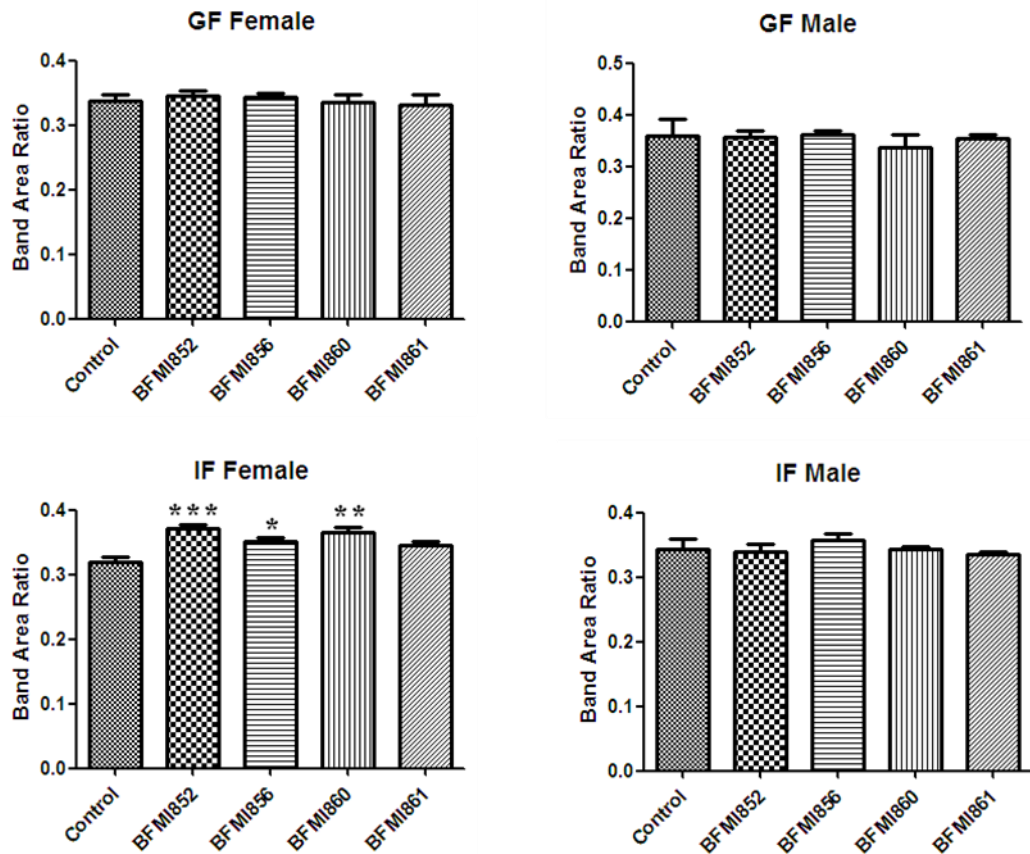


Figure 33. The CH₂ anti-sym. str./total lipid band area ratio. The degree of significance was denoted with * for the comparison of control DBA/J2 strain with other BFM lines, with # for the comparison of BFM852 with other BFM lines, with ‡ for the comparison for BFMI856 and with † for the comparison of BFM860 with other BFM lines. *P* values less than or equal to 0.05 were considered as statistically significant; **p* ≤ 0.05; ***p* ≤ 0.01; ****p* ≤ 0.001.

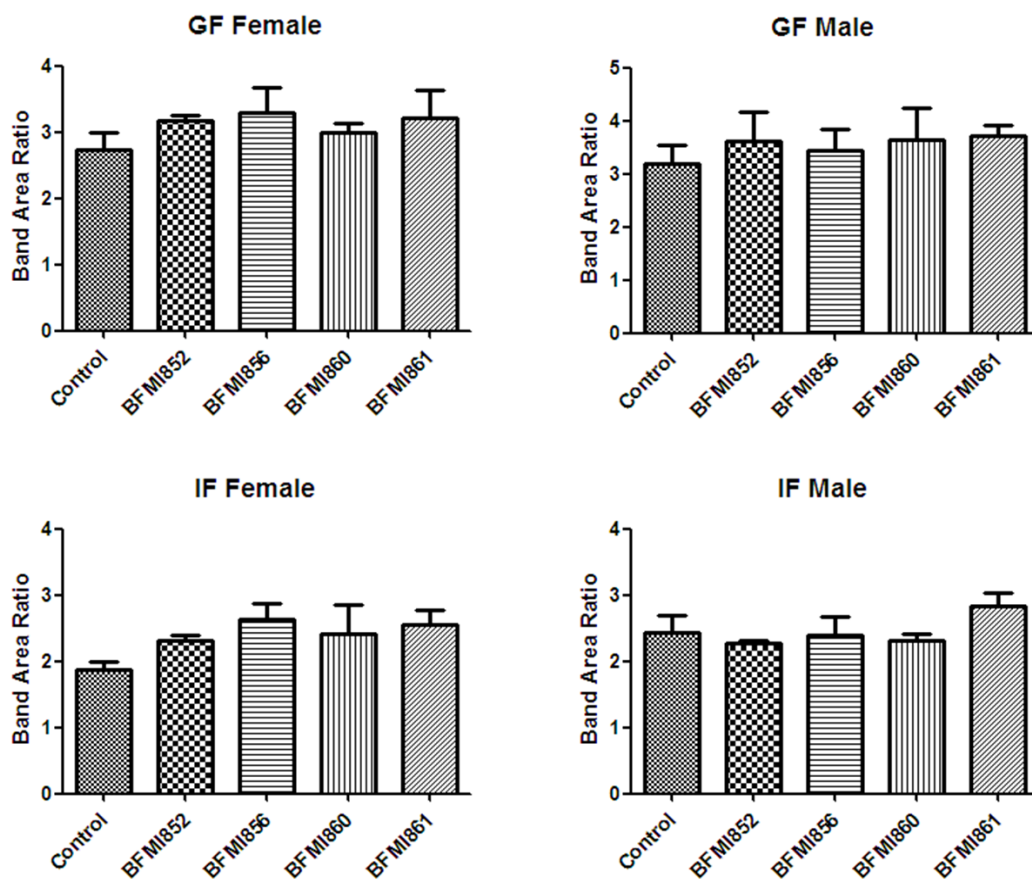


Figure 34. The amide I / amide II band area ratio. The degree of significance was denoted with * for the comparison of control DBA/J2 strain with other BFM lines, with # for the comparison of BFM852 with other BFM lines, with ‡ for the comparison for BFM856 and with † for the comparison of BFM860 with other BFM lines. *P* values less than or equal to 0.05 were considered as statistically significant; * $p \leq 0.05$; ** $p \leq 0.01$; *** $p \leq 0.001$.

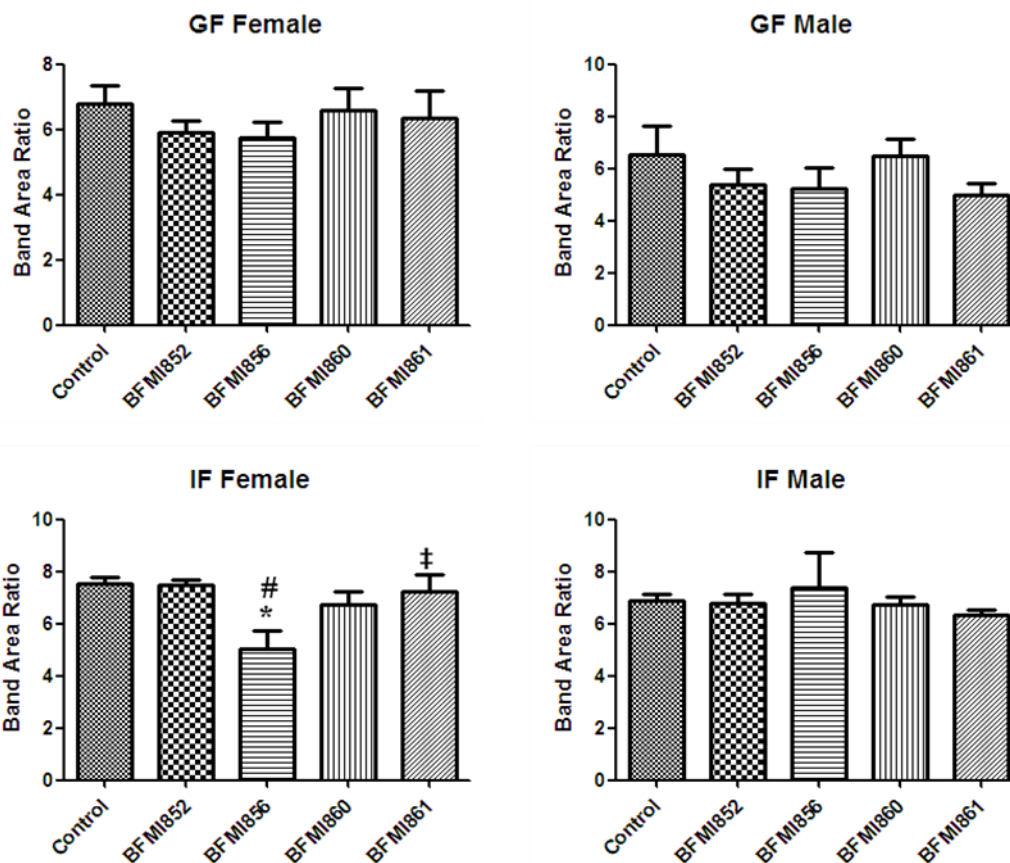


Figure 35. The amide II/ 1345 cm^{-1} band area ratio. The degree of significance was denoted with * for the comparison of control DBA/J2 strain with other BFM lines, with # for the comparison of BFM852 with other BFM lines, with ‡ for the comparison for BFMI856 and with † for the comparison of BFMI860 with other BFM lines. P values less than or equal to 0.05 were considered as statistically significant; * $p \leq 0.05$; ** $p \leq 0.01$; *** $p \leq 0.001$.

Ratio of the C=O carbonyl stretching band area to total lipid area gives information about the triglyceride amount in total lipid (Cakmak et al, 2011). According to the data shown in Figure 27, all BFMI lines represented slight increase in TG amount and especially in BFMI856 and BFMI860 lines, there was a significant increase in the TG /total lipid ratio in IF adipose tissues of female mice.

In order to observe the methyl group amount in lipids, the ratio of area of CH₃ anti-symmetric stretching band to total lipid content was calculated (Figure 28) (Bozkurt et al, 2010; Cakmak et al, 2011). There was a significant increase in methyl amount in BFMI856 line compared to the control group. Also, BFMI860 and BFMI861 lines showed that they had the lowest methyl amount among all BFMI lines in male IF adipose tissue.

Unsaturation amount was deduced from the ratio of olefinic band area to total lipid content and unsaturated/saturated lipid ratio was calculated by dividing the olefinic band area to the sum of the CH₂ anti-symmetric and symmetric stretching band area values which gives information about the saturated lipid content (Bozkurt et al, 2010; Cakmak et al, 2012; Cakmak et al, 2011; Ozek et al, 2010). According to the calculated values for the both band ratios which are shown in Figures 29 and 30, all BFMI lines except BFMI856 represented a significant decrease in comparison to the control in both male and female IF. Moreover, in female GF, there was a significant increase in unsaturated lipid amount in all BFMI lines and especially in BFMI860, significantly higher unsaturation was observed.

The CH₂ sym. str. / CH₃ sym. str. band area ratio was calculated in order to obtain information about lipid to protein ratio (Boyar et al, 2004; Severcan et al, 2000b). According to the results (Figure 31), slight increase was observed in male and female GF adipose tissues in all BFMI lines compared to the control. In addition, BFMI860 line in male GF and BFMI856 and BFMI861 lines in female GF represented significant increase in the lipid to protein ratio.

The CH₂ anti-sym. str. / CH₃ anti-sym. str. band area ratio was calculated to achieve information about the hydrocarbon chain length of the lipids and results are given in Figure 32 (Bozkurt et al, 2010; Cakmak et al, 2011; Gasper et al, 2009). In female IF tissue, there was a slight increase in all BFMI lines except BFMI860 line which showed a significantly higher value in comparison to the control. Increase in this ratio value especially in BFMI860 line is an indicator of longer lipid acyl chains in female IF tissue. Moreover, the CH₂ anti-sym. str./ total lipid ratio was also calculated in order to observe phospholipid chain length alterations (Antoine et al, 2010). In female IF, BFMI852, BFMI856 and BFMI860 lines represented a significant increase in the ratio value with respect to the control (Figure 33). This result reveals that IF adipose tissues of female BFMI852, BFMI856 and BFMI860 mice may be mainly consist of lipids with longer acyl chains.

The amide I /amide II band area ratio gives information about the alterations in the structure of proteins (Cakmak et al, 2011). According to the results, there were no significant changes in both female and male mice adipose tissues (IF and GF) (Figure 34). Therefore, no structural changes were observed in proteins within the adipose tissues.

The amide II/ 1345 cm⁻¹ band area ratio gives information about collagen integrity. According to the results given in Figure 35, there was a significant decrease in BFMI856 line in female IF adipose tissue. The decrease in this ratio value indicates that collagen integrity alters and the quality of the collagens within the tissue decreases (Bi et al, 2006; Bozkurt et al, 2010; West et al, 2004).

3.4 Comparison of the Bandwidth Values of Control and Obese Mice

Bandwidth values were achieved with spectral analysis and the the results of the CH₃ anti-symmetric stretching, the CH₂ anti-symmetric stretching, the CH₂ symmetric stretching, the amide I and amide II bandwidth values are given in

Table 11-14. Dynamics of the lipid membranes can be monitored by the information from the alterations in the bandwidth values of the CH₃ anti-symmetric stretching, the CH₂ anti-symmetric stretching, the CH₂ symmetric stretching bands (Bozkurt et al, 2010). In these bands located at C-H region, there were not any significant changes in BFMI lines in both IF and GF tissues of female and male mice with respect to the control DBA/2J mice and no variety was observed between the lines. However, in the amide II band which gives information about proteins, significant changes was observed in BFMI861 line in male IF. There was a significant increase in the bandwidth values of the amide II band compared to the control (Table 14). This change indicated that there might be alterations in the structure of proteins in BFMI861 line in male IF adipose tissue (Cakmak et al, 2006). However, it should be supported by the information achieved from the band wavenumber shift in the amide I and amide II bands and also the amide I / amide II band area ratios.

Table 11. Detailed numerical summary of the differences in the bandwidth value of the bands observed in female control (DBA/2J) and obese (BFMI lines) mice GF adipose tissues.

Bands	Control	BFMI852	BFMI856	BFMI860	BFMI861
CH ₃ anti-sym. str.	14.76± 0.46	14.21± 0.72	14.20± 0.83	14.14± 0.94	14.00± 1.03
CH ₂ anti-sym. str.	16.29± 0.18	16.70± 0.28	16.70± 0.32	16.89± 0.42	16.95± 0.37
CH ₂ sym str.	10.18± 0.07	10.25± 0.09	10.20± 0.10	10.27± 0.12	10.19± 0.08
Amide I	36.85± 0.36	37.29± 0.20	37.00± 0.53	36.88± 0.37	37.14± 0.41
Amide II	28.12± 1.56	33.35± 1.23	32.88± 1.65	29.45± 0.78	32.19± 1.42

The values are the mean ± standard error of the mean for each group. Comparison was performed by one-way ANOVA and Tukey's test was used as a post test. The degree of significance was denoted with * for the comparison of control DBA/J2 strain with other BFM lines, with # for the comparison of BFMI852 with other BFM lines, with ‡ for the comparison for BFMI856 and with † for the comparison of BFMI860 with other BFM lines. *P* values less than or equal to 0.05 were considered as statistically significant; **p* ≤ 0.05; ***p* ≤ 0.01; ****p* ≤ 0.001.

Table 12. Detailed numerical summary of the differences in the bandwidth value of the bands observed in male control (DBA/2J) and obese (BFMI lines) mice GF adipose tissues.

Bands	Control	BFMI852	BFMI856	BFMI860	BFMI861
CH ₃ anti-sym. str.	14.15± 0.93	14.61± 0.27	13.54± 0.77	14.41± 0.31	14.33± 0.22
CH ₂ anti-sym. str.	16.71± 0.36	16.09± 0.19	16.14± 0.31	16.01± 0.27	15.98± 0.13
CH ₂ sym str.	10.34± 0.16	10.08± 0.06	10.14± 0.15	10.07± 0.08	9.97± 0.03
Amide I	36.88± 0.61	36.15± 0.48	36.29± 0.62	35.57± 0.72	36.22± 0.30
Amide II	31.47± 1.96	32.44± 1.38	34.53± 0.61	32.19± 1.45	34.69± 0.98

The values are the mean ± standard error of the mean for each group. Comparison was performed by one-way ANOVA and Tukey's test was used as a post test. The degree of significance was denoted with * for the comparison of control DBA/J2 strain with other BFM lines, with # for the comparison of BFM852 with other BFM lines, with ‡ for the comparison for BFM856 and with † for the comparison of BFM860 with other BFM lines. *P* values less than or equal to 0.05 were considered as statistically significant; **p* ≤ 0.05; ***p* ≤ 0.01; ****p* ≤ 0.001.

Table 13. Detailed numerical summary of the differences in the bandwidth value of the bands observed in female control (DBA/2J) and obese (BFMI lines) mice IF adipose tissues.

Bands	Control	BFMI852	BFMI856	BFMI860	BFMI861
CH ₃ anti-sym. str.	11.78± 1.11	11.04± 1.21	8.80± 0.80	11.46± 1.64	10.81± 1.01
CH ₂ anti-sym. str.	19.08± 0.87	18.16± 0.31	19.40± 1.10	20.31± 2.45	18.43± 0.32
CH ₂ sym str.	11.64± 0.50	10.86± 0.13	11.42± 0.51	11.31± 0.40	10.80± 0.24
Amide I	38.37± 0.09	38.46± 0.15	38.55± 0.06	38.46± 0.42	38.60± 0.15
Amide II	26.27± 0.20	27.76± 0.46	30.20± 1.32	27.92± 1.13	29.54± 1.70

The values are the mean ± standard error of the mean for each group. Comparison was performed by one-way ANOVA and Tukey's test was used as a post test. The degree of significance was denoted with * for the comparison of control DBA/J2 strain with other BFM lines, with # for the comparison of BFMI852 with other BFM lines, with ‡ for the comparison for BFMI856 and with † for the comparison of BFMI860 with other BFM lines. *P* values less than or equal to 0.05 were considered as statistically significant; **p* ≤ 0.05; ***p* ≤ 0.01; ****p* ≤ 0.001.

Table 14. Detailed numerical summary of the differences in the bandwidth value of the bands observed in male control (DBA/2J) and obese (BFMI lines) mice IF adipose tissues.

Bands	Control	BFMI852	BFMI856	BFMI860	BFMI861
CH ₃ anti-sym. str.	10.56± 1.86	9.89± 1.43	14.00± 1.99	13.20± 1.34	12.18± 1.06
CH ₂ anti-sym. str.	18.05± 0.77	19.33± 1.10	19.23± 1.00	17.85± 0.42	18.15± 0.52
CH ₂ sym str.	10.85± 0.32	11.30± 0.30	12.15± 0.82	10.82± 0.16	10.74± 0.24
Amide I	38.87± 0.31	39.04± 0.16	38.86± 0.22	38.89± 0.21	38.71± 0.21
Amide II	26.60± 0.60	27.05± 0.40	27.54± 0.93	27.25± 0.76	30.00± 1.04*†

The values are the mean ± standard error of the mean for each group. Comparison was performed by one-way ANOVA and Tukey's test was used as a post test. The degree of significance was denoted with * for the comparison of control DBA/J2 strain with other BFM lines, with # for the comparison of BFMI852 with other BFM lines, with ‡ for the comparison for BFMI856 and with † for the comparison of BFMI860 with other BFM lines. *P* values less than or equal to 0.05 were considered as statistically significant; **p* ≤ 0.05; ***p* ≤ 0.01; ****p* ≤ 0.001.

CHAPTER 4

DISCUSSION

This current study aims to investigate the effects of obesity on macromolecular compositional, structural and functional alterations in order to characterize BFMI mice, new models for obesity research, which will contribute to understanding of; spontaneous obesity without induction of a high fat diet, with macromolecular alterations in different adipose tissues and gender effect on obesity. For this purpose, Attenuated Total Reflectance-Fourier Transform Infrared (ATR-FTIR) spectroscopy was used to characterize content and structure of macromolecules in male and female control (DBA/2J) and BFMI lines; namely BFMI856, BFMI860 and BFMI861, in two different adipose tissues; inguinal fat (IF) which is SAT, gonadal fat (GF) which is VAT. According to the results, there were significant alterations in the unsaturated and saturated lipid, proteins, collagen, RNA, glycogen and triglyceride content and structure in different adipose tissues of female and male BFMI lines.

Polyunsaturated fatty acids (PUFAs) which are the constituents of the structural phospholipids of the biological membranes, are prone to be attacked by free radicals. The reaction of free radicals with the double bonds of PUFAs lead to lipid peroxidation, which in turn results in the loss of unsaturation in lipid structure together with the breakdown of longer chains into shorter lipid acyl chains (Levine et al, 1998, Olusi, 2002). Lipid peroxidation also alters the unsaturated/saturated lipid composition of the membranes and results in the generation of cross-linked lipid-lipid and lipid-protein moieties, which culminates in more rigid membranes (Niranjan et al., 2000). In turn, rigid

membranes might be associated with insulin resistance since there can be some limitations for the correct insulin-receptor binding due to rigidity (Russo, 2009).

The results of the current study revealed that the unsaturated lipid content, the unsaturated/saturated lipid and the unsaturated/ total lipid ratios were significantly lower in especially BFMI860 and BFMI861 lines in male and female IF adipose tissues, which indicate that these lines are more prone to lipid peroxidation among BFMI lines. IF as a subcutaneous adipose tissue has low antioxidant protein levels and GF as a VAT has high antioxidant protein levels (Sackmann-Sala et al, 2012). Therefore, IF may become more prone to lipid peroxidation under oxidative stress, ER stress and mitochondrial stress conditions due to obesity. The results are supporting this idea because lipid peroxidation was thought to be occurred only in IF and unsaturation increased in GF adipose tissues especially in female BFMI860 and BFMI861 lines. Supporting the results, accumulation of excessive fat in white adipose tissues seen in obesity was found to increase the thiobarbituric acid reactive substances (TBARS) content, indicator of lipid peroxidation within the tissue itself in different obese mice models (Vincent et al 2006; Furukawa et al., 2004). Moreover, in a previous study, FTIR spectroscopic results on lipid peroxidation by monitoring the olefinic band was supported with TBARS test in diabetic microsomal membranes, where same results were achieved in both techniques (Severcan et al., 2005).

In contrary to IF adipose tissues, GF adipose tissues of female BFMI mice represented an increase in unsaturated lipid content especially in BFMI860 and BFMI861 lines. Deposition of TGs within GF as a VAT may be composed of unsaturated fatty acids since they can be easily mobilized from VAT toward other tissues for the need of energy. It is also thought that fatty acids are not mobilized from adipocytes due to their TG contents. However, they may be mobilized according to their unsaturation level. And, PUFAs are preferentially mobilized compared to saturated fatty acids from VAT (Giarola et al, 2011; Halliwell et al, 1996).

The CH₂ anti-symmetric and symmetric stretching band positions give information about lipid acyl chain flexibility and so, information about the degree of the conformational disorders within the lipids can be obtained from these bands (Bozkurt et al, 2010; Casal & Mantsch, 1984; Umemura et al, 1980). The CH₂ anti-symmetric stretching band value of wavenumber decreased significantly in BFMI852, BFMI856 and BFMI861 lines in male GF adipose tissue. Also, there was a significant decrease in the CH₂ symmetric stretching band wavenumber value in BFMI856 and BFMI861 lines in comparison to the control. The decrease seen in these band wavenumber value represents that acyl chains in lipids are more ordered and trans/gauche ratio value of the lipids is lower, which is the indicator of structural changes especially in male GF adipose tissues (Liu et al, 2002; Mantsch, 1984; Severcan et al, 1997). This increase in order results in more rigid membranes (Niranjan et al., 2000).

The CH₃ anti-symmetric stretching band can be used to monitor the methyl concentration in the structure of lipids and an increased methyl amount indicates the presence of shorter acyl chains (Cakmak et al., 2011; Cakmak et al., 2012; Zwart et al., 1999, Bozkurt et al., 2010, Gasper et al., 2009). The results of the current study revealed an increase in the CH₃ anti-symmetric band area and the CH₃ anti-sym. str./total lipid ratio, which were higher in BFMI856 line in both adipose tissues. This observed increase in the amount of methyl groups in lipids can be interpreted as reduction of hydrocarbon chain length of lipids which are dominantly found in BFMI856 line in comparison to the other BFMI lines including the control (Cakmak et al., 2011).

The CH₂ anti-symmetric stretching/CH₃ anti-symmetric stretching band area ratio was also calculated to achieve information about the hydrocarbon chain length of the lipids (Bozkurt et al, 2010; Cakmak et al, 2011). The results revealed that BFMI lines tend to possess lipids with longer hydrocarbon chain length. In female IF tissue, there was a slight increase in this ratio in all BFMI lines except BFMI860 line which showed a significantly higher value in comparison to the control. Increase in this ratio value especially in BFMI860 line is an indicator of

longer lipid acyl chains in female IF tissue. Moreover, the CH_2 anti-sym. str./total lipid ratio was also calculated in order to observe phospholipid chain length alterations (Antoine et al, 2010). In female IF, BFMI852, BFMI856 and BFMI860 lines represented a significant increase in this ratio value with respect to the control. This result reveals that IF adipose tissues of female BFMI852, BFMI856 and BFMI860 mice may be mainly consist of lipids with longer acyl chains. Enhanced lipid peroxidation generally accompanies with the shortening of acyl chain length. However, in the current study, despite the increase in lipid peroxidation in IF tissues of female and male BFMI mice, these tissues have lipids with longer acyl chains. One possible explanation is that the synthesis of longer chained lipids are dominantly formed in these adipose tissues. Since adipose tissues are the TG depots of the body, increase in the amount of longer chained lipids may be due to the continuously synthesized newly formed TGs.

The CH_2 sym. str./ CH_3 sym. str. band area ratio was calculated in order to obtain information about lipid to protein ratio. According to the results, slight increase was observed in male and female GF adipose tissues in all BFMI lines compared to the control. In addition to this, BFMI860 line in male GF and BFMI856 and BFMI861 lines in female GF represented significant increase in lipid to protein ratio. It may be interpreted as, in GF adipose tissues of both male and female mice, having an increase in the amount of lipids compared to proteins.

Although it has been showed in many studies that obesity is related with disturbed glucose and lipid metabolism, it is controversial whether protein metabolism is also affected. Some studies in the literature have reported that basal leucine turnover rate increases in obesity (Bruce et al, 1990; Jensen & Haymond, 1991; Welle et al, 1992). Other studies have shown that protein anabolism is affected by insulin hormone and obesity induced insulin resistance may have a role in protein metabolism especially in females (Caballero & Wurtman, 1991; Luzi et al, 1996). In addition to these studies, increased mass of adipose tissue was found to be correlated with the decreased relative total protein content (Seraphim et al, 2001). Therefore, differences in protein metabolism and increased protein turnover may

be seen even in moderate obesity additionally to the disturbed glucose and FFA metabolism (Jensen & Haymond, 1991; Welle et al, 1992). Increased proteolysis may occur since anti-proteolytic activity of insulin is disrupted during obesity and proteolysis can contribute to impaired glucose disposal and further insulin resistance (Jensen & Haymond, 1991). Moreover, especially VAT was found to be inversely correlated with endogenous leucine flux which is an index of proteolysis in response to hyperinsulinemia (Solini et al, 1997). However, proteolysis was also found to be increased in SAT in females (Patterson et al, 2002).

The results revealed that, area values of amide I and amide II bands decreased in both female GF and IF adipose tissues of obese lines and the decrease in the band area values was significant in all BFMI lines in female IF with respect to the control group. This decrease represented that in female IF, all BFMI lines had lower protein content significantly compared to control (Bozkurt et al, 2010; Ozek et al, 2010). Increase in the depletion of proteins could be explained due to the higher levels of FFA and the increased rate of lipid oxidation during obesity (Ferrannini et al, 1986; Tessari et al, 1986). Moreover, visceral adiposity is associated with the alterations in the cortisol metabolism and androgens such that insulin represses sex hormone-binding globulin production. That is why, in obese women who are hyperinsulinemic and have large amounts of VAT, sex hormone-binding globulin concentrations are lowered and free androgens amount increases in the circulation. Increased levels of steroid hormones are responsible for the improved antiproteolytic effect of insulin in during visceral obesity in females (Solini et al, 1997). Another possible reason may be that alterations in muscle fiber composition and muscle capillarization in obese individuals due to the amount of visceral fat, are negatively related with the protein metabolism (Lillioja et al, 1987). Although, protein content of female adipose tissues decreased significantly, the structure of the proteins did not alter compared to the control according to the information achieved by the amide I / amide II band area ratio (Cakmak et al, 2011). It may be interpreted that obesity may induce the

proteolysis especially in IF adipose tissues of female mice but it may not effect the structure of the proteins.

The 995-970 cm^{-1} region in the spectra is assigned to symmetric stretching mode of dianionic phosphate monoester of nucleic acids (Cakmak et al, 2003; Chiriboga et al, 2000). The C-N+-C stretching vibration band located at 970-971 cm^{-1} arises from nucleic acids especially ribose-phosphate main chain vibrations (Banyay et al, 2003; Chiriboga et al, 2000). There was not any significant change in the wavenumber value of this band in both tissues in both sexes. However, in band area values, there was a decrease in all lines in female IF and in BFMI860 and BFMI861 lines in male IF compared to the control. BFMI861 had the lowest band area value in IF adipose tissues of the female and male mice. Moreover, this decrease in RNA could be the result of lower RNA expression supporting the decrease in protein content of BFMI lines in female IF.

Adipocytes are surrounded by collagens, specifically type I collagens are densely found within adipose tissues (Chun et al, 2006). They are thought to be responsible for supplying integrity and elasticity to adipose tissues in order to provide the appropriate structure to maintain their form and function (Prockop & Kivirikko, 1995). It was found that obesity induces collagenolytic activity in adipose tissue, which leads the degradation of collagens results in the decreased amount of collagen in adipose tissues (Chun et al, 2010). The band located at 1343 cm^{-1} originates mainly from the CH_2 side-chain vibrations and a little contributions from the C-N and the C-C stretching and the N-H bending vibrations of collagen (Camacho et al, 2001; Gough et al, 2003; West et al, 2004). It has previously shown that decrease in band area value resulted in denaturation of the collagens (West et al, 2004). Supportingly, in male GF, BFMI860 line and in female IF, BFMI852 and BFMI861 lines represented a decrease in area value of this band with respect to the control. Moreover, the amide II/ 1345 cm^{-1} band area ratio gives information about the collagen integrity. Significant decrease was observed in BFMI856 line in female IF adipose tissue. The decrease in this ratio value indicates the alteration in the collagen integrity (Bi et al, 2006; West et al,

2004). While the collagen content did not change, disruption of the collagen integrity in BFMI856 line in female IF adipose tissues can be interpreted as increase in the disease state (Bi et al, 2006).

Spectral range between 1300-1000 cm^{-1} is the region where bands of the stretching modes of the P=O bond phosphate moieties of phospholipids and nucleic acids are present (Diem et al, 1999; Liquier & Taillender, 1996). The bands arising from phosphate-stretching vibrations are thought to give valuable information about phospholipid head groups in the polar and non-polar interface of membrane structures (Mendelsohn & Mantsch, 1986). Moreover, bands located at this region also give information about the changes in the conformational state, quantity and position of nucleic acid phosphorylation in RNA and DNA (Dovbeshko et al, 2000; Kneipp et al, 2000). In the PO₂- symmetric stretching band which was located around 1237 cm^{-1} , there was no significant difference in wavenumber values in all lines in both adipose tissues compared to the control group. In female IF, there was a significant decrease in all BFMI lines except BFMI860 line and in male GF and IF, BFMI861 line showed the lowest band area value among all lines including control line. Therefore, it was interpreted as reduction in nucleic acid and phospholipid content in male BFMI861 line in both GF and IF adipose tissues. Although, there was not a significant alteration in female GF adipose tissues, all BFMI lines were seem to have lower nucleic acid and membrane phospholipid content compared to the control (Severcan et al, 2003).

Band located at 1050 cm^{-1} arises from the C–O stretching vibrations of polysaccharides especially glycogen within the tissues (Ozek et al, 2010). There was no significant decrease in the wavenumber value of this band in both female and male IF and GF adipose tissues compared to the control group, which means that no structural changes were found in glycogens. However, in band area values, all lines represented a decrease in female GF and IF adipose tissues. In addition to this, BFMI860 and BFMI861 lines had significantly lower band area values in both IF and GF adipose tissue of male mice. Importantly, BFMI861 line seemed

to have the lowest value of band area. The decrease in area value of this band indicated a decrease in glycogen content of the tissues (Ozek et al, 2010; Toyran et al, 2006). For the storage of the glycogen, skeletal muscle is the most important tissue. If glucose in the blood cannot be converted into glycogen in skeletal muscle, much of this glucose is taken up by adipocytes. Insulin is the major hormone that is responsible for the uptake of glucose and its conversion to triglycerides which are stored in adipocytes by promoting GLUT4 transporters. The reason for the decrease in the glycogen content in obese lines in both adipose tissues can be the storage of glucose as TGs instead of glycogen. Moreover, decrease in the glycogen content in both SAT and VAT of obese lines without having diabetes was an indicator that these adipose tissues might not response to insulin. The results support the finding that both SAT and VAT are associated with insulin resistance in obese subjects (Stolic et al, 2002). BFMI861 line seemed to be more prone to have insulin resistance with respect to other BFMI lines since it had the least amount of glycogen within the both IF and GF adipose tissues. This result is supported by the intraperitoneal insulin tolerance test (IPITT) results that were carried out in Humboldt University, Berlin. It was found that BFMI860 and BFMI861 lines represented the slowest response to insulin whereas BFMI852 and BFMI856 lines responded faster than BFMI860 and BFMI861 lines according to the blood glucose measurement upon insulin injection (unpublished data). Enhanced glycolysis results in the formation of α -glycerol-phosphate that is esterified with free fatty acids and converted to triglycerides. During this process, insulin decreases hormone sensitive triglyceride lipase activity in order to block the breakdown of triglycerides and therefore, inhibits lipolysis (Delibegovic et al, 2003).

Accumulation of TGs in adipose tissues is one of the major determinants of obesity. There are contradictory results in the literature about the TG amount in female and male VAT and SAT. Some studies in the literature revealed that women have a higher percentage of body fat and have a greater storage capacity especially in gluteal-femoral region than men who tend to store adipose tissue in visceral and abdominal depots (Blaak, 2001). Adipose tissue depots in gluteal-

femoral region in women is related to increased stimulated lipolysis, larger fat cell size and increased triglyceride synthesis. Conversely in men, increment in abdominal adipose tissue is related to decreased stimulation of lipolysis and decreased synthesis of triglyceride (Fried et al, 1993). According to another study, men have more plasma TG value in comparison to women (Williams, 2004). Also, it was found that men having higher visceral adiposity, represent more elevated postprandial insulin, FFAs, and TG level than in women (Couillard et al, 1999). According to the results, male mice were found to be affected more than female mice in both VAT and SAT regarding their TG amount. Band located around 1743 cm^{-1} in fingerprint region of the spectra, which arise from ester C=O stretching vibrations, originating from triglycerides (Nara et al, 2002). Although there were not any significant changes in band area and wavenumber values in all BFMI lines in female IF and GF adipose tissues, BFMI860 in male IF and BFMI856, BFMI860 lines in male GF represented significant increase in band area value as an indicator of increment in triglyceride content compared to the control DBA/J2 group. In addition, BFMI856 and BFMI861 lines in GF adipose tissues of male mice showed significantly lower band wavenumber values in comparison to the control, which indicated that structural changes might occur in triglycerides due to obesity. Furthermore, ratio of C=O carbonyl stretching band area to total lipid area gives information about the triglyceride amount in total lipid (Cakmak et al, 2011). According to the results, all BFMI lines represented slight increase in TG amount and especially in BFMI856 and BFMI860 lines, there was a significant increase in TG/total lipid ratio in IF adipose tissues of female mice. Results are in agreement with the studies in the literature that larger adipocytes which SAT consists of, synthesize more triglycerides than smaller adipocytes constituting VAT (Edens et al, 1993; Farnier et al, 2003). Moreover, contradict to many studies, SAT may become more hyperlipolytic than VAT and have a higher rate of triglyceride turnover (Tchernof et al, 2006). In addition, triglyceride structure and content seemed to be affected more in male mice adipose tissues than females since triglyceride content in GF adipose tissues of female mice decreased and no structural changes were found in both IF and GF adipose tissues of female obese lines.

In the literature, several studies have been conducted in order for the understanding of the relationship between sex difference and obesity. Some of these studies were carried out to enlighten the differences in body fat distribution (Blaak, 2001; Nguyen et al, 1996), energy expenditure (Quevedo et al, 1998; Valle et al, 2005), metabolic rate (Henderson et al, 2008; Tarnopolsky et al, 1995), physical activity (Kautzky-Willer & Handisurya, 2009), oxidative capacity (Rodriguez & Palou, 2004), adipokine signaling (Havel et al, 1996; Matsuda et al, 2005) and sex hormones (Rodriguez-Cuenca et al, 2002). According to the studies, males compared to females have a higher tendency to obesity (Hong et al, 2009; Legato, 1997) but there are also some contradictory results due to the differences in nutritional state and strains of the male and female animals (Justo et al, 2005; Kautzky-Willer & Handisurya, 2009). Therefore, the role of gender effect in obesity could not be fully understood. This study aimed to contribute the discrimination of effect of obesity on different adipose tissues of mice with different genders. The results of this study revealed that insulin resistance and lipid peroxidation might be formed both in female and male mice due to the decreased amount of glycogen and decreased unsaturation in the lipids within both adipose tissues. In addition to this, TG amount was increased especially in male adipose tissues. Structural changes in lipids were observed especially in GF adipose tissues of male obese mice. Protein and RNA content significantly decreased in female IF adipose tissues. Chain length of the lipids were longer particularly in IF adipose tissues female obese mice and collagen integrity was disrupted in IF adipose tissues of female mice. However, these alterations also varied between BFMI lines and obesity affected IF and GF adipose tissue macromolecules differently.

BFMI852 line was found to be the least affected line compared to the other BFMI lines due to obesity. It showed significant differences in the content of unsaturated, saturated lipids, proteins, collagens and glycogens especially and almost only in female IF adipose tissues. Significant increase in the amount of saturated lipids were determined according to the information from CH₂

symmetric stretching band. In addition, chain length of the lipids was found to be increased. According to the olefinic band area value, unsaturated/saturated lipid ratio and unsaturated/total lipid ratio, unsaturated lipid content decreased in female and male IF adipose tissues as an indicator of lipid peroxidation. Protein and collagen amount decreased in IF adipose tissue of female BFMI852 line. Moreover, glycogen content decreased in female GF and IF adipose tissues in comparison to the control but it had the highest glycogen content among the other BFMI lines.

BFMI856 line represented higher saturated lipid content with longer acyl chained lipids according to the CH_2 anti-symmetric band area value and CH_2 anti-symmetric stretching band/total lipid band area ratio. Moreover, triglyceride amount and triglyceride amount in total lipid increased. In IF adipose tissues of both female BFMI856 mice, unsaturated lipid content decreased according to olefinic band, olefinic/ total lipid and unsaturated/ saturated lipid ratios, which might be due to lipid peroxidation. However, unsaturated lipid content did not change in male IF and GF adipose tissues compared to the control, which means that there was no sign for lipid peroxidation in the IF and GF adipose tissues belong to BFMI852 line. Structural changes in the lipids were observed especially in the GF adipose tissues of BFMI856 male mice since there were frequency shifts in the bands belonging to saturated lipids and triglycerides. Protein content decreased especially in female IF adipose tissues and collagen integrity was found to be corrupted in IF adipose tissues of female BFMI856 mice. However, no significant alterations was found in glycogen content or structure different than BFMI860 and BFMI861 which might become insulin resistant. This line seemed to represent obesity induced changes especially on lipids together with alterations on proteins and collagens.

BFMI860 line represented many significant changes in saturated and unsaturated lipids, proteins, glycogens, collagens, triglycerides and total RNA amount without structural changes within these macromolecules. In IF adipose tissues of both male and female BFMI860 mice, unsaturated lipid content decreased according to

olefinic band, olefinic/ total lipid and unsaturated/ saturated lipid ratios, which might be due to lipid peroxidation. However, different than the BFMI852 and BFMI856 lines, in GF adipose tissues of female BFMI860 line, there was an increment in the unsaturated lipid content and chain length of the lipids. This may be the result of that unsaturated lipids are preferentially stored for the release of FFAs into circulation from VAT during obesity, which in turn can affect other organs with the accumulation of lipids (van Herpen & Schrauwen-Hinderling, 2008). Supporting these results, triglyceride content also increased in GF and IF adipose tissues of male mice. It may be an indicator of the increase in the severity of the disease in female BFMI860 lines. BFMI860 line together with BFMI861 line had lower glycogen content among all BFMI lines and compared to the control as an indicator of insulin resistance. No significant changes were observed in the protein content and structure. However, collagen content decreased in GF adipose tissues of male mice.

BFMI861 line showed considerable alterations in the content of lipids, proteins, RNAs, glycogens and also structural changes were observed especially in the saturated lipids and triglycerides of male GF adipose tissues. In IF adipose tissues of both male and female BFMI861 mice, the decrease in the olefinic band area, the olefinic/ total lipid and the unsaturated/ saturated lipid band area ratios was also observed in BFMI860 line. These findings further implicate the loss of unsaturation which is an indicator of lipid peroxidation. However, different than the BFMI852 and BFMI856 lines, in GF adipose tissues of female BFMI861 line like BFMI860 line, there was an increment in the unsaturated lipid content. Unsaturated lipids are more preferentially stored in order for the release of FFAs into circulation from VAT during obesity, which in turn cause the accumulation of lipids in other organs. This ectopic lipid accumulation results in the formation of metabolic complications such as insulin resistance in skeletal muscle and hepatic insulin resistance and non-alcoholicsteatohepatitis (Ferris & Crowther, 2011; van Herpen & Schrauwen-Hinderling, 2008). The increase in unsaturation content in GF adipose tissues may also contribute to these metabolic complications. Moreover, total RNA and protein content decreased especially in

male and female IF adipose tissues. Importantly, BFMI861 line seemed to be more prone to have insulin resistance with respect to other BFMI lines since it had the least amount of glycogen within the both IF and GF adipose tissues.

Moreover, although approximately 80% of total body fat is deposited in SAT and nearly 20% of fat in VAT, VAT has more impact on the release of FFAs into blood circulation since it is located closer to the portal circulation (Oka et al., 2009). Most studies have demonstrated a significant relation between VAT and prediabetes hyperglycemia and very few studies have shown the effect of SAT on metabolic complications of obesity (Goodpaster et al., 2003; Hayashi et al., 2007). The results of this study revealed that IF adipose tissue also demonstrated considerable obesity-induced alterations in addition to GF tissue. The findings of the signs of insulin resistance, decrease of glycogen content and increase of triglyceride content together with the decrease in unsaturation, implying the increased lipid peroxidation was observed in IF tissues of male and female BFMI lines. This implicated that not only VAT but also SAT may be important in the formation of metabolic complications of obesity. One possible reason for this observation is that SAT might have become insulin resistant and therefore resistant to fat storage, which might lead to fat deposition in VAT (Frayn, 2000). Indeed, in the current study an increase in saturated lipid content in GF tissues was observed in BFMI lines. The other explanation can be the expansion of SAT depots until it reaches the maximum capacity for storing FAs, then SAT adipocytes may contribute to insulin resistance by releasing FAs into the systemic circulation (Freedland, 2004).

CHAPTER 5

CONCLUSION

In this current study IF and GF adipose tissues of male and female BFMI lines were characterized in order to determine the alterations in macromolecules due to spontaneous obesity without high fat diet induction by ATR-FTIR spectroscopy. Detailed analysis of spectral data revealed the following findings;

Most of the studies in the literature have demonstrated significant alterations in VAT during obesity, while very few studies have shown the possible effect of SAT on metabolic complications of obesity. Supportingly, in this study, GF as a VAT represented alterations in different macromolecules, significantly. However, IF as a SAT was found to be affected dramatically and might have a role in obesity related complications on the contrary of its protective property. The findings of the signs of insulin resistance, decrease of glycogen content and increase of triglyceride content together with the decrease in unsaturation, implying the increased lipid peroxidation was observed in IF tissues of male and female BFMI lines. This implicated that not only VAT but also SAT may be important in the formation of metabolic complications of obesity

In the literature, number of studies were conducted to determine the relation between gender and obesity. However, the role of gender effect in obesity could not be fully understood. In this current study, female and male mice were found to be affected differently. TG amount was increased especially in male adipose tissues. Structural changes in lipids were observed especially in GF adipose tissues of male obese mice. Protein and RNA content significantly decreased in female IF adipose tissues. Moreover, chain length of the lipids were longer

particularly in IF adipose tissues female obese mice and collagen integrity was disrupted in IF adipose tissues of female mice. Although, there seemed to be more lipid accumulation and structural alterations in lipids in male mice, total RNA and protein content decreased especially in female mice. However, similar effects have been observed in terms of insulin resistance and lipid peroxidation both in female and male mice especially due to the decreased amount of glycogen and decreased unsaturation level of the lipids within both adipose tissues.

In this study, BFMI852 line was found to be the least affected line due to obesity compared to other BFMI lines. Especially, alterations in the macromolecules such as a decrease in unsaturated lipid, total protein, collagen content and an increase in saturated lipid content with longer chain length in IF adipose tissues of the BFMI852 female mice were determined. BFMI856 and BFMI861 lines represented structural alterations especially in lipids belonging to GF adipose tissues different than the other lines. BFMI856 lines showed increased saturated lipid and triglyceride content and decreased protein and collagen content without changes in unsaturated lipid and glycogen content. That is why, this line was not found to be related with lipid peroxidation and insulin resistance. However, BFMI861 line represented lower unsaturated lipid, protein, RNA content with the least glycogen amount in adipose tissues. It was thought to be the most insulin resistant line in addition to the lipid peroxidation found in IF adipose tissues due to the effect of obesity. Also, increased unsaturated lipid deposition found in GF adipose tissues of this line together with BFMI860 line might imply the increased FFA release to the circulation which may be an indicator of the severity of obesity in these lines. BFMI860 line represented significant alterations in macromolecules such as decreased collagen and RNA content, increased triglyceride amount and lipids with longer acyl chains. In addition, decreased amount of unsaturated lipid and glycogen, which are the indicators of lipid peroxidation and insulin resistance were determined in this line.

To conclude, BFMI860 and BFMI861 lines were found to be the most affected lines since they showed the indications of lipid peroxidation and insulin resistance

more severely as they had lower glycogen in all tissues and unsaturated content especially in IF adipose tissues. Also, BFMI856 and BFMI861 lines were determined to have alterations in the structure of lipids, especially in GF adipose tissues. Protein content was lowered significantly specifically in female IF adipose tissues but there was no change found in the structure. Furthermore, BFMI852 line was found to be affected different than other lines and had effect on especially female IF. Therefore, obesity induced changes differently according to the gender, adipose tissue type and distinctness in the strains. However, further studies should be conducted to understand these differences more accurately. Important adipokine levels may be determined in order to observe the metabolic complications of obesity and to observe whether there is an inflammation developed in these adipose tissues of male and female BFMI mice. This will enable the determination of the severity of the disease and its relation with metabolic syndrome in these mice.

REFERENCES

Abate N, Garg A, Peshock RM, Stray-Gundersen J, Grundy SM (1995) Relationships of generalized and regional adiposity to insulin sensitivity in men. *J Clin Invest* 96: 88-98

Adams M, Montague CT, Prins JB, Holder JC, Smith SA, Sanders L, Digby JE, Sewter CP, Lazar MA, Chatterjee VK, O'Rahilly S (1997) Activators of peroxisome proliferator-activated receptor gamma have depot-specific effects on human preadipocyte differentiation. *J Clin Invest* 100: 3149-3153

Ahima RS (2006) Adipose tissue as an endocrine organ. *Obesity (Silver Spring)* 14 Suppl 5: 242S-249S

Aksoy C, Guliyev A, Kilic E, Uckan D, Severcan F (2012) Bone Marrow Mesenchymal Stem Cells in Patients with Beta Thalassemia Major: Molecular Analysis with Attenuated Total Reflection-Fourier Transform Infrared Spectroscopy Study as a Novel Method. *Stem Cells Dev*

Alessi MC, Peiretti F, Morange P, Henry M, Nalbone G, Juhan-Vague I (1997) Production of plasminogen activator inhibitor 1 by human adipose tissue: possible link between visceral fat accumulation and vascular disease. *Diabetes* 46: 860-867

Andreasen CH, Andersen G (2009) Gene-environment interactions and obesity--further aspects of genomewide association studies. *Nutrition* 25: 998-1003

Antoine KM, Mortazavi S, Miller AD, Miller LM (2010) Chemical differences are observed in children's versus adults' latent fingerprints as a function of time. *J Forensic Sci* 55: 513-518

Arner P (1995) Differences in lipolysis between human subcutaneous and omental adipose tissues. *Ann Med* 27: 435-438

Arner P (1999) Catecholamine-induced lipolysis in obesity. *Int J Obes Relat Metab Disord* 23 Suppl 1: 10-13

Balaban G, Silva GA (2004) Protective effect of breastfeeding against childhood obesity. *J Pediatr (Rio J)* 80: 7-16

Banyay M, Sarkar M, Graslund A (2003) A library of IR bands of nucleic acids in solution. *Biophys Chem* 104: 477-488

Bi X, Yang X, Bostrom MP, Camacho NP (2006) Fourier transform infrared imaging spectroscopy investigations in the pathogenesis and repair of cartilage. *Biochim Biophys Acta* 1758: 934-941

Bizeau ME, Solano JM, Hazel JR (2000) Menhaden oil feeding increases lipolysis without changing plasma membrane order in isolated rat adipocytes. *Nutr Res* 20: 1633-1644

Bjorntorp P (1990) "Portal" adipose tissue as a generator of risk factors for cardiovascular disease and diabetes. *Arteriosclerosis* 10: 493-496

Blaak E (2001) Gender differences in fat metabolism. *Curr Opin Clin Nutr Metab Care* 4: 499-502

Boyar H, Zorlu F, Mut M, Severcan F (2004) The effects of chronic hypoperfusion on rat cranial bone mineral and organic matrix. A Fourier transform infrared spectroscopy study. *Anal Bioanal Chem* 379: 433-438

Bozkurt O, Severcan M, Severcan F (2010) Diabetes induces compositional, structural and functional alterations on rat skeletal soleus muscle revealed by FTIR spectroscopy: a comparative study with EDL muscle. *Analyst* 135: 3110-3119

Brockmann GA, Tsaih SW, Neuschl C, Churchill GA, Li R (2009) Genetic factors contributing to obesity and body weight can act through mechanisms affecting muscle weight, fat weight, or both. *Physiol Genomics* 36: 114-126

Brownlee M (2001) Biochemistry and molecular cell biology of diabetic complications. *Nature* 414: 813-820

Bruch RC, Thayer WS (1983) Differential effect of lipid peroxidation on membrane fluidity as determined by electron spin resonance probes. *Biochim Biophys Acta* 733: 216-222

Cakmak G, Miller LM, Zorlu F, Severcan F (2012) Amifostine, a radioprotectant agent, protects rat brain tissue lipids against ionizing radiation induced damage: an FTIR microspectroscopic imaging study. *Arch Biochem Biophys* 520: 67-73

Cakmak G, Togan I, Severcan F (2006) 17Beta-estradiol induced compositional, structural and functional changes in rainbow trout liver, revealed by FT-IR spectroscopy: a comparative study with nonylphenol. *Aquat Toxicol* 77: 53-63

Cakmak G, Togan I, Uguz C, Severcan F (2003) FT-IR spectroscopic analysis of rainbow trout liver exposed to nonylphenol. *Appl Spectrosc* 57: 835-841

Cakmak G, Zorlu F, Severcan M, Severcan F (2011) Screening of protective effect of amifostine on radiation-induced structural and functional variations in rat liver microsomal membranes by FT-IR spectroscopy. *Anal Chem* 83: 2438-2444

Camacho NP, West P, Torzilli PA, Mendelsohn R (2001) FTIR microscopic imaging of collagen and proteoglycan in bovine cartilage. *Biopolymers* 62: 1-8

Campbell ID, Dwek RA (1984) *Biological spectroscopy*: Benjamin/Cummings Publishing Company, USA.

Canello R, Zingaretti MC, Sarzani R, Ricquier D, Cinti S (1998) Leptin and UCP1 genes are reciprocally regulated in brown adipose tissue. *Endocrinology* 139: 4747-4750

Cannon B, Hedin A, Nedergaard J (1982) Exclusive occurrence of thermogenin antigen in brown adipose tissue. *FEBS Lett* 150: 129-132

Cannon B, Nedergaard J (2004) Brown adipose tissue: function and physiological significance. *Physiol Rev* 84: 277-359

Casal HL, Mantsch HH (1984) Polymorphic phase behaviour of phospholipid membranes studied by infrared spectroscopy. *Biochim Biophys Acta* 779: 381-401

Catala-Niell A, Estrany ME, Proenza AM, Gianotti M, Llado I (2008) Skeletal muscle and liver oxidative metabolism in response to a voluntary isocaloric intake of a high fat diet in male and female rats. *Cell Physiol Biochem* 22: 327-336

Chiriboga L, Yee M, Diem M (2000) Infrared spectroscopy of human cells and tissue. Part VI: A comparative study of histopathology and infrared microspectroscopy of normal, cirrhotic, and cancerous liver tissue. *Appl Spectrosc* 54: 1-8

Ci YX, Gao TY, Feng J, Guo ZQ (1999) Fourier transform infrared spectroscopic characterization of human breast tissue: Implications for breast cancer diagnosis. *Appl Spectrosc* 53: 312-315

Cinti S (2005) The adipose organ. *Prostaglandins Leukot Essent Fatty Acids* 73: 9-15

Cinti S (2006) The role of brown adipose tissue in human obesity. *Nutr Metab Cardiovasc Dis* 16: 569-574

Cinti S (2008) Reversible transdifferentiation in the adipose organ. *Int J Pediatr Obes* 3 Suppl 2: 21-26

Colthup NB, Daly LH, Wiberley SE (1975) *Introduction to infrared and raman spectroscopy*: Academic Press, New York.

Cortes VA, Curtis DE, Sukumaran S, Shao X, Parameswara V, Rashid S, Smith AR, Ren J, Esser V, Hammer RE, Agarwal AK, Horton JD, Garg A (2009) Molecular mechanisms of hepatic steatosis and insulin resistance in the AGPAT2-deficient mouse model of congenital generalized lipodystrophy. *Cell Metab* 9: 165-176

Couillard C, Mauriege P, Imbeault P, Prud'homme D, Nadeau A, Tremblay A, Bouchard C, Despres JP (2000) Hyperleptinemia is more closely associated with adipose cell hypertrophy than with adipose tissue hyperplasia. *Int J Obes Relat Metab Disord* 24: 782-788

Curtis MT, Gilfor D, Farber JL (1984) Lipid peroxidation increases the molecular order of microsomal membranes. *Arch Biochem Biophys* 235: 644-649

Danforth E, Jr. (2000) Failure of adipocyte differentiation causes type II diabetes mellitus? *Nat Genet* 26: 13

Diem M (1993) *Introduction to modern vibrational spectroscopy*: John Wiley & Sons, USA.

Diem M, Boydston-White S, Chiriboga L (1999) Infrared spectroscopy of cells and tissues: Shining light onto a novel subject. *Appl Spectrosc* 53: 148A-161A

Dogan A, Ergen K, Budak F, Severcan F (2007) Evaluation of disseminated candidiasis on an experimental animal model: a fourier transform infrared study. *Appl Spectrosc* 61: 199-203

Dovbeshko GI, Gridina NY, Kruglova EB, Pashchuk OP (2000) FTIR spectroscopy studies of nucleic acid damage. *Talanta* 53: 233-246

Duplus E, Glorian M, Forest C (2000) Fatty acid regulation of gene transcription. *J Biol Chem* 275: 30749-30752

Dusserre E, Moulin P, Vidal H (2000) Differences in mRNA expression of the proteins secreted by the adipocytes in human subcutaneous and visceral adipose tissues. *Biochim Biophys Acta* 1500: 88-96

Federico A, D'Aiuto E, Borriello F, Barra G, Gravina AG, Romano M, De Palma R (2010) Fat: a matter of disturbance for the immune system. *World J Gastroenterol* 16: 4762-4772

Fernandez-Sanchez A, Madrigal-Santillan E, Bautista M, Esquivel-Soto J, Morales-Gonzalez A, Esquivel-Chirino C, Durante-Montiel I, Sanchez-Rivera G, Valadez-Vega C, Morales-Gonzalez JA (2011) Inflammation, oxidative stress, and obesity. *Int J Mol Sci* 12: 3117-3132

Ferris WF, Crowther NJ (2011) Once fat was fat and that was that: our changing perspectives on adipose tissue. *Cardiovasc J Afr* 22: 147-154

Frayling TM, Timpson NJ, Weedon MN, Zeggini E, Freathy RM et al. (2007) A common variant in the FTO gene is associated with body mass index and predisposes to childhood and adult obesity. *Science* 316: 889-894

Frayn KN (2000) Visceral fat and insulin resistance--causative or correlative? *Br J Nutr* 83 Suppl 1: S71-77

Frayn KN (2002) Adipose tissue as a buffer for daily lipid flux. *Diabetologia* 45: 1201-1210

Freedland ES (2004) Role of a critical visceral adipose tissue threshold (CVATT) in metabolic syndrome: implications for controlling dietary carbohydrates: a review. *Nutr Metab (Lond)* 1: 12

Freifelder D (1982) *Physical Chemistry, Applications to Biochemistry and Molecular Biology*: New York.

Fruhbeck G (2008) Overview of adipose tissue and its role in obesity and metabolic disorders. *Methods Mol Biol* 456: 1-22

Fujita K, Nishizawa H, Funahashi T, Shimomura I, Shimabukuro M (2006) Systemic oxidative stress is associated with visceral fat accumulation and the metabolic syndrome. *Circ J* 70: 1437-1442

Furukawa S, Fujita T, Shimabukuro M, Iwaki M, Yamada Y, Nakajima Y, Nakayama O, Makishima M, Matsuda M, Shimomura I (2004) Increased oxidative stress in obesity and its impact on metabolic syndrome. *J Clin Invest* 114: 1752-1761

Garaulet M, Hernandez-Morante JJ, Lujan J, Tebar FJ, Zamora S (2006) Relationship between fat cell size and number and fatty acid composition in adipose tissue from different fat depots in overweight/obese humans. *Int J Obes (Lond)* 30: 899-905

Garip S, Bozoglu F, Severcan F (2007) Differentiation of mesophilic and thermophilic bacteria with fourier transform infrared spectroscopy. *Appl Spectrosc* 61: 186-192

Garip S, Yapici E, Ozek NS, Severcan M, Severcan F (2010) Evaluation and discrimination of simvastatin-induced structural alterations in proteins of different rat tissues by FTIR spectroscopy and neural network analysis. *Analyst* 135: 3233-3241

Gasper R, Dewelle J, Kiss R, Mijatovic T, Goormaghtigh E (2009) IR spectroscopy as a new tool for evidencing antitumor drug signatures. *Biochim Biophys Acta* 1788: 1263-1270

Geloën A, Roy PE, Bukowiecki LJ (1989) Regression of white adipose tissue in diabetic rats. *Am J Physiol* 257: E547-553

Gough KM, Zelinski D, Wiens R, Rak M, Dixon IM (2003) Fourier transform infrared evaluation of microscopic scarring in the cardiomyopathic heart: effect of chronic AT1 suppression. *Anal Biochem* 316: 232-242

Gray DS, Fujioka K (1991) Use of relative weight and Body Mass Index for the determination of adiposity. *J Clin Epidemiol* 44: 545-550

Gregor MF, Hotamisligil GS (2007) Thematic review series: Adipocyte Biology. Adipocyte stress: the endoplasmic reticulum and metabolic disease. *J Lipid Res* 48: 1905-1914

Gupta P, Tyagi S, Mukhija M, Saini AS, Goyal R, Sharma PL (2011) Obesity: An Introduction and Evaluation. *Journal of Advanced Pharmacy Education & Research* 2: 125-137

Hageman RS, Wagener A, Hantschel C, Svenson KL, Churchill GA, Brockmann GA (2010) High-fat diet leads to tissue-specific changes reflecting risk factors for diseases in DBA/2J mice. *Physiol Genomics* 42: 55-66

Hajer GR, van Haften TW, Visseren FL (2008) Adipose tissue dysfunction in obesity, diabetes, and vascular diseases. *Eur Heart J* 29: 2959-2971

Hantschel C, Wagener A, Neuschl C, Teupser D, Brockmann GA (2011) Features of the metabolic syndrome in the Berlin Fat Mouse as a model for human obesity. *Obes Facts* 4: 270-277

Haris PI, Severcan F (1999) FTIR spectroscopic characterization of protein structure in aqueous and non-aqueous media. *J Mol Catal B-Enzym* 7: 207-221

Haugen F, Drevon CA (2007) Activation of nuclear factor-kappaB by high molecular weight and globular adiponectin. *Endocrinology* 148: 5478-5486

Hauner H, Wabitsch M, Pfeiffer EF (1988) Differentiation of adipocyte precursor cells from obese and nonobese adult women and from different adipose tissue sites. *Horm Metab Res Suppl* 19: 35-39

Havel PJ, Kasim-Karakas S, Dubuc GR, Mueller W, Phinney SD (1996) Gender differences in plasma leptin concentrations. *Nat Med* 2: 949-950

Henderson GC, Fattor JA, Horning MA, Faghihnia N, Johnson ML, Luke-Zeitoun M, Brooks GA (2008) Glucoregulation is more precise in women than in men during postexercise recovery. *Am J Clin Nutr* 87: 1686-1694

Hevener AL, Febbraio MA (2010) The 2009 stock conference report: inflammation, obesity and metabolic disease. *Obes Rev* 11: 635-644

Holtz WA, Turetzky JM, Jong YJ, O'Malley KL (2006) Oxidative stress-triggered unfolded protein response is upstream of intrinsic cell death evoked by parkinsonian mimetics. *J Neurochem* 99: 54-69

Hong J, Stubbins RE, Smith RR, Harvey AE, Nunez NP (2009) Differential susceptibility to obesity between male, female and ovariectomized female mice. *Nutr J* 8: 11

Hotamisligil GS (2006) Inflammation and metabolic disorders. *Nature* 444: 860-867

Ibrahim MM (2010) Subcutaneous and visceral adipose tissue: structural and functional differences. *Obes Rev* 11: 11-18

Jackson M, Ramjiawan B, Hewko M, Mantsch HH (1998) Infrared microscopic functional group mapping and spectral clustering analysis of hypercholesterolemic rabbit liver. *Cell Mol Biol (Noisy-le-grand)* 44: 89-98

Justo R, Boada J, Frontera M, Oliver J, Bermudez J, Gianotti M (2005) Gender dimorphism in rat liver mitochondrial oxidative metabolism and biogenesis. *Am J Physiol Cell Physiol* 289: C372-378

Kautzky-Willer A, Handisurya A (2009) Metabolic diseases and associated complications: sex and gender matter! *Eur J Clin Invest* 39: 631-648

Keaney JF, Jr., Larson MG, Vasan RS, Wilson PW, Lipinska I, Corey D, Massaro JM, Sutherland P, Vita JA, Benjamin EJ (2003) Obesity and systemic oxidative stress: clinical correlates of oxidative stress in the Framingham Study. *Arterioscler Thromb Vasc Biol* 23: 434-439

Kershaw EE, Flier JS (2004) Adipose tissue as an endocrine organ. *J Clin Endocrinol Metab* 89: 2548-2556

Klaus S, Casteilla L, Bouillaud F, Ricquier D (1991) The uncoupling protein UCP: a membraneous mitochondrial ion carrier exclusively expressed in brown adipose tissue. *Int J Biochem* 23: 791-801

Klein J, Permana PA, Owecki M, Chaldakov GN, Bohm M, Hausman G, Lapiere CM, Atanassova P, Sowinski J, Fasshauer M, Hausman DB, Maquoi E, Tonchev AB, Peneva VN, Vlachanov KP, Fiore M, Aloe L, Slominski A, Reardon CL, Ryan TJ, Pond CM (2007) What are subcutaneous adipocytes really good for? *Exp Dermatol* 16: 45-70

Kneipp J, Lasch P, Baldauf E, Beekes M, Naumann D (2000) Detection of pathological molecular alterations in scrapie-infected hamster brain by Fourier transform infrared (FT-IR) spectroscopy. *Biochim Biophys Acta* 1501: 189-199

Lafontan M, Berlan M (2003) Do regional differences in adipocyte biology provide new pathophysiological insights? *Trends Pharmacol Sci* 24: 276-283

Lefterova MI, Lazar MA (2009) New developments in adipogenesis. *Trends Endocrinol Metab* 20: 107-114

Legato MJ (1997) Gender-specific aspects of obesity. *Int J Fertil Womens Med* 42: 184-197

Lemieux S, Despres JP (1994) Metabolic complications of visceral obesity: contribution to the aetiology of type 2 diabetes and implications for prevention and treatment. *Diabete Metab* 20: 375-393

Lyman DJ, Murray-Wijelath J (1999) Vascular graft healing: I. FTIR analysis of an implant model for studying the healing of a vascular graft. *J Biomed Mater Res* 48: 172-186

MacDougald OA, Burant CF (2007) The rapidly expanding family of adipokines. *Cell Metab* 6: 159-161

Maddux BA, See W, Lawrence JC, Jr., Goldfine AL, Goldfine ID, Evans JL (2001) Protection against oxidative stress-induced insulin resistance in rat L6 muscle cells by micromolar concentrations of alpha-lipoic acid. *Diabetes* 50: 404-410

Manoharan R, Wang Y, Feld MS (1996) Histochemical analysis of biological tissues using Raman spectroscopy. *Spectrosc Acta Pt A-Molec Biomolec Spectr* 52: 215-249

Mantsch HH (1984) Biological Applications Of Fourier Transform Infrared Spectroscopy - A Study Of Phase-Transitions In Biomembranes. *J Mol Struct* 113: 201-212

Marcelli A, Cricenti A, Kwiatek WM, Petibois C (2012) Biological applications of synchrotron radiation infrared spectromicroscopy. *Biotechnol Adv*

Marin P, Andersson B, Ottosson M, Olbe L, Chowdhury B, Kvist H, Holm G, Sjostrom L, Bjorntorp P (1992) The morphology and metabolism of intraabdominal adipose tissue in men. *Metabolism* 41: 1242-1248

Martinez JA (2006) Mitochondrial oxidative stress and inflammation: an slalom to obesity and insulin resistance. *J Physiol Biochem* 62: 303-306

Matsuda Y, Tanioka T, Yoshioka T, Nagano T, Hiroi T, Yoshikawa K, Okabe K, Nagamine I, Takasaka Y (2005) Gender differences in association of plasma adiponectin with obesity reflect resultant insulin resistance in non-diabetic Japanese patients with schizophrenia. *Psychiatry Clin Neurosci* 59: 266-273

Matsuoka T, Kajimoto Y, Watada H, Kaneto H, Kishimoto M, Umayahara Y, Fujitani Y, Kamada T, Kawamori R, Yamasaki Y (1997) Glycation-dependent, reactive oxygen species-mediated suppression of the insulin gene promoter activity in HIT cells. *J Clin Invest* 99: 144-150

Melin AM, Perromat A, Deleris G (2000) Pharmacologic application of Fourier transform IR spectroscopy: In vivo toxicity of carbon tetrachloride on rat liver. *Biopolymers* 57: 160-168

Mendelsohn R, Mantsch H (1986) *Fourier transform infrared studies of lipid-protein interaction, Progress in Protein-Lipid Interactions*, Vol. 2: Elsevier Science Publishers, Netherlands.

Mendez-Sanchez N, Arrese M, Zamora-Valdes D, Uribe M (2007) Current concepts in the pathogenesis of nonalcoholic fatty liver disease. *Liver Int* 27: 423-433

Meyer CW, Wagener A, Rink N, Hantschel C, Heldmaier G, Klingenspor M, Brockmann GA (2009) High energy digestion efficiency and altered lipid metabolism contribute to obesity in BFMI mice. *Obesity (Silver Spring)* 17: 1988-1993

Misra A, Vikram NK (2003) Clinical and pathophysiological consequences of abdominal adiposity and abdominal adipose tissue depots. *Nutrition* 19: 457-466

Mitra S, Bansal VS, Bhatnagar PK (2008) From a glucocentric to a lipocentric approach towards metabolic syndrome. *Drug Discov Today* 13: 211-218

Miyazaki Y, Mahankali A, Matsuda M, Mahankali S, Hardies J, Cusi K, Mandarino LJ, DeFronzo RA (2002) Effect of pioglitazone on abdominal fat distribution and insulin sensitivity in type 2 diabetic patients. *J Clin Endocrinol Metab* 87: 2784-2791

Montague CT, O'Rahilly S (2000) The perils of portliness: causes and consequences of visceral adiposity. *Diabetes* 49: 883-888

Motoshima H, Wu X, Sinha MK, Hardy VE, Rosato EL, Barbot DJ, Rosato FE, Goldstein BJ (2002) Differential regulation of adiponectin secretion from cultured human omental and subcutaneous adipocytes: effects of insulin and rosiglitazone. *J Clin Endocrinol Metab* 87: 5662-5667

Movasaghi Z, Rehman S, Rehman IU (2008) Fourier transform infrared (FTIR) spectroscopy of biological tissues. *Appl Spectrosc Rev* 43: 134-179

Nakazono K, Watanabe N, Matsuno K, Sasaki J, Sato T, Inoue M (1991) Does superoxide underlie the pathogenesis of hypertension? *Proc Natl Acad Sci U S A* 88: 10045-10048

Nara M, Okazaki M, Kagi H (2002) Infrared study of human serum very-low-density and low-density lipoproteins. Implication of esterified lipid C=O stretching bands for characterizing lipoproteins. *Chem Phys Lipids* 117: 1-6

Neuschl C, Hantschel C, Wagener A, Schmitt AO, Illig T, Brockmann GA (2010) A unique genetic defect on chromosome 3 is responsible for juvenile obesity in the Berlin Fat Mouse. *Int J Obes (Lond)* 34: 1706-1714

Nguyen DM, El-Serag HB (2010) The epidemiology of obesity. *Gastroenterol Clin North Am* 39: 1-7

Nguyen TT, Hernandez Mijares A, Johnson CM, Jensen MD (1996) Postprandial leg and splanchnic fatty acid metabolism in nonobese men and women. *Am J Physiol* 271: E965-972

Nissen-Meyer LS, Svalheim S, Tauboll E, Gjerstad L, Reinholt FP, Jemtland R (2008) How can antiepileptic drugs affect bone mass, structure and metabolism? Lessons from animal studies. *Seizure* 17: 187-191

Ohara Y, Peterson TE, Harrison DG (1993) Hypercholesterolemia increases endothelial superoxide anion production. *J Clin Invest* 91: 2546-2551

Oka R, Miura K, Sakurai M, Nakamura K, Yagi K, Miyamoto S, Moriuchi T, Mabuchi H, Koizumi J, Nomura H, Takeda Y, Inazu A, Nohara A, Kawashiri MA, Nagasawa S, Kobayashi J, Yamagishi M (2010) Impacts of visceral adipose tissue and subcutaneous adipose tissue on metabolic risk factors in middle-aged Japanese. *Obesity (Silver Spring)* 18: 153-160

Otto TC, Lane MD (2005) Adipose development: from stem cell to adipocyte. *Crit Rev Biochem Mol Biol* 40: 229-242

Ouchi N, Kihara S, Arita Y, Okamoto Y, Maeda K, Kuriyama H, Hotta K, Nishida M, Takahashi M, Muraguchi M, Ohmoto Y, Nakamura T, Yamashita S, Funahashi T, Matsuzawa Y (2000) Adiponectin, an adipocyte-derived plasma

protein, inhibits endothelial NF-kappaB signaling through a cAMP-dependent pathway. *Circulation* 102: 1296-1301

Ozek NS, Tuna S, Erson-Bensan AE, Severcan F (2010) Characterization of microRNA-125b expression in MCF7 breast cancer cells by ATR-FTIR spectroscopy. *Analyst* 135: 3094-3102

Pepys MB, Hirschfield GM (2003) C-reactive protein: a critical update. *J Clin Invest* 111: 1805-1812

Phillips MS, Liu Q, Hammond HA, Dugan V, Hey PJ, Caskey CJ, Hess JF (1996) Leptin receptor missense mutation in the fatty Zucker rat. *Nat Genet* 13: 18-19

Pou KM, Massaro JM, Hoffmann U, Vasan RS, Maurovich-Horvat P, Larson MG, Keaney JF, Jr., Meigs JB, Lipinska I, Kathiresan S, Murabito JM, O'Donnell CJ, Benjamin EJ, Fox CS (2007) Visceral and subcutaneous adipose tissue volumes are cross-sectionally related to markers of inflammation and oxidative stress: the Framingham Heart Study. *Circulation* 116: 1234-1241

Pouliot MC, Despres JP, Lemieux S, Moorjani S, Bouchard C, Tremblay A, Nadeau A, Lupien PJ (1994) Waist circumference and abdominal sagittal diameter: best simple anthropometric indexes of abdominal visceral adipose tissue accumulation and related cardiovascular risk in men and women. *Am J Cardiol* 73: 460-468

Quevedo S, Roca P, Pico C, Palou A (1998) Sex-associated differences in cold-induced UCP1 synthesis in rodent brown adipose tissue. *Pflugers Arch* 436: 689-695

Rajala MW, Scherer PE (2003) Minireview: The adipocyte--at the crossroads of energy homeostasis, inflammation, and atherosclerosis. *Endocrinology* 144: 3765-3773

Razani B, Engelman JA, Wang XB, Schubert W, Zhang XL, Marks CB, Macaluso F, Russell RG, Li M, Pestell RG, Di Vizio D, Hou H, Jr., Kneitz B, Lagaud G, Christ GJ, Edelmann W, Lisanti MP (2001) Caveolin-1 null mice are viable but show evidence of hyperproliferative and vascular abnormalities. *J Biol Chem* 276: 38121-38138

Reaven GM (1997) Banting Lecture 1988. Role of insulin resistance in human disease. 1988. *Nutrition* 13: 65; discussion 64, 66

Rigas B, Morgello S, Goldman IS, Wong PTT (1990) Human Colorectal Cancers Display Abnormal Fourier-Transform Infrared-Spectra. *Proc Natl Acad Sci U S A* 87: 8140-8144

Rodriguez-Cuenca S, Pujol E, Justo R, Frontera M, Oliver J, Gianotti M, Roca P (2002) Sex-dependent thermogenesis, differences in mitochondrial morphology and function, and adrenergic response in brown adipose tissue. *J Biol Chem* 277: 42958-42963

Rodriguez AM, Palou A (2004) Uncoupling proteins: gender dependence and their relation to body weight control. *Int J Obes Relat Metab Disord* 28: 500-502

Rudich A, Tirosh A, Potashnik R, Hemi R, Kanety H, Bashan N (1998) Prolonged oxidative stress impairs insulin-induced GLUT4 translocation in 3T3-L1 adipocytes. *Diabetes* 47: 1562-1569

Rytka JM, Wueest S, Schoenle EJ, Konrad D (2011) The portal theory supported by venous drainage-selective fat transplantation. *Diabetes* 60: 56-63

Schaffer JE (2003) Lipotoxicity: when tissues overeat. *Curr Opin Lipidol* 14: 281-287

Schenk S, Saberi M, Olefsky JM (2008) Insulin sensitivity: modulation by nutrients and inflammation. *J Clin Invest* 118: 2992-3002

Severcan F, Gorgulu G, Gorgulu ST, Guray T (2005) Rapid monitoring of diabetes-induced lipid peroxidation by Fourier transform infrared spectroscopy: evidence from rat liver microsomal membranes. *Anal Biochem* 339: 36-40

Severcan F, Haris PI (2003) Fourier transform infrared spectroscopy suggests unfolding of loop structures precedes complete unfolding of pig citrate synthase. *Biopolymers* 69: 440-447

Severcan F, Kaptan N, Turan B (2003) Fourier transform infrared spectroscopic studies of diabetic rat heart crude membranes. *Spectr-Int J* 17: 569-577

Severcan F, Okan Durmus H, Eker F, Akinoglu BG, Haris PI (2000a) Vitamin D(2) modulates melittin-membrane interactions. *Talanta* 53: 205-211

Severcan F, Toyran N, Kaptan N, Turan B (2000b) Fourier transform infrared study of the effect of diabetes on rat liver and heart tissues in the CH region. *Talanta* 53: 55-59

Sies H (1997) Oxidative stress: oxidants and antioxidants. *Exp Physiol* 82: 291-295

Simsek Ozek N, Sara Y, Onur R, Severcan F (2010) Low dose simvastatin induces compositional, structural and dynamic changes in rat skeletal extensor digitorum longus muscle tissue. *Biosci Rep* 30: 41-50

Sjostrom L, William-Olsson T (1981) Prospective studies on adipose tissue development in man. *Int J Obes* 5: 597-604

Smith GC, Jackson SP (1999) The DNA-dependent protein kinase. *Genes Dev* 13: 916-934

Sonmez K, Akcakoyun M, Akcay A, Demir D, Duran NE, Gencbay M, Degertekin M, Turan F (2003) Which method should be used to determine the obesity, in patients with coronary artery disease? (body mass index, waist circumference or waist-hip ratio). *Int J Obes Relat Metab Disord* 27: 341-346

Speliotes EK, Willer CJ, Berndt SI, Monda KL, Thorleifsson G, Jackson AU et al. (2010) Association analyses of 249,796 individuals reveal 18 new loci associated with body mass index. *Nat Genet* 42: 937-948

Struve WS (1989) *Fundamentals of molecular spectroscopy*: John Wiley, New York.

Stuart B (1997) *Biological Applications of Infrared Spectroscopy*: John Wiley and Sons, Ltd. England.

Stuart BH (2004) *Infrared Spectroscopy-Fundamentals and Applications. (Analytical Techniques in the Sciences (AnTs))*: John Wiley and Sons.

Svenson KL, Von Smith R, Magnani PA, Suetin HR, Paigen B, Naggert JK, Li R, Churchill GA, Peters LL (2007) Multiple trait measurements in 43 inbred mouse strains capture the phenotypic diversity characteristic of human populations. *J Appl Physiol* 102: 2369-2378

Takahashi H, French SW, Wong PT (1991) Alterations in hepatic lipids and proteins by chronic ethanol intake: a high-pressure Fourier transform infrared spectroscopic study on alcoholic liver disease in the rat. *Alcohol Clin Exp Res* 15: 219-223

Tarnopolsky MA, Atkinson SA, Phillips SM, MacDougall JD (1995) Carbohydrate loading and metabolism during exercise in men and women. *J Appl Physiol* 78: 1360-1368

Toyran N, Lasch P, Naumann D, Turan B, Severcan F (2006) Early alterations in myocardia and vessels of the diabetic rat heart: an FTIR microspectroscopic study. *Biochem J* 397: 427-436

Trayhurn P, Drevon CA, Eckel J (2011) Secreted proteins from adipose tissue and skeletal muscle - adipokines, myokines and adipose/muscle cross-talk. *Arch Physiol Biochem* 117: 47-56

Trayhurn P, Wood IS (2004) Adipokines: inflammation and the pleiotropic role of white adipose tissue. *Br J Nutr* 92: 347-355

Tritos NA, Mantzoros CS (1997) Leptin: its role in obesity and beyond. *Diabetologia* 40: 1371-1379

Umemura J, Cameron DG, Mantsch HH (1980) A Fourier-Transform Infrared Spectroscopic Study Of The Molecular Interaction Of Cholesterol With 1,2-Dipalmitoyl-Sn-Glycero-3-Phosphocholine. *Biochimica Et Biophysica Acta* 602: 32-44

Unger RH, Orci L (2001) Diseases of liporegulation: new perspective on obesity and related disorders. *FASEB J* 15: 312-321

Valle A, Catala-Niell A, Colom B, Garcia-Palmer FJ, Oliver J, Roca P (2005) Sex-related differences in energy balance in response to caloric restriction. *Am J Physiol Endocrinol Metab* 289: E15-22

van Herpen NA, Schrauwen-Hinderling VB (2008) Lipid accumulation in non-adipose tissue and lipotoxicity. *Physiol Behav* 94: 231-241

Vendemiale G, Grattagliano I, Altomare E (1999) An update on the role of free radicals and antioxidant defense in human disease. *Int J Clin Lab Res* 29: 49-55

Vincent HK, Taylor AG (2006) Biomarkers and potential mechanisms of obesity-induced oxidant stress in humans. *Int J Obes (Lond)* 30: 400-418

Wagener A, Goessling HF, Schmitt AO, Mauel S, Gruber AD, Reinhardt R, Brockmann GA (2010) Genetic and diet effects on Ppar-alpha and Ppar-gamma signaling pathways in the Berlin Fat Mouse Inbred line with genetic predisposition for obesity. *Lipids Health Dis* 9: 99

Wagener A, Schmitt AO, Aksu S, Schlote W, Neuschl C, Brockmann GA (2006) Genetic, sex, and diet effects on body weight and obesity in the Berlin Fat Mouse Inbred lines. *Physiol Genomics* 27: 264-270

Wajchenberg BL (2000) Subcutaneous and visceral adipose tissue: their relation to the metabolic syndrome. *Endocr Rev* 21: 697-738

Wang TD, Triadafilopoulos G, Crawford JM, Dixon LR, Bhandari T, Sahbaie P, Friedland S, Soetikno R, Contag CH (2007) Detection of endogenous biomolecules in Barrett's esophagus by Fourier transform infrared spectroscopy. *Proc Natl Acad Sci U S A* 104: 15864-15869

Weisberg SP, McCann D, Desai M, Rosenbaum M, Leibel RL, Ferrante AW, Jr. (2003) Obesity is associated with macrophage accumulation in adipose tissue. *J Clin Invest* 112: 1796-1808

West PA, Bostrom MP, Torzilli PA, Camacho NP (2004) Fourier transform infrared spectral analysis of degenerative cartilage: an infrared fiber optic probe and imaging study. *Appl Spectrosc* 58: 376-381

Westcott E, Windsor A, Mattacks C, Pond C, Knight S (2005) Fatty acid compositions of lipids in mesenteric adipose tissue and lymphoid cells in patients with and without Crohn's disease and their therapeutic implications. *Inflamm Bowel Dis* 11: 820-827

Wong PT, Wong RK, Caputo TA, Godwin TA, Rigas B (1991) Infrared spectroscopy of exfoliated human cervical cells: evidence of extensive structural changes during carcinogenesis. *Proc Natl Acad Sci U S A* 88: 10988-10992

Yano K, Ohoshima S, Shimizu Y, Moriguchi T, Katayama H (1996) Evaluation of glycogen level in human lung carcinoma tissues by an infrared spectroscopic method. *Cancer Lett* 110: 29-34

Yu BP (1994) Cellular defenses against damage from reactive oxygen species. *Physiol Rev* 74: 139-162

Zhang Y, Proenca R, Maffei M, Barone M, Leopold L, Friedman JM (1994) Positional cloning of the mouse obese gene and its human homologue. *Nature* 372: 425-432